The interplay between glucose and fat metabolism

A biosimulation approach

Hallgreen, Christine E.

Publication date:
2010

Document Version
Publisher's PDF, also known as Version of record

THE INTERPLAY BETWEEN GLUCOSE AND FAT METABOLISM:
A BIOSIMULATION APPROACH

PHD THESIS

BY

CHRISTINE E. HALLGREEN

BIOSIMULATION, NOVO NORDISK A/S

DEPARTMENT OF PHYSICS, TECHNICAL UNIVERSITY OF DENMARK

COPENHAGEN, NOVEMBER 2009

PREFACE

This thesis presents the work I have preformed during my PhD studies at Clinical Pharmacology – Biosimulation Novo Nordisk A/S (Earlier under Developments Projects – Biosimulation) and Department of Physics, Technical University of Denmark. The thesis has kindly been supervised by Professor Erik Mosekilde, Department of Physics, Technical University of Denmark, and Professor Morten Colding-Jørgensen, Biosimulation, Novo Nordisk A/S. My work was finically supported by Corporate Research Affairs, Novo Nordisk, and the Industrial PhD Initiative under the Danish Ministry of Science, Technology and Innovation. In addition to the guidance and support from my two supervisors, many other persons have guided my through my period as a ph.d student. Especially I would like to thank Dr. Kevin D. Hall who supervised me during my external research stay at his lab, at the National Institute of Health, NIDDK, Laboratory of Biological Modelling. Katarina Jelic is thanked for her help and guidance with the literature of lipid metabolism, for scientific discussions, as well as for general support during my work. I would also like to thank Rene Norman Hansen for an endogamous help with the application of this PhD project, and more recently, for help in filing out an application for a PostDoc project. Rene also provided a lot of constructive criticism of the structure of this thesis. More over I like to thank Christian Hove Rasmussen for his help with converting figures to the right format. Finally, I must express a word of appreciation to my family for outstanding support and encouragement.

Christine E. Hallgreen

Copenhagen, November 2009

ABSTRACT

This thesis covers different aspects of glucose and fat metabolism and of the interplay between the two metabolic pathways. The glucose and fat metabolism and mechanisms involved in the regulation have been investigated through the formulation of four mechanistic models and one simple allometric model, each covering different aspects of the metabolism. The goal of the modelling efforts is not primarily to predict but rather to explain the behavior of and test various hypotheses about the involved biological /physiological processes and mechanisms, with a view to gain a better understanding of the human glucose and fat metabolism.

The formulation of a quasi steady state model of the flows and transformations in human glucose and fat metabolism was used to illustrate the importance of the interplay between glucose and fat metabolism. The regulation of glucose and fat metabolism is complex and, combined with at simple model of hexokinase, the glucose and fat steady state model illustrate how important it is not only to focus on the uptake of glucose into the cell but also to consider how the utilisation of intercellular glucose in regulated. Simulation of hyperinsulinemic glucose clamp studies with the glucose and fat metabolism steady state model showed that that the nutritional state of the metabolism can influence the conclusion of an experimental glucose clamp study. The clamp simulation also showed that changes in the regulation of lipid metabolism influence the glucose utilisation rate at lower insulin levels.

Through the construction of a model of hepatic glucose metabolism I found that both stimulation of glycogen synthesis by glucose and inhibition of glycogen breakdown by glucose were necessary in order to explain the experimentally observed relation between hepatic glucose output and plasma glucose concentration (45). The hepatic glucose metabolism model was also used to test the effect of either glycogen stimulation of its own breakdown or glycogen inhibition of its own synthesis. It was found that both

mechanisms separately could explain the experimentally observed linear relation between net glycogen breakdown and hepatic glycogen content experimentally observed (77;106).

Through the formation of a model of postprandial plasma non-esterified fatty acid dynamics, the mechanism involved in the experimental observed plasma non-esterified fatty acid overshoot in the late postprandial period was investigated. Simulation with this the model showed that the stimulatory effect of insulin on lipoprotein lipase, and especially the long response time for this effect, is the main mechanism responsible for the observed overshoot. The postprandial plasma non-esterified fatty acid dynamics model was used to simulate plasma non-esterified fatty acid profile for healthy as well as for obese and diabetic subjects. Regulation of adipose tissue lipase by insulin was found to be essential in explaining the differences in the plasma non-esterified fatty acid profiles in relation to plasma insulin profiles observed in studies of postprandial metabolism. The model indicated a relation between overnight fasted insulin concentration and half maximal suppression insulin concentration for adipose tissue lipase (EC50).

A small model describing the allometric relationship between changes in visceral fat and total fat mass was made. This is the first model to reveal an allometric relationship between changes of visceral and total fat mass that holds for both genders as well as for a wide range of weight loss interventions including bariatric surgery, caloric restriction with or without exercise, and exercise alone. From this relationship it can be concluded that changes of visceral fat are primarily determined by total fat mass changes and by the initial visceral to total fat mass ratio. For future investigations of visceral fat loss the allometric model predictions could be used as a null hypothesis to test for an additional independent effect of weight loss.

Publications:

Jelic, K., Hallgreen, C.E., Colding-Jørgensen, M., A model of NEFA dynamics with focus on the postprandial state, *Annals of biomedical engineering* (2009) 37(9):1897-1909.

Hall, K.D. & Hallgreen, C.E., Increasing Weight Loss Attenuates the Preferential Loss of Visceral Compared with Subcutaneous Fat: A predicted result of an allometric model, *International Journal of Obesity* (2008) 32, 722

Hallgreen, C.E., & Hall, K.D., Allometric Relationship between Changes of Visceral Fat and Total Fat Mass, *International Journal of Obesity* (2008) 32, 845-852

Hallgreen, C.E., Korsgaard, T.V, Hansen, R.N., Colding-Jørgensen, M., The Glucose-Insulin Control System, in Biosimulation of Drug Development, Edited by; Bertau, M., Mosekilde, E., Westerhoff, H.V., (2008) Wiley-VDH verlag GmbH & Co, KGaA Weinheim.

DANSK OPSUMERING / DANISH SUMMERY

Denne ph.d afhandling omhandler forskellige facetter af det menneskelige glukose og fedt stofskifte. Glukose og fedt stofstiftet og de fysiologiske mekanismer, som regulerer stofskiftet, er blevet undersøgt gennem beskrivelsen af fire mekanisme-baserede modeller samt en simple allometrisk model. Målet med modellerne er ikke kun at forudsige, men også at forklare dynamikken af og teste hypoteser om de involverede biologiske/fysiologiske processer og mekanismer, for derved opnå en større forståelse af det menneskelige glukose og fedt stofskifte.

Beskrivelsen af en steady state model af glukose og fedt metabolismen blev brugt til at illustrere hvor vigtig samspillet mellem glukose og fedt stofskiftet er. Regulering af glukose og fedt stofskiftet er meget kompleks, og sammen med en simpel model at hexokinase blev glukose og fedt steady state modellen brugt til at vise, hvor vigtigt det er ikke kun at fokusere på optaget af glukose i cellerne, men også på hvordan forbruget af glukose i cellerne bliver reguleret. Simuleringer af hyperinsulinemic glukose clamp studier med glukose og fedt steady state modellen viste, at den ernæringsmæssige tilstand af metabolismen kan have indflydelse på resultatet af glukose clamp studier. Desuden viste simuleringerne at ændringer i fedt stofskiftet kan have indflydelse på størrelsen af glukose forbruget for lavere insulin niveauer.

Gennem beskrivelsen af en model af lever glukose stofskifte har jeg vist at både en stimulering af lever glykogen syntesen af glukose og en hæmning af lever glykogen nedbrydningen af glukose er nødvendig for at forklare det eksperimentelt fundne forhold mellem leverens glukose produktion og plasma glukose koncentration under forhold med basale insulin og glukagon niveauer (45). Lever glukose stofskifte modellen blev også brugt til at teste om en mekanisme hvor lever glykogen stimulerer sin egen nedbrydning, eller en mekanisme, hvor lever glykogen hæmmer sin egen syntese, kan forklare det lineære forhold mellem net lever glykogen nedbrydning af lever glykogen niveau som er observeret eksperimentelt (77;106). Gennem denne undersøgelse blev det vist at begge

mekanismer hver for sig kunne forklare det observerede forhold mellem net glykogen nedbrydning og glykogen niveau.

Ved hjælp af en model, der beskriver plasma fedtsyre dynamikken efter et måltid, har jeg undersøget, hvilke mekanismer der er med til at give den eksperimentalt observerede plasma fedtsyre over kompensation i den sene fase efter et måltid (43;86;113). Denne undersøgelse viste, at den observerede overkompensation i plasma fedtsyre kan forklares gennem insulin stimulering af nedbrydningen af plasma triglycerid til fedt syre (lipoprotein lipase), samt den lange tids forskydning (omkring 4 timer) denne stimulering sker under. Med den beskrevne model af plasma fedtsyre dynamikken efter et måltid kunne jeg reproducere plasma fedtsyre tidsserier efter et måltid for både normale, overvægtige og diabetiske personer. For overvægtige og diabetiske personer krævede det dog ændringer af et mindre antal model parametre. Gennem simuleringen af plasma fedtsyre dynamikken efter et måltid, blev det fundet at insulin regulering af fedtvævets frigivelse af fedtsyre (adipose tissue lipase) er afgørende for at forklare de forskelle mellem plasma fedtsyre profiler efter et måltid som kan observeres for normale, overvægtige og diabetiske personer. Desuden indikerede model simuleringer en relation mellem den basale insulin koncentration (efter en nats faste) og den insulin koncentration der giver halv maksimal hæmning på adipose tissue lipase (EC50).

Under mit ophold ved NIH har jeg været med til at opstille en lille model, der beskriver det allometriske forhold mellem ændringer i visceral fedt og total fedtmasse. Modellen er den første, der afslører et allometrisk forhold mellem ændringen i visceral fedt masse og total fedt masse, som gælder for begge køn, samt for mange forskellige vægt tabs metoder, herunder reduktion af mave sækkens volumen, kalorie restriktion med og uden motion samt motion alene. Gennem dette allometriske forhold kan det konkluderes, at ændringer i visceral fedt masse primært er bestemt af ændringen i total fedt masse samt af det initiale forhold mellem visceral fedtmasse og total fedtmasse. For fremtidige

undersøgelser af visceral fedttab kan den allometriske model bruges som nul hypotese til at teste for, om der er en ekstra uafhængig effekt af et vægttab, på visceral fedttab.

TABLE OF CONTENT

1 INTRODUCTION

The food composition and the content of carbohydrate, fat and protein in the food differ considerably from person to person and from culture to culture. The human metabolism must be able to cope with them all; sometimes immediately and sometimes after a period of adaptation. The nutrients are broken down in the intestine and appear in the blood mainly as glucose, amino acids, and fatty acids coupled to albumin or triglycerides stored in the lipoproteins. The blood transports the nutrients – or metabolites of the nutrients – from organ to organ, and the different organs collaborate in the utilization of the nutrients for energy needs, building or replacement of cells and tissues, and storage. The storage option is important, since food intake is discontinuous with intervals of hours or even days, so in some periods the uptake from the intestine exceeds the organism's demands and in other periods there is no uptake, and the organism must rely on its nutrient stores. Consequently there is interchange of nutrients and metabolites back and forth, and the regulation of this traffic is one of the major challenges of our metabolic control. In the blood, glucose concentration is held within narrow limits. The fasting plasma glucose is normally 4-5 mM (66), and even during large meals, the increase is only a few mM in healthy persons and lasts only for a few hours. In contrast, the concentration of fatty acids varies from up to around 1.5 mM during long fast (66) to 0.1 mM after a meal (66). Both the glucose and the fatty acid metabolism are mainly controlled by the hormone insulin, although insulin in not released in response to a signal related to fatty acid metabolism, at lease not directly. So it appears to be a fair conclusion that insulin is controlling the plasma glucose concentration and that the effect on fatty acids is secondary to the glucose control. The view has led to the notion that the insulin-glucose system acts as an isolated, classic control system to keep the plasma glucose constant. If the glucose concentration increases, the beta cells release more insulin that increases the glucose uptake mainly in muscle, and decreases the hepatic glucose output, so the glucose concentration is brought down again. However, the fate of the glucose is complex, and the control of the intracellular utilisation may be even more important than the regulation of the glucose uptake. The glucose and fat should rather be thought of as a complex system that controls

the detailed metabolic interchange, and where the movements of fatty acids play an integral role.

Experiments on isolated organs, tissues and cells have contributed significantly to our understanding of the metabolic system. However, glucose and fat homeostasis requires integrated control by the whole organism, and the used of biosimulation can help us to gain insight into the complex regulation of the metabolism, by combining our physiological knowledge in mechanistic models.

1.1 BIOSIMULATION

To improve the understanding of physiology, diseases and drug action one can introduce physiology or mechanism based models. This approach will be referred to as biosimulation. Mechanism based models describes the dynamics of a system expressed by the physiological processes and interaction we know or assume exists in the biological system. This is done by translating knowledge about biological systems into mathematical expressions. The relevant biological processes and mechanisms are represented as realistically as possible, and parameters and relations are determined from independent experiments. Beside experience with mathematical modelling, this approach requires a good overview of the relevant literature and an extensive biochemical and physiological expertise as well as mathematical. It is also important that the modelling work is preformed in close collaboration with scientists or clinicians who can perform the relevant experiments. The mechanistic models are validated by their ability to reproduce observed phenomena and to predict the outcome of other experiments. Biosimulation can be used to increase our understanding of complex biological systems, predictions ("what if scenarios") and test hypotheses about possible biological processes and mechanisms involved

The models described in the thesis are ordinary differential equations models, where each differential equation represents a metabolite or hormone. The descriptions of metabolic fluxes are in general formulated in terms of the rate determining steps of a process. The metabolic fluxes are by and large expressed as Michaelis-Menten type functions. The kinetic parameters are found in the literature, when possible. It has not been possible to find values for all relevant kinetic parameters. Hence, the values are estimated based on measured rates of the metabolic fluxes and estimated concentrations of the metabolites, and relations between fluxes.

The models described in this thesis are set up in MATLAB R2008b student edition and solved using MATLAB solver ode45 and ode15s.

1.2 THESIS OBJECTIVES AND OUTLINES

Through the formulation of physiological mechanistic models, this thesis will investigate the regulation and interplay between the metabolism of glucose and fat. The goal is not only to predict specific outcomes, but also to explain the general behaviour of the systems and to test hypotheses about biological /physiological processes and mechanisms, all in view of gaining a better understanding of the human glucose and fat metabolism.

The first section; "The Interplay between Glucose and Fat" is concerned with the relationship between glucose and fat metabolism, and the utilisation of the two metabolites. Through formulation of a glucose and fat metabolism steady state model and simulation of glucose clamp studies it is first illustrated how important the interplay between the two metabolic pathways is for the selection of nutrition used for oxidation, and for the way the two metabolic pathways indirectly influence each others dynamics. To further illustrate the importance of metabolite utilisation, a simple model of hexokinase is described. This model captures a mechanism not described in the glucose and fat steady state model, namely the reduced glucose uptake by cells without intercellular glucose utilisation.

In the second section "Hepatic Glucose Metabolism" a model of the hepatic glucose metabolism is described. The model looks into possible mechanisms involved in the regulation of hepatic glucose production during fasting. Focusing on how glucose regulates its own hepatic production, and how the hepatic glycogen content is involved in this regulation. In relation to the interplay between glucose and fat metabolism the hepatic capacity for glucose production during fasting and its capacity for glycogen storages have impact not only on glucose metabolism, but also on the utilisation of glucose, and thereby also indirectly on insulin, fat metabolism.

The section “Postprandial Lipid Metabolism” focuses on the dynamics of postprandial plasma non-estrified fatty acids after a meal, especially on the late postprandial plasma fatty acid overshoot. The overshoot is observed 6-8 hours after a meal is given, under normal conditions a new meal would be consumed before the overshoot is observed. However, this overshoot might be able to explain why the dynamics of glucose, insulin and fatty acids of the second meal is different from that of the first meal. This is why it is relevant to look into the mechanism responsible for this late postprandial fatty acid overshoot. The model was used to simulated studies of postprandial fatty acid metabolism, for different subjects groups, in order to see if the model could reveal any changes in lipid metabolism between for example lean, obese and diabetic subjects.

The last section is concerned with the relationship between visceral fat and total fat mass, and the changes in the though fat masses associated with weight loss. The model described in this section is the first model to reveal an allometric relationship between changes of visceral and total fat mass that holds for both genders as well as for a wide variety of weight loss interventions including bariatric surgery, caloric restriction with or without exercise, and exercise alone.

2 THE INTERPLAY BETWEEN GLUCOSE AND FAT

As mentioned the regulation of the glucose and fat metabolism in very complex, and there are several areas where the two metabolic pathways interplay. One of the major regulators for both systems are is insulin (66). Insulin regulates the glucose transport into the cells, and it regulates the release and uptake of non-esterified fatty acid from adipose tissue, and thereby indirectly fatty acid oxidation and glucose oxidation. The literature has a strong focus on the glucose uptake, *i.e.,* only the removal of glucose from the blood into the cells. This is, however, a too simplified view. The removal takes place mainly by facilitated diffusion via special glucose transporters like GLUT1 and GLUT4 (66). Inside the cell glucose is phosphorylated to glucose-6-phosphate, which traps the glucose inside the cell. Only a few cell types, mainly in the liver and kidney, are able to de-phosphorylate G6P back into glucose (7;66). The fate of the G6P is complex and differs from cell type to cell type and with the nutritional situation of the body. For an illustration

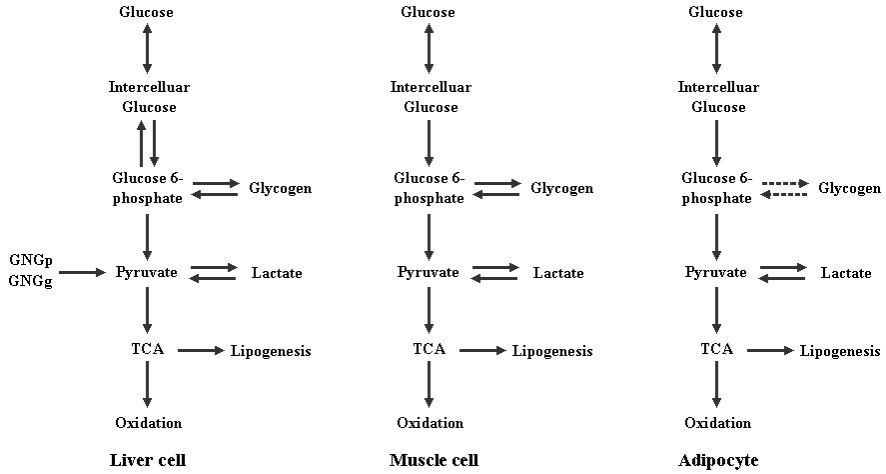

Figure 1: The main routes of glucose breakdown in liver cells, muscle cells and adipocytes.

of the routes of glucose utilisation see figure 1. Once glucose is phosphorylated, the quantitatively most important fates of glucose 6-phosphate are as follows:

- Oxidation, glucose 6-phosphate enters glycolysis and the Krabs TCA cycle to be oxidised into CO_2 and H_2O.
- Storages, glucose 6-phophate is stored as glycogen inside primarily the liver and muscle cells. The capacity for glycogen storages are limited to about 500g glucose which is less that a days worth of energy (66).
- Glucose re-cycling, glucose 6-phosphate can also be converted into lactate. In this way excess glucose can escape the cell. Lactate can be taken up by all cells in the body, where it can be converted to pyruvate and be utilised. In the liver lactate can be transformed back to glucose and re-enter the systemic circulation.
- Fat synthesis, glucose 6-phosphate can also enter glycolysis so that instead of oxidation it is used for fat synthesis though de novo lipogenesis.

As mentioned insulin is a major actor in the interplay between glucose and fat metabolism. Another major aspect of this interplay is oxidation which, as mentioned, is indirectly regulated by insulin. The turnover of non-esterifed fatty acids seems to depend more of less on the level of non-esterified fatty acids, at least during rest (64;125). Total body energy expenditure is covered by oxidation of fatty acids, glucose and protein. Thus, in situations with high fatty acid oxidation the need for glucose oxidation is low, and glucose will have to be utilised by other routes. Glucose re-cycling, which normally amounts to around 50 g glucose per day (21), gives a possibility to increase the fatty acid oxidation in situation of excess glucose. If glucose in the cells are not oxidised or stored, it can re-enter the systemic circulation through the cori-cycle (lactate-glucose cycle), and thereby stimulate insulin production, which inhibits plasma non-esterified fatty acid concentration and thereby fatty acid oxidation.

The effect of insulin on the glucose metabolism is investigated though glucose clamps studies, as well as through oral or intravenous glucose tolerance tests (OGTT and IVGTT). In glucose clamp studies, glucose is kept at a constant level by intervenous infusion of glucose. The glucose infusion rate (GIR) is used to determine the effect of insulin at the given insulin and glucose concentrations. In OGTT's and IVGTT's glucose in given orally or intravenously, respectively. The plasma response of glucose (AUC) is then used to evaluate the effect of insulin. However neither of these tests can tell us how the glucose is utilised. Through the formulation of a glucose and fat steady state model, the utilisation of glucose is investigated from a more systematic point of view.

2.1 GLUCOSE AND FAT STEADY STATE MODEL

The steady state or quasi steady state is a hypothetical situation in which the daily variation in plasma glucose, insulin, triglyceride and non-esterified fatty acids are averaged out over the whole day, and so are the metabolic fluxes. The steady state model applied to get an overview of how the daily energy intake (in the form of glucose and fat) is utilised and to illustrate the complexity of the regulation of glucose and fat metabolism.

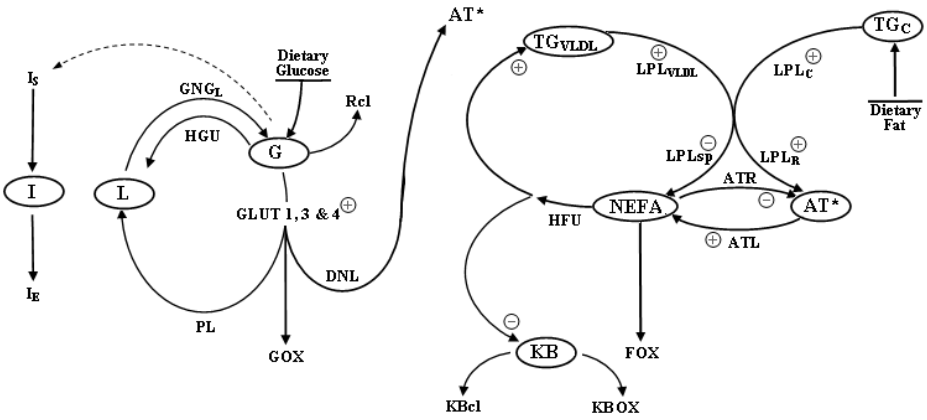

TG_{VLDL} – Plasma VLDL-triglyceride
TG_C – Plasma Chylomicron-triglyceride
NEFA – Plasma non esterified fatty acids
KB – Ketone bodies
AT – Adipose tissue
G – Glucose
L – Lactate
I – Insulin

LPL_C – Chylomicron lipoprotein lipase
LPL_{VLDL} – VLDL lipoprotein lipase
LPL_{SP} – Lipoprotein lipase spillover
LPL_R – Lipoprotein lipase reesterification
ATL – Adipose tissue lipase
ATR – Adipose tissue reesterification
HFU – Hepatic fatty acid uptake
FOX – Fatty acid oxidation
KBOX – Ketone body oxidation
KBcl – Ketone body clearence

HGU – Hepatic glucose uptake
PL – Lactate production
GNG_L – Gluconeogenesis from lactate
DNL – De novo lipogenesis
GOX – Glucose oxidation
GLUT1,3&4 Glucose transporters
Rcl – Renal glucose clearence

I_S – Insulin secretion
I_E – Insulin elimination

Figure 2: Schematic presentation of the glucose fat steady state model. The full line represents fluxes; except for glucose stimulatory effect on insulin secretion (broken line) the effectors of the different fluxes are not shown.

Part of the steady state model has previous been described in the Master Thesis "Modelling the Interplay between the Fat and Glucose Metabolism" by Hallgreen, C.E and Nielsen, B (2005). However, the steady state model described in the master thesis has

since been modified in several ways in order to describe situations with negative or positive energy balance. The following section will start with a short summary of the steady state model as describe in my Master Thesis. The parts of the model that has been modified will be described more toroughly. Figure 2 shows a schematic overview of the steady state model. The circled capitals represent state variables and the full lines represent fluxes between the different metabolites. The stimulatory effect of glucose on insulin secretion is represented by a broken line, and insulin's effect on different fluxes are shown by + or -, stimulation or inhibition, respectively. The regulatory effects of other metabolites on different fluxes are not shown.

The plasma glucose concentration stimulates the production of insulin from the beta-cells in pancreas. In this model the secretion of insulin is regulated by plasma glucose concentration, this is described through a Hill function. Elimination of insulin occurs in liver, kidneys, and fat and muscle cells. The liver is responsible for about 50% of the insulin clearance, the hepatic insulin clearance in considered to be saturated as is the elimination of insulin by fat and muscle cells (78).

In the steady state model, dietary glucose and fat intakes are considered to be constant rates. The rate of dietary glucose is released into plasma as is the rate of dietary fat. Note, however that rate of dietary fat is released into plasma as triglycerides.

Triglycerides in the plasma are carried by lipoproteins (66). An example is the chylomicrons that are secreted form the intestinal wall, and contain the triglyceride entering our system from dietary triglyceride. Another major lipoprotein, referred to as very low density lipoprotein (VLDL), VLDL triglyceride is primarily secreted from the liver. Other lipoproteins are low density lipoprotein (LDL) and high density lipoprotein (HDL). These two lipoproteins carry cholesterol (66). LDL and HDL will not be considered further in this model. The Chylomicro-triglyceride and the VLDL-triglyceride are hydrolysed by lipoprotein lipase (LPL) to non-esterified fatty acids. Lipoprotein lipase

prefers larger particles (66;166), and in comparison to VLDL-triglyceride the Chylomicro-Triglyceride are cleared quickly from plasma. The major contribution to lipoprotein lipase activity is adipose tissue, although lipoprotein lipase also occurs in connection to muscle and liver. Adipose tissue lipoprotein lipase is stimulated by insulin, and in the same time insulin also stimulates re-esterification of lipoproteins in to adipose tissue. However, there is a spillover of non-esterified fatty acids in to plasma.

Another route for non-esterified fatty acids into plasma is from adipose tissue lipolysis. This process is known to be inhibited by insulin and the inhibition is saturated at high insulin levels (40;50;66;150). Adipose tissue also takes up plasma non-esterified fatty acids. Here they are re-esterified to triglyceride and stored, and this process in stimulated by insulin, again the effect of insulin will be saturated at high insulin levels (39;50).

Another fate of plasma fatty acids is to be taken up by different cells for oxidation, primarily muscle cells. Under resting condition this uptake is closely related to plasma non-esterified fatty acid concentration, and with in the muscle cell fatty acids are oxidised in accordance with their rate of uptake (64).

Further more plasma non-esterified fatty acids are taken up by the liver, where they are either re-esterified and released into plasma as VLDL-triglyceride, or go through beta-oxidation to produce ketone bodies, which are important sources for oxidation during starvation. In this model the formation of either VLDL-triglyceride or ketone bodies from hepatic fatty acid uptake is stimulated and inhibited by insulin, respectively. Ketone bodies is either oxidised or eliminated, for example though expiration, both are regulated by the availability of ketone bodies (118).

One of the major connections between the glucose and fat metabolism in this model is obviously insulin. Insulin secretion is regulated by plasma glucose concentration and as mentioned, insulin regulates fat metabolism in several ways, especially by regulating the

direction of flux to the adipose tissue. High insulin stimulates triglyceride storing in adipose tissue while low insulin favours release of fatty acids into the plasma. But glucose and fat metabolism is also connected through oxidation and gluconeogenesis.

In the glucose and fat steady state model, glucose oxidation is the difference between total oxidation and lipid and protein oxidation. Protein oxidation is minimum 7% of total oxidation, however 50% of protein intake in considered to be oxidised in steady state. The other 50% of protein intake is considered to contribute to gluconeogenesis. In the steady state model, gluconeogenesis from glycogen is considered to be proportional to lipid oxidation (5), this will be explained further later in this section, see "2.1.4 Glyconeogenesis". Gluconeogenesis is one of the paths for glucose to enter the system. Besides gluconeogenesis from protein and glycerol, glucose is also produced from lactate; the rate of gluconeogenesis from lactate is regulated by substrate availability

Glucose is removed from plasma and taken up by different cells through glucose transporters. The brain needs a continuous uptake of glucose for oxidation, since it can not take up and utilise fatty acids (64). Glucose is transported into the brain cells by the GLUT3 glucose transporter. The rate of glucose uptake through GLUT3 is saturated for glucose levels within the normal range and and can be described through a Michaelis-Menten function, with a low *Km* (66). The effects from insulin are assumed negligible (95).

The GLUT1 is another insulin independent glucose transporter. Insulin independent glucose transport takes place in muscle cells, adipose tissue, nerve cells and blood cells (51). Again the rate of glucose uptake through the transporter is described through a Michaelis- Menten function. The GLUT1 glucose transporter has a low affinity for glucose (high *Km*) and is not saturated at glucose concentrations within the normal range (66;72).

The last glucose transporter described in the model is the GLUT4 glucose transporter. This transporter is insulin dependent. Insulin increase the glucose transport by GLUT4, by increasing the density of GLUT4 in the membrane of the cells (66). The effect of insulin in thought to be co-operative, with a Hill constant of about 2 (51;82).

Another possibility for removal of glucose from plasma is the kidneys. Plasma glucose can be cleared by the kidneys, however this occur only when the plasma glucose concentration is elevated with respect to the normal level, for example in diabetes.

The metabolite lactate is included in the steady state model. There is a small production of lactate from the liver, but lactate is mainly produced in muscle and fat cells. In the glucose and fat steady state model the majority of lactate is produced from excess glucose. Excess glucose is defined as the glucose taken up from plasma which is not utilised through glucose oxidation. Through gluconeogenesis, in the liver, lactate is used to produce glucose, which is then released back into plasma, completing the glucose-lactate futile cycle (the cori cycle). Despite its name, this cycle clearly plays an important role by allowing a continuous redistribution of glucose among the various cells and organs.

Another possibility for excess glucose in the cells is de novo lipogenesis (fat synthesis). The distribution of surplus glucose between lactate production and de novo lipogenesis is determined by the lactate concentration. De novo lipogenesis is considered to occur in the liver, in adipose tissue, and to some extent in muscle cells.

The model was named glucose fat steady state model, but in reality it operates with a quasi steady state, at least when there is an energy imbalance, when dietary calorie intake exceeds or is lower than total energy expenditure. In quasi steady state the insulin level, the metabolite levels and the fluxes between metabolites are constant except for adipose tissue content. This means that in quasi steady state there can be a net gain or loss of fat tissue.

2.1.1 Glycogen

The steady state model is based on the assumption, that over a day there is no net build up or break down of glycogen. The body glycogen stores is fairly limited, muscle and hepatic glycogen constitutes about 1% of the body's total energy storages, corresponding to about 1500-2000 kcal which is less that a days worth of energy (66). Hence, a longer lasting excess or shortage of glucose can not be dealt with through the glycogen storages.

2.1.2 Glucose Oxidation

As mentioned above, oxidation is one of the major areas of interplay between the glucose and fat metabolism. In the glucose fat steady state model the rate of glucose oxidation is determined by the total need for energy (total energy expenditure), and the rate of non-esterified fatty acid oxidation, ketone body oxidation, and protein oxidation. Both fatty acid oxidation and ketone oxidation is regulated by the availability of substrates (64;118). However the availability of both fatty acids and ketones is indirectly regulated by insulin.

2.1.3 The Cori Cycle and De novo Lipogenesis

A continuous excess of glucose, for example through a high level of carbohydrate in the diet, is in the steady state model primarily dealt with by formation of lactate. Glyconeogenesis from lactate, the cori cycle, is important in the regulation between glucose and fat metabolism in the steady state model. When the glucose uptake into the cells, is higher than the need for glucose oxidation, the excess glucose can escape the cells through the cori cycle. All cells can produce lactate through glycolysis and, contrary to glucose lactate can be transported out of the cells. Lactate can be taken up by the liver, where it is regenerated as glucose and again released into the systemic circulation. In a situation of excess energy, the glucose-lactate cycle increases the flow of glucose in the system and there by also insulin production. In situations of energy fatigue the cori cycle makes the possible for the body to utilise the energy stored as muscle glycogen, in other parts of the body. During fatigue the cori cycle can also have an important function in maintaining the plasma glucose level. Even though the cori cycle does not contribute to

any net glucose production, it makes sure that the glucose taken up by muscle and adipose tissue despite the relative low glucose and insulin levels are redirected back into plasma. Hyperlactaemia is defined for a lactate concentration between 2 mM and 5 mM, and severe lactic acidosis (metabolic acidoses) is said to occur when the lactate concentration exceeds 5 mM. So, when excess glucose is too high to be dealt with through the glucose-lactate cycle, the secondary choice is production of fat, de novo lipogenesis. In the steady state model, the lactate concentration regulated the production of fat through lipogenesis. The activity of de novo lipogenesis is strongly dependent of the pyruvate and lactate concentrations (120).

2.1.4 Glyconeogenesis

One of the areas where the glucose and fat steady state model has been modified is glyconeogenesis. Gluconeogenesis from lactate is described in the section above, the cori cycle. Gluconeogenesis from glycerol is also an important source of glucose, especially during fasting or starvation. Glycerol is released when triglycerides are hydrolysed to yield 3 fatty acids and one glycerol. This means the glycerol release in proportional to the rate of adipose tissue lipolysis and lipoprotein lipase, all is made in to glucose. However when fatty acids are re-esterified, the glycerol needed is produced from glucose. Therefore the net contribution of glycerol to glyconeogenesis in steady state is considered to be proportional to the rates of fat oxidation and ketone body formation, which are end roads for fatty acids. Gluconeogenesis from amino acids and glycerol are slower than the rate of gluconeogenesis from lactate (84). The rates depend on the concentration of the precursors, and half-maximal rates are observed at concentrations that exceed the usual plasma concentrations (84), which means the rates are not saturated. The model production of glucose from amino acids is considered to be 50% of dietary protein intake, the other 50% are considered to be oxidised.

2.1.5 Glucose and Fat Steady State Model Equations

The differential equation representing the change in concentration of the eight metabolites (including insulin) described in the steady state model, and the related fluxes between metabolites are shown below. All glucose fluxes (including to and from lactate) are in mmol glucose/min, one mmol glucose yield two mmol lactate. All lipid fluxes are in µmol NEFA/min, including ketone bodies. It takes three µmol NEFA to yield one µmol triglyceride, while one µmol NEFA yields 4 µmol ketone bodies. All state variables are presented at concentrations. This means that the net change in flux is divided by the relevant distribution volume (V). For plasma triglyceride and NEFA the distribution volume (V_P) is 3 litre (13). For Ketone bodies the distribution volume is higher (V_{KB}) 14 litre (118). The distribution volume for insulin (V_I) is also 14 litre (78). For lactate and glucose it is even higher (V_L and V_G) 17 litre (78).

Plasma chylomicron triglyceride:

$$\frac{dTG_C}{dt} = \frac{1}{V_P} \cdot \left(\tfrac{1}{3} \cdot LMeal - \tfrac{1}{3} \cdot LPL_C \right)$$

eq. 1

Plama VLDL triglyceride

$$\frac{dTG_{VLDL}}{dt} = \frac{1}{V_P} \left(\tfrac{1}{3} \cdot HFD \cdot HFU - \tfrac{1}{3} \cdot LPL_{VLDL} \right)$$

eq. 2

Plasma non-esterified fatty acids

$$\frac{dNEFA}{dt} = \frac{1}{V_P} \left(LPLsp \cdot \left(LPL_C + LPL_{VLDL} \right) + ATL - ATR - HFU - FOX \right)$$

eq. 3

Adipose tissue

$$\frac{dAT}{dt} = (1 - LPLsp) \cdot \left(\tfrac{1}{3} \cdot LPL_C + \tfrac{1}{3} \cdot LPL_{VLDL}\right) + \tfrac{1}{3} \cdot ATL - \tfrac{1}{3} \cdot ATR + DNL$$

eq. 4

Plasma ketone bodies

$$\frac{dKB}{dt} = \frac{1}{V_{KB}} \cdot \left(4 \cdot (1 - HFD) \cdot HFU - 4 \cdot KBOX - 4 \cdot KBcl\right)$$

eq. 5

Plasma glucose

$$\frac{dG}{dt} = \frac{1}{V_G} \cdot \left(GMeal + GNG_G + GNG_L + GNG_P - GLUT1 - GLUT3 - GLUT4 - Rcl - HGU\right)$$

eq. 6

Plasma lactate

$$\frac{dL}{dt} = \frac{1}{V_L} \cdot \left(2 \cdot HGU + 2 \cdot LP - 2 \cdot GNGl\right)$$

eq. 7

Plasma insulin

$$\frac{dI}{dt} = \frac{1}{V_I}\left(SC_I - CL_I\right)$$

eq. 8

Lipoprotein lipase rates:

$$LPL_C = \frac{V_{LPL} \cdot (\varepsilon \cdot [TG_C])}{K_{LPL,TG} + \varepsilon \cdot [TG_C] + [TG_{VLDL}]} \cdot \frac{[I] + K_I}{K_{LPL,I} + [I]}$$

eq. 9

$$LPL_{VLDL} = \frac{V_{LPL} \cdot [TG_{VLDL}]}{K_{LPL,TG} + \varepsilon \cdot [TG_C] + [TG_{VLDL}]} \cdot \frac{[I] + K_I}{K_{LPL,I} + [I]}$$

eq. 10

Regulation of lipoprotein lipase spillover into plasma:

$$LPL_{sp} = \frac{1}{1 + \exp\left(a_{SP} \cdot \left([I]\right) - K_{sp}\right)}$$

eq. 11

Adipose tissue lipase rate:

$$ATL = \frac{V_{ATL} \cdot K_{ATL}}{K_{ATL} + [I]} + B_{ATL}$$

eq. 12

Adipose tissue re-esterification rate:

$$ATR = \frac{V_{ATR} \cdot [NEFA]}{K_{ATR}} \cdot \frac{[I]}{K_{ATR,I} + [I]}$$

eq. 13

Fatty acid oxidation rate:

$$FOX = \frac{V_{FOX} \cdot EE \cdot [NEFA]}{K_{FAOX} + [NEFA]}$$

eq. 14

Ketone body oxidation rate:

$$KBOX = \frac{V_{KBOX} \cdot [KB]}{K_{KBOX} + [KB]}$$

eq. 15

Hepatic fatty acid uptake rate:

$$HFU = \frac{V_{HFU} \cdot [HFU]}{K_{HFU} + [HFU]}$$

eq. 16

Insulin stimulation of hepatic re-esterification and VLDL secretion rate:

$$HFD = \frac{[I]}{K_{HFD} + [I]}$$

eq. 17

Ketone body clearance:

$$KBcl = R_{KBcl} \cdot [KB]$$

eq. 18

Rate of glyconeogenesis from glycerol:

$$GNG_G = \mathrm{C_G} \cdot (FOX + (1 - HFD) \cdot HFU)$$

eq. 19

Rate of glucose transport through GLUT1:

$$GLUT1 = \frac{V_{GLUT1} \cdot [G]}{K_{GLUT1} + [G]}$$

eq. 20

Rate of glucose transport through GLUT3:

$$GLUT3 = \frac{V_{GLUT3} \cdot [G]}{K_{GLUT3} + [G]}$$

eq. 21

Rate of glucose transport through GLUT4:

$$GLUT4 = \frac{V_{GLUT1} \cdot [G]}{K_{GLUT1} + [G]} \cdot \frac{[I]^{\alpha}}{K_{GLUT4,I}{}^{\alpha} + [I]^{\alpha}}$$

eq. 22

Renal clearance of glucose:

$$Rcl = \frac{V_R \cdot (G_1 - [G]) \cdot b_1}{\exp((G_1 - [G]) \cdot b_1) - 1}$$

eq. 23

Rate of glucose oxidation:

$$GOX = EE - FOX - KBOX - POX$$

eq. 24

Rate of gluconeogenesis from lactate:

$$GNG_L = \frac{V_{GNG,L} \cdot [L]}{K_{GNG,L} + [L]}$$

eq. 25

Hepatic lactate production rate:

$$HGU = \frac{K_{HGU}}{K_{HGU} + [L]}$$

eq. 26

Rate of lactate production:

$$LP = \left(1 - \frac{[L]^{\beta}}{{K_{DNL}}^{\beta} + [L]^{\beta}}\right) \cdot (GLUT1 + GLUT3 + GLUT4 - GOX)$$

eq. 27

Rate of de novo lipogenesis:

$$DNL = \frac{[L]^{\beta}}{{K_{DNL}}^{\beta} + [L]^{\beta}} \cdot (GLUT1 + GLUT3 + GLUT4 - GOX)$$

eq. 28

Insulin secretion rate:

$$SC_I = \frac{V_{SC} \cdot [G]^{\gamma}}{{K_{SC}}^{\gamma} + [G]^{\gamma}}$$

eq. 29

Insulin clearance rate:

$$CL_I = \frac{V_{CL1} \cdot [I]}{K_{CL1} + [I]} + \frac{V_{CL2} \cdot [I]}{K_{CL2} + [I]} + k3 \cdot [I]$$

eq. 30

Table 1: Glucose Fat Steady State Model Parameters

V_P	3	L	Estimated from (13)
V_{KB}	14	L	Estimated from (118)
V_G	17	L	(78)
V_L	17	L	
V_I	14	L	(78)
V_{LPL}	1750	µmol/min	*Estimated from (3;35;56;96)
$K_{LPL,TG}$	200	µM	(22;33).
ε	10		
$K_{LPL,I}$	200	pM	(35;55;65)
I_0	30	pM	
a_{SP}	0.02	pM^{-1}	Estimated from (38)
K_{SP}	200	pM	Estimated from (38)
V_{ATL}	50	µmol/kg fat/min	*Estimated from (25;26;35;165)
K_{ATL}	50	µM	(17;25;26;40;150)
B_{ATL}	10	µmol/kg fat/min	(25;26)
V_{RST}	150	µmol/kg fat/min	*Estimated from (25;164)
$K_{RST,FA}$	1500	µM	(104)
$K_{RST,I}$	200	pM	Estimated from (74)
V_{FOX}	370	µmol /kcal	*Estimated from (2;11;113;159)
K_{FOX}	478	µM	*Estimated from (2;11;113;159)
V_{HFU}	600	µmol /min	*Estimated from (80)
K_{HFU}	1500	µM	(80)
K_{HFD}	25	pM	Estimated from (111)
V_{KBOX}	200	µmol /min	(118)
K_{KBOX}	1000	µM	(118)
R_{KBcl}	0.15	L/min	
C_G	0.0005	mmol glucose/ µmol glycerol	
V_{GLUT1}	1.2	mmol/min	(78)
K_{GLUT1}	10	mM	(72)
V_{GLUT3}	0.6	mmol/min	*Estimated from (66)
K_{GLUT3}	1.6	mM	(66)
V_{GLUT4}	7.1	mmol/min	*Estimated from (82)
K_{GLUT4}	5	mM	(66)
$K_{GLUT4,I}$	180	pM	*Estimated from (82)
α	2		*Estimated from (51;82)
$V_{GNG,L}$	2	mmol/min	*Estimated from (84)
$K_{GNG,L}$	0.5	mM	*Estimated from (66;84)
V_{HGU}	1	mmol/min	*Estimated from (84)
K_{HGU}	0.5	mM	*Estimated from (66;84)
β	4		

K_{DNL}	2	mM	*Estimated from (66;84)
V_{SC}	2000	pmol/min	(78)
K_{SC}	7.4	mM	(78)
γ	6.4		(78)
V_{CL1}	1400	pmol/min	(78)
K_{CL1}	2000	pM	(78)
V_{CL2}	2750	pmol/min	(78)
K_{CL2}	5000	pM	(78)
k3	0.18	L/min	(78)

* The estimation is based on the assumption about the mathematical relationship made here when describing the flux.

Total energy expenditure EE, and total fat mass is set for each simulation.

2.2 GLUCOSE FAT STEADY STATE MODEL SIMULATIONS

As mentioned the glucose and fat steady state model in used to simulate a hypothetical situations where the daily variations in metabolites and hormones (insulin) and the fluxes between metabolites are averaged out. Therefore it is difficult to validate the model. In an attempt to validate the model it is used to simulate a study of massive carbohydrate overfeeding. The study and the model simulation of massive carbohydrate overfeeding are described in the following section "Massive Carbohydrate Overfeeding". In the section "Simulation of Hyperinsulinaemic Glucose Clamp" the glucose and fat steady state model is used to simulate hyperinsulinemic glucose clamp studies. The setup of glucose clamp studies is very similar to the setup of the steady state model. In a glucose clamp study insulin and glucose concentrations are kept constant, through infusion of insulin and/ or glucose. Often, the body's own production of insulin is set out of function through infusion of the drug somatostatin. These simulations are done to show the complexity of the regulation of glucose metabolism and the importance in considering glucose utilisation and not only glucose uptake into the cell. And further more the importance in taking the nutritional condition of the person into account, when evaluation results of glucose clamp studies. To further illustrate the importance of including the glucose utilisation in the cells when describing the glucose metabolism, a simple model of hexokinase was made. The model shows how intercellular glucose inhibits glucose uptake, if glucose utilisation within the cells is not stimulated simultaneous to stimulation of glucose transport. The mechanism of the regulation of glucose uptake by intercellular glucose is not described in the glucose and fat steady state model.

2.2.1 Massive Carbohydrate Overfeeding

The model is used to simulate situations of underfeeding (negative energy balance) and of massive carbohydrate overfeeding in humans (positive energy balance). In a study by Acheson et al (1988), healthy subjects first underwent three days on a low calorie diet, consisting of 1600 kcal per day, which is composted of 15% protein, fat and carbohydrate.

After three days of low calorie diet, glycogen stores are considered depleted. Therefore the subjects will be considered to be in a "steady state", which is attempted to simulate using the glucose and fat steady state model. After the 3 days on a low calorie diet, the subjects are massively overfeed with carbohydrates for 10 days. During the 10 days the diet consists of an energy surplus of 1500 kcal/day, relative to the energy requirements of the subjects. The diet is composed of 11% protein, 3% fat and 86% carbohydrate. At day 10 of the high kcal high carbohydrate diet the glycogen stores are considered to be replenished, and again the subjects can be considered to be in a "steady state (1). This situation is simulated with the glucose fat steady state model. The simulations of the two situations are used to see if the model is able to replicate the utilization of the food intake during negative and positive energy balance.

One of the values used to evaluate energy expenditure and nutrition oxidation is the non-protein respiratory coefficient (npRQ). The npRQ are calculated as follows:

$$\mathrm{npRQ} = \frac{V_{O2}}{V_{CO2}} = \frac{0.746 \cdot c_0 + 2.03 \cdot f_0 + 0.028 \cdot c_f}{0.746 \cdot c_0 + 1.43 \cdot f_0 + 0.239 \cdot c_f}$$

eq. 31

Where c_0 is the rate of carbohydrate oxidation in g glucose/min, f_0 is the rate of fat oxidation in g fat/min and c_f in the rate of de novo lipogenesis in g glucose/min (62).

In figure 3 results of simulation of low calorie high fat diet and high calorie, high carbohydrate diet are shown. Model input are dietary protein, fat and glucose intake and total energy expenditure in the two situations. These values for total energy expenditure and dietary intake are found in the Acheson, *et al* (1988) study described above. The figure shows the experimental found values for energy expenditure and the contribution of glucose, fat and protein to total energy expenditure, non protein RQ, total carbohydrate

utilization which includes carbohydrate oxidation and de novo lipogenesis, and total carbohydrate intake. These value are compared the corresponding simulated values.

For the low calorie, high fat diet the model seems to underestimate fat. Instead the model predicts a considerable ketone body oxidation, which is probably included in the experimental fat oxidation. For the low calorie, high fat diet the model predicts protein oxidation fairly well, but overestimates protein oxidation in the high calorie, high carb diet. The model can only include protein metabolism in a very simplified way, where it is assumed that all protein provided to the metabolism through meals are utilized, so when there is a net storage of protein, as found experimentally for the high kcal, high carb diet, the model will not be able to capture this. For the simulation shown in figure 3 the model was modified a bit, so the protein provided through the meal is considered fully oxidised instead contributing to glucose production through glyconeogenesis, with 50% of protein

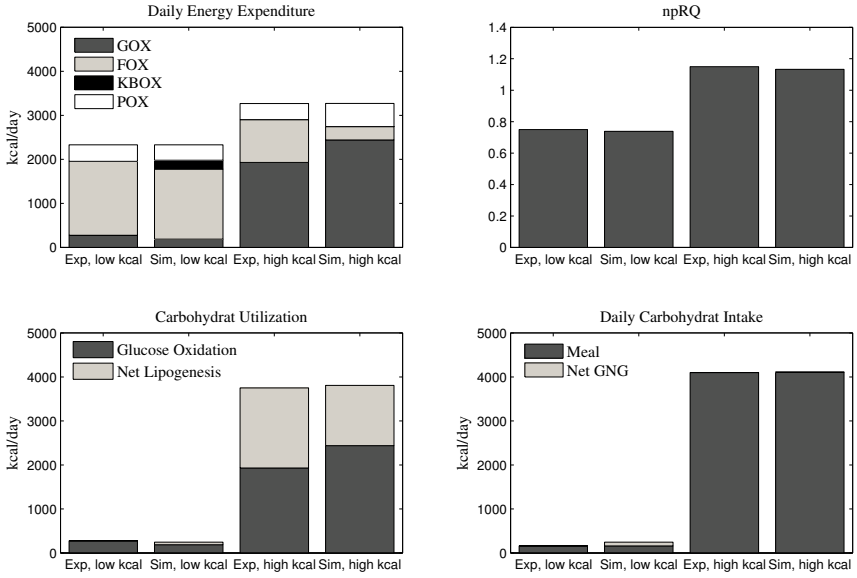

Figure 3: Glucose-Fat Steady State Model Simulation of Acheson, *et al* (1988) study with low kcal - high fat diet and high kcal - high carbohydrate diet. The steady state simulation fluxes (Sim, low kcal and Sim, high kcal) are compared to the fluxes found in the study after three day of low kcal high fat diet (Exp, low kcal) and after 7 days of high kcal high carbohydrate diet (day 10 of study) (Exp, high kcal), respectively. GNG from protein is set to zero instead all protein provided though the meals is oxidised.

provided through meals. This is done since, gluconeogenesis from protein will experimentally be considered as protein oxidation, which is measured by the amount of nitrogen in the urine. Simulated non-protein RQ corresponds to the non-protein RQ found in the study, and both simulation and study finds that the rate of de novo lipogenesis is zero.

For the high calorie, high carbohydrate diet the model again under estimate fatty acid oxidation while overestimating protein oxidation and glucose oxidation is. As for protein oxidation, the simple form in which protein in included in the model does not allow for protein storages therefore all protein provided through meals are oxidised. Compared to the study the model underestimates non-protein RQ a bit, which can be ascribed to the overestimation of glucose oxidation and underestimation of net de novo lipogenesis, see figure 3 in the bottom left corner.

2.2.2 Simulation of Hyperinsulinaemic Glucose Clamp

The glucose and fat steady state model is used to simulate situations compatible with hyperinsulinaemic glucose clamp. The set up of a clamp study is a situation that is close to that of the steady state model. During a glucose clamp, insulin and glucose concentrations are kept at a constant level, through invervenous infusions of insulin and/ or glucose. Figure 4 shows the glucose infusion rate during an 8 hour hyperinsulinemic hyperglycaemic clamp study, where glucose was kept with in 20-22 mM and insulin concentration was 12000 pM. The study involved two male healthy subjects (76). The figure shows how the glucose infusion rate (GIR) decreases with in the duration of the study; this decrease is considered to by due to the limitation of glycogen storages capacity. The glucose and fat steady state model stimulation of hyperinsulinemic glucose clamp will find GIR in a situation where there are no glycogen storages. The glucose and fat steady state model predicts a GIR of 4.7 mmol/min which corresponds to around 70 µmol/kg/min, for at 70 kg person, with plasma glucose concentration of 22 mM and insulin concentration of 12000 pM (total energy expenditure was set to 1.66 kcal/min).

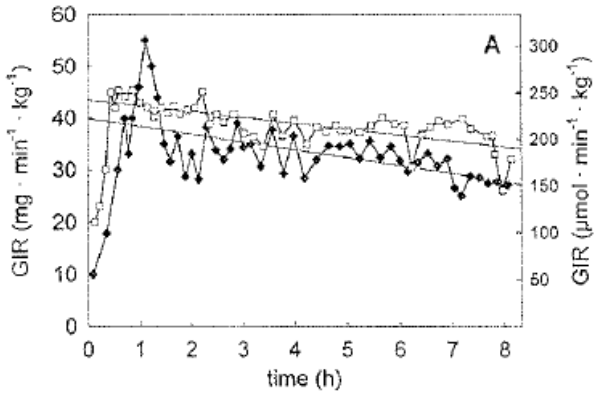

Figure 4: Figure tatken from Hansen, B.F, *et al* (1999). Glucose infusion rate (GIR) during an 8 hour hyperinsulinaemic hyperglycaemic clamp study, ♦ subject 1 and ○ subject 2. Glucose concentration 20-22 mM insulin concentration of 12000 pM (76).

The steady state rate of glucose infusion needed to keep glucose concentration constant is found as follows:

$$GIR = Glucose\ uptake + Renal\ clearence - Gluconeogenesis$$

For the simulation model insulin secretion and elimination is set to zero. The GIR found in the simulation is about 4 fold lower than the initially experimental GIR and about 2.5 fold lower than the experimental determined GIR after 8 hours with hyperinsulinemic hyperglycaemic glucose clamp (76).

Figure 5 shows a model simulation of a hyperinsulinemic euglycemic clamp. The steady state GIR, is found for a glucose concentration of 4.8 mM and a variety of insulin concentration from 50 pM to 1000 pM. The glucose infusion rate needed to keep glucose constant at 4.8 mM increases with insulin, but saturates at an insulin concentration around 600 pM, at a rate just below 3 mmol/min. The fate of a majority of the glucose is oxidation, however from an insulin concentration around 150 pM the model predicts lipogenesis to occur. The rate of glucose oxidation and lipogenesis increases with insulin,

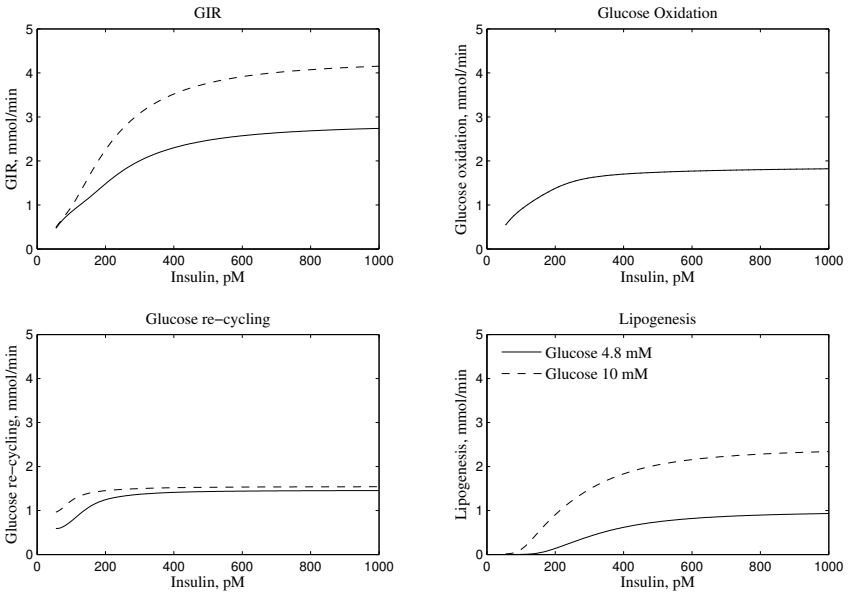

Figure 5: Glucose and fat steady state model simulation of hyperglycaemic glucose clamp in steady state. Insulin in varied from 50 pM to 1000 pM, glucose kept constant at 4.8 mM and 10 mM

but as with GIR the rates saturate for high insulin levels. An experimental hyperinsulinemic euglycemic clamp study with glucose 4.8 mM and insulin 360 pM, finds GIR to be around 3.9 mmol/min and glucose oxidation to be 1.36 mmol/min (147). The glucose and fat steady state model GIR is about 2.2 mmol/min and glucose oxidation 1.6 mmol/min, for the same glucose and insulin concentrations (model total energy expenditure was 1.66 kcal/min). The difference between the experimentally found GIR and the model simulated GIR (1.7 mmol/min) could be due to glycogen stores, which (as mentioned) are not included in the steady state model.

Alterations in insulin's regulation of lipid metabolism can influence the results of glucose clamp studies, see figure 6. The model regulation of adipose tissue lipase and re-esterification by insulin was altered by a two fold increase in the Km values for inhibition

by insulin of lipase and its stimulation on re-esterification. For lower insulin concentrations this resulted in a decrease in GIR, due to decrease in glucose oxidation, and failure of insulin to suppress plasma non-esterified fatty acid concentration. The simulation show the lower than expected GIR is not necessarily a result of decreased insulin effect on glucose metabolism, but can also be explained by decreased inhibition of net adipose tissue release of fatty acids to plasma by insulin.

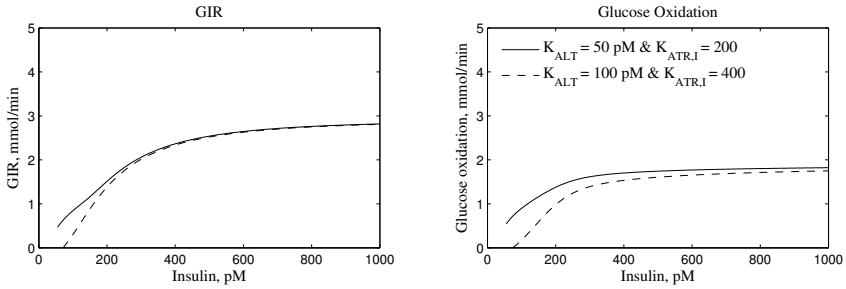

Figure 6: Simulation of hyperinsulinimic glucose clamp study with alteration in insulin's regulation of lipid metabolism, glucose is kept constant at 5 mM and steady state is found for insulin concentration varied between 50 and 1000 pM.

2.3 A SMALL MODEL OF HEXOKINASE

To further illustrate the importance of considering the utilisation of glucose when looking at glucose metabolism a small model of hexokinase is constructed, for schematic presentation see figure 7. Hexokinase is the enzyme that phosphorylates glucose to glucose 6-phosphate in the muscle and fat cells. Hexokinase is inhibited by its product, glucose 6-phosphate. The model will illustrate how important it is not only to consider stimulation of glucose uptake into the cells but also to stimulate the utilisation of glucose with the cells. The rate of hexokinase is described by a Michaelis-Menten function with so-called mixed inhibition (155), see eq. 35. The rate of glucose uptake into the cell is also described by at Michaelis-Menten function, it is in general believed that the GLUT transporter are symmetric (93), see eq. 34. The rate of removal of glucose 6-phosphate is for simplicity considered to be proportional to the glucose 6-phosphate concentration eq. 36. The parameters A and B represent the relative maximal velocity of glucose transport

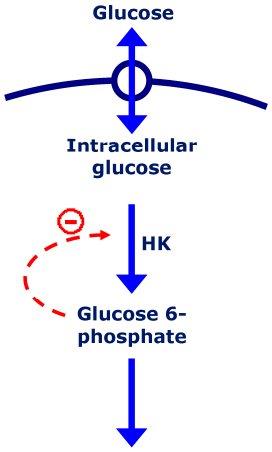

Figure 7: Schematic presentation of hexokinase model. The red line illustrates the product inhibition of hexokinase by glucose 6-phosphate.

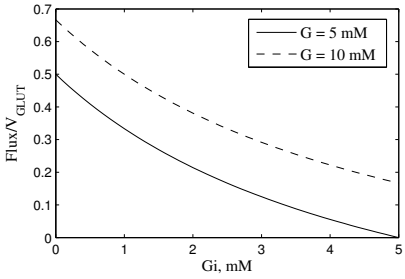

Figure 8: The relative flux through the glucose transporter for increasing intercellular glucose.

and glucose 6-phosphate utilisation to maximal hexokinase rate, respectively. When A increases is represent a stimulation of glucose transport for example by insulin, and when B increase it represent a stimulation of glucose 6-phosphate utilisation.

2.3.1 Simple Hexokinase Model Equations

$$\frac{dGi}{dt} = \frac{1}{V}(GLUT - HK)$$

eq. 32

$$\frac{dG6P}{dt} = \frac{1}{V}(HK - GU)$$

eq. 33

$$GLUT = A \cdot \left(\frac{G}{K_G + G} - \frac{Gi}{K_G + Gi} \right)$$

eq. 34

$$HK = \frac{Gi}{\left(1 + G6P / K_{G6P}\right) \cdot K_{HK} + \left(1 + G6P / K_{G6P}{}^{*}\right) \cdot Gi}$$

eq. 35

$$GU = B * G6P$$

eq. 36

The model consists of two differential equations, one representing intercellular glucose (Gi), and one intercellular glucose 6-phophate (G6P). G stands for plasma glucose concentration, GLUT is the rate of transport into the cell, HK is the rate of hexokinase and GU is the rate of glucose 6-phoshate utilisation. Parameter values are shown in table 2, for graphical illustration see figure 7.

Table 2: Parameter values for hexokinase model

K_G	5	mM	Estimated from (66)
K_{HK}	0.188	mM	(155)
K_{G6P}	0.068	mM	(155)
K_{G6P}*	0.022	mM	(155)

2.3.2 Simulation with the Simple Hexokinase Model

If only glucose uptake into the cell is stimulated with out stimulating the rate of glucose utilisation within the cell there will be an accumulation of glucose 6-phosphate which inhibits hexokinase and thereby also an accumulation of intercellular glucose. This is illustrated in figure 9. The effect of increasing intercellular glucose is an inhibition of the glucose transport into the cell, see figure 8. When the utilisation of glucose 6-phosphate is also stimulated, the accumulation of metabolites does not happen, and the glucose uptake increases with increases stimulation (increasing A). The relative flux is shown in figure 9 in the top right corner.

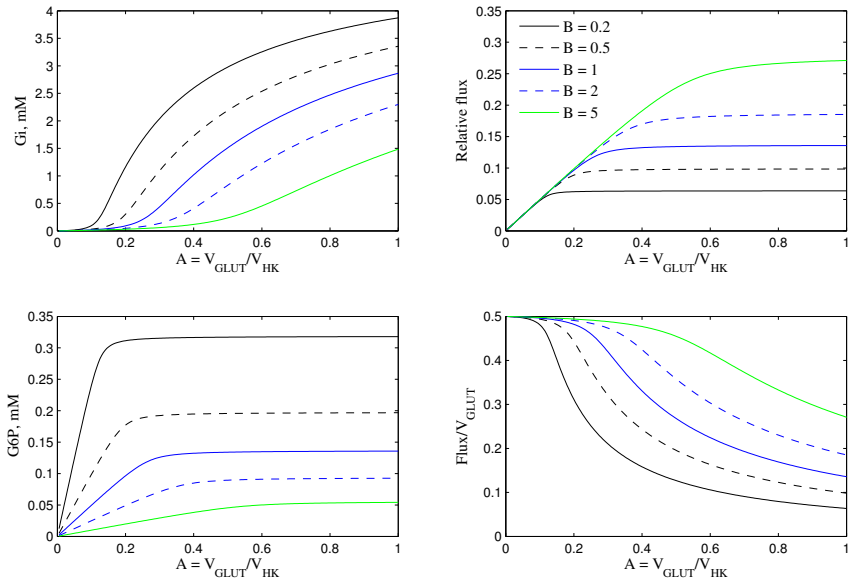

Figure 9: The two left plots show the relation between intercellular glucose (in the top) and glucose 6-phosphate (in the bottom) and the parameter A for different values of the parameter B. The two right plots shows the inhibition of glucose uptake as a function of the parameter A for different values of B.

2.4 DISCUSSION OF GLUCOSE FAT STEADY STATE MODEL

The glucose fat steady state model describes a hypothetical situation where all metabolic fluxes and metabolite concentrations are averaged over the day. The model does not represent dynamical changes in metabolites over the day, but relations between fluxes and metabolites for different nutritional situations. The model was sought validated through simulation of an underfeeding study and an overfeeding study. In the simulation of the underfeeding study (negative energy balance) the model result resembled those observed experimentally. The results of the overfeeding simulation were not similar good. Glucose oxidation was overestimated and the rate of fatty acid oxidation and lipogenesis was underestimated.

Although the model predicts the utilization of the metabolites at least during the underfeeding simulation fairly well, it is difficult to say whether the metabolite concentration corresponds to the physiological averages. However the saturating rates of Michaelis-Menten functions, by which most of the metabolic fluxes are described, will in general overestimate the average metabolic fluxes.

The simulation of hyperinsulinemic glucose clamp shows how important it is to consider the not only the uptake of glucose into the cells as being regulated by insulin, but also the possible routs of glucose utilisation and there regulation. Especially the first example with the hyperinsulinemic hyperglycemic clamp shows, how decreased GIR might not be a symptom of insulin resistance but merely a result of the nutritional state of the metabolism. For example the difference between having depleted glycogen depots or only having partly depleted glycogen stores.

To further illustrate that it is not enough to consider the transport of glucose into the cells but also the utilisation of glucose within the cells, a simple model of hexokinase was made. The hexokinase model captures an effect which is not described in the glucose fat steady state model. The concentration of glucose inside the cells will inhibit the rate of

glucose uptake into the cells. The model shows how an accumulation of intercellular glucose occur if utilisation of glucose 6-phosphate in the cell is not stimulated when glucose uptake is stimulated. The result of this is decreased glucose uptake. If decreased glucose uptake is observed in relation insulin concentration, it is considered to be due to insulin resistance, which might by the case. But it is not necessarily the stimulation of the insulin dependent glucose transporter that is responsible for the observed insulin resistance. In could for example by related the level of glycogen in the cells, if glycogen storage is close to its maximal capacity it could influence the rate of glycogen synthesis a path for glucose utilisation within the cells. The next section will focus more on the mechanisms of glycogen formation and breakdown. Another possibility for decreased glucose utilisation could be changes in the fat metabolism. In the simulation of hyperinsulinemic glucose clamp, alterations were made in insulin's ability to suppress adipose tissue lipase and stimulate adipose tissue re-estrification. The results show decreased glucose oxidation for lower insulin concentration compared to the normal regulation capacity of insulin.

3 HEPATIC GLUCOSE METABOLISM

As mentioned in the section "The Interplay between Glucose and Fat" a route of glucose utilisation is to be stored as glycogen, and this happens in part in the liver. After a meal, nutritions that enter the body form the intestine, reach the liver first. The liver acts as a buffer, taking up glucose when concentration outside is high and releasing glucose when it is required elsewhere in the body. During fasting most of the body's energy requirements are meet by fatty acids oxidation and to some extent also protein oxidation. However a portion of the energy requirement, about 20% (66) comes from glucose oxidation, and during fasting the liver releases glucose in to circulation to prevent hypoglycaemia. After an overnight fast, the hepatic glucose output is about 10 µmol/kg/min (161), where about 50% comes from gluconeogenesis and 50% from glucogenolysis (161). In the postabsorptive fase (often refered to as basal state) plasma glucose concentrations are about 5 mM and plasma insulin about 40 pM (66).

In this section a physiological model of hepatic glucose metabolism will be described. Earlier attempts to construct a physiological model of hepatic glucose metabolism have been made Bergman et al. (8;52). This earlier model was validated by simulating the

Table 3: Metabolite concentrations and fluxes from simulation of overnight fast hepatic glucose metabolism with Bergman model (8;52) – gluconeogenesis rate 0.1 µmol/g liver/min, compared to measured values

Overnight fast	Bergman model (52)	Measured values for human liver	
Glucose 6-phosphate	0.13 mM	0.2 - 0.4 mM	(54)
UDP-glucose	0.35 mM	0.43 - 0.82 mM	(54)
Hepatic glucose output	0.31 µmol/g liver/min	0.46 - 0.53 µmol/g liver/min	(45;81;161)
Glycogen synthesis	0.58 µmol/g liver/min	0 - 0.12 µmol/g liver/min	(81;122)
Glycogenolysis	0.79 µmol/g liver/min	0.5 - 0.25 µmol/g liver/min	(81;122)

overnight fasting state and comparing intracellular metabolite concentrations with measured concentration. For the simulation, a fasting glucose concentration of 5.55 mM, hepatic glycogen content of 242 µmol/g liver and a gluconeogenesis rate of 0.1 µmol/g liver/min, were used. However the simulated rates of hepatic glucose output, glycogen

synthesis and glycogenolysis do not fit with measured rates for healthy humans, see table 3. The rate of net hepatic glucose output is close to the measured rate, especially taking into account that the gluconeogenesis rate is only 0.1 μmol/g liver/min. In the healthy human it is considered to be around 0.23 μmol/g liver/min after an overnight fast (161). However, the simulated rates of glycogen synthesis and glycogenolysis are several times higher than the measured rates. The Bergman model was used to investigate mechanisms involved in the regulation of hepatic glucose metabolism in response to increased glucose and insulin concentrations.

The model of hepatic glucose metabolism described here will take regulatory effect of glucose on hepatic glycogen synthesis and breakdown into account and incorporate them in the model. The model is used to investigate mechanisms relevant for the regulation of hepatic glucose metabolism by glucose and glycogen.

3.1 HEPATIC GLUCOSE METABOLISM MODEL

The mechanistic model of hepatic glucose metabolism is presented in figure 10. Glucose enters the liver primarily through the glucose transporter GLUT2. GLUT2 has a high half maximum velocity concentration (*Km*) and a high maximal rate which allows glucose to "equilibrate" across the membrane (66). The GLUT2 transporter is not responsive to

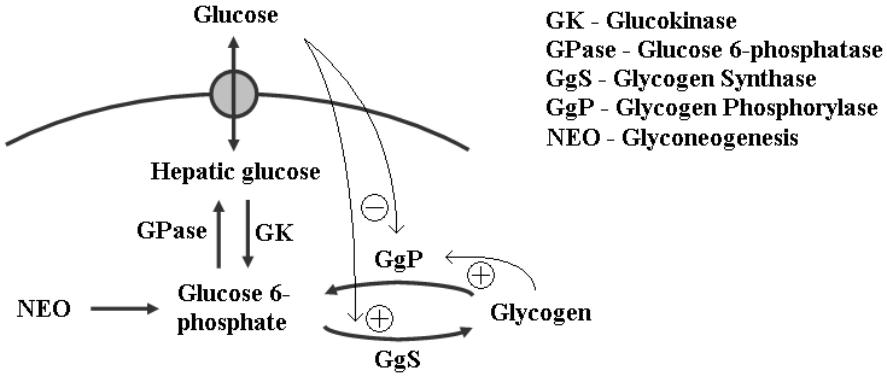

Figure 10: Schematic presentation of hepatic glucose metabolism. The thick lines represent fluxes and the thin lines represent regulation of flux by metabolite (+ stimulation, - inhibition).

insulin (66). The low affinity towards glucose and the high capacity for GLUT2, results in glucose concentration in the liver is very close to glucose concentration outside. Inside the liver cell glucose is phosphorylated by glucokinase to glucose 6-phosphate. In the liver, contrary to other tissues, glucose 6-phosphate can be dephosphorylated back to glucose though glucose 6-phosphatase. The pathway of glycogen synthesis and breakdown goes through glucose 1-phosphate. Glucose 6-phosphate and glucose 1-phosphate are assumed to be in rapid equilibrium, due to the high activity of phosphoglucomutase in the liver (149), and will be considered to equilibrate instantly. Therefore, the liver glucose 1-phosphate will not be included in the model. Total liver volume is found to be around 1.5 l (32;135). Liver mass is considered to be 1500 g (61;66;135).

3.1.1 Glucokinase

Glucose entering the liver cell is phosphorylated to glucose 6-phsophate in order to be utilized in the liver cells (as for any other cell); in the liver cell it is the enzyme glucokinase that catalyzes the glucose phosphorylation. The rate of gucokinase (or hexokinase D) in relation to glucose concentration follows a sigmoid curve (42;105;124;160). Glucokinase differs kinetically form the other hexokinases by virtue of its cooperative glucose dependence (42;105;124;160), low affinity for glucose *Km* 7-8 mM (105;124) and lack of product inhibition by glucose 6-phosphate (42;105;124). These kinetic properties allow glucokinase to respond quickly to changes in glucose concentrations under physiological conditions.

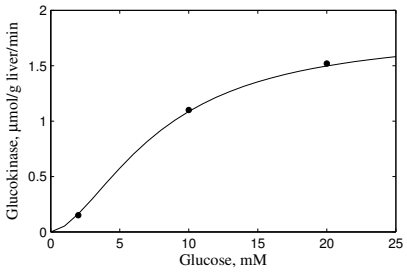

- Youn, J.H., J.Biol.Chem., 264: 168−172, 1989

Figure 11: Rate of Glucokinase in the liver as a function of glucose concentration (line). The dots are data points of hepatic glucose phosphorylation vs glucose concentration in fasted rats (167).

The glucose concentration for half maximal velocity, *Km*, equals 7.8 mM (124), and the Hill coefficient *h* equals 1.7 (105;124). The maximal velocity, V_{max} , is found to be 1.8 µmol/g liver/min, by fitting the Hill function to experimental data of hepatic glucose phosphorylation versus glucose concentration in fasted rats (167), see figure 11. In *in vitro*

studies with rats, V_{max} for flucokinase was found to 1.46 µmol/g liver/min (8;94). The mathematical function describing the flux through glucokinase is as follows:

$$GK = \frac{V_{GK} \cdot [G]^{\alpha}}{K_{KG}{}^{\alpha} + [G]^{\alpha}}$$

eq. 37

The enzymes affinity for MgATP (S_{50} 0.3-0.4 mM), its other substrate, is well below the intracellular concentration of MgATP (~2.5 mM). This assured that the metabolic flux depends almost entirely on the concentration of glucose and the amount of glucokinase within the cell (105).

3.1.2 Glucose-6-phosphatase

The *Km* of Glucose 6-phosphatase is 2-3 mM, which is higher than the intracellular concentration of glucose 6-phoshate considered to be between 0.05 and 1 mM (54;54;84;158) in the liver. The inhibition exerted by glucose on G6Pase is probably of little physiological significance, since the half maximal suppression constant (*Ki* ~ 0.1 M) is more than one order of magnitude above glycemia (158). The controle of glucose 6-phosphatase activity therefore appears simple since it does not involve factors other than V_{max} and Km, and the substrate concentration. The function describing the flux through glucose 6-phosphatase is shown below.

$$GPase = \frac{V_{GPase} \cdot [G6P]}{K_{GPase} + [G6P]}$$

eq. 38

In the fed state, V_{max} is close to 10 µmol/g liver/min (83).This value is doubled during starvation and diabetes (83). In fasted state (overnight fast) V_{max} for glucose 6-phosphatase is found to be 13 µmol/g liver/min (94) and 12.3 µmol/g liver/min (142) in rats. This agrees with basal Glucose 6-phosphatase rate based on total hepatic glucose output of 0.53

umol/g liver/min (45), with a fasting glucose 6-phoshate concentration of 0.2 mM (54) and a *Km* of glucose 6-phophatase of 2 mM (84) and glucose phosphorylation/ dephosphorylation recycling of about 50%. The glucose/glucose 6-phosphate cycle is found to be 20-50% in normally fed rats (83). As glucokinase glucose 6-phosphatase is not directly regulated in short term by hormonal signals. However, over a matter of some hours by changes in enzyme amount (66).

3.1.3 Glycogen phosphorylase

Glycogen phosphorylase is the rate determining step in the breakdown of glycogen to glucose 6-phosphate (103). Glycogen phosphorylase in regulated by its substrate, by glycogen and by orthophosphate (103). In the normal fasted human liver the orthophosphate concentration is about 1.4 mM (14), and her it will be considered to remain constant at this level. The *Km* for glycogen is low compared with the overnight fasted glycogen concentration of about 250 mM. For glycogen concentrations above 50

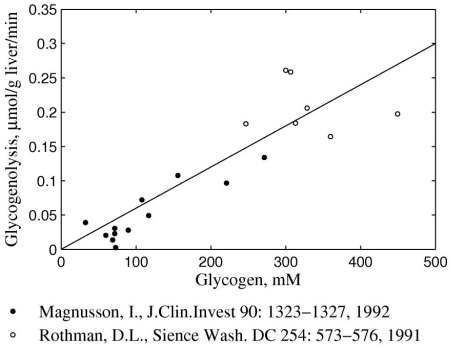

Figure 12: Correlation between net glycogenolysis and hepatic glycogen concentration, from (106). The Rothman data are mean net glycogenolysis during-22 hours fast – glycogen concentration after 15 hours fast, glucose concentration 4.6 mM, insulin 66 pM. Magnusson data shows net glycogenolysis and hepatic glycogen content after 4, 13.5, 17, 19.5 and 22.5 hours fast, for both healthy and diabetic subjects.

mM the glycogen phosphorylation rate is more or less constant. However, there are several studies that suggest the net glycogenolysis decreases with glycogen concentration in a linear fashion (107;135). This indicate that the glycogen concentration may regulate its rate of breakdown and that liver glycogen turnover may be an important factor in limiting the accumulation of liver glycogen in humans (106;161), see figure 12.

The decreasing net glycogneolysis with decreasing glycogen concentration, could be due to either inhibition of glycogen synthase by glycogen (77) or stimulation of glycogen phosphorylase by glycogen (106;161), or a combination of both. However in the description of glycogen phosphorylase in is assumed that glycogen stimulates its own breakdown. In the section "Simulation of Hepatic glucose production" this will be discussed further.

Hepatic glucose metabolism was studied by Hellerstein, et al. (81) after 11 hours fast and after 60 hour fast. Net glycogenolysis decreased from 0.24 μmol/g liver/min to close to zero between 11 and 60 hours fast. Total glycogen phosphorylase decreased from 0.36 μmol/g liver/min to 0.09 μmol/g liver/min, during the 11 hour and the 60 hour fast, respectively. At the same time glycogen syntesis flux decreased from 0.12 μmol/g liver/min to 0.09 μmol/g liver/min (81). This drastic decrease in glycogen phosphorylase occurs despite that, after 60 hours fast it would be expected that glucagon concentration is increased and glucose concentration decreased a bit, both favouring increased glycogen phosphorylase activity. This could indicate that glucogen phosphorylase flux decreases with glycogen concentration. Hepatic glycogen content is between 185 – 444 mM (50-120 g) (66), after an overnight fast (12-15 hours fast). In healthy subjects hepatic glycogen content is 251 mM (135), 230 mM (between 191-288 mM) (122).

Glycogen phosphorylase activity is regulated through phosphorylation and de-phosphorylastion of the enzyme. Glycogen phosphorylase is active in its de-phosphorylated form (glycogen phosphorylase a) (7).

Glucose is a major regulator of human glycogen phophorylase, while UDP-glucose, glucose 6-phophate and fructose 1-phosphate are only minor inhibitors of the enzyme in human liver (54). Moreover glucose is the only of these for which the concentration changes greatly *in vivo* (54). Glucose inhibit glycogen phosphorylase, by reducing the amount of glycogen phosphorylase a (16;54), which is the active from in the liver, and by increasing the *Km* for orthophosphate (54). In the absence of glucose, *Km* for orthophosphate for glycogen phosphorylase a was measured to be 5 mM in human liver. At a glucose concentration of 8 mM it was found to be 10 mM (54). The activity of glycogen phophorylase decreased with increasing glucose concentration, at a glucose concentration of 8 mM the activity of phosphorylase was 31% of its activity with no glucose present. The activity fell to 10% at a glucose concentration of 20 mM (54). Both measured at an orthophosphate concentration of 1 mM which is close to the fasting human hepatic level of 1.4 mM. The maximal rate of glucogen phorylase with no glycogen present and an orthophosphate concentration of 1 mM was 1.3 µmol/ g liver/min (54). In figure 13 (left) the inhibition of glycogen phosphorylase activity enforced by glucose is shown. Figure 13 (right) shows the rate of glycogen phosphorylase as a function of glucose concentration.

Glycogen phosphorylase flux has been measured during glucose clamps after an overnight fast. In the basal state glucose 5 mM and insulin 40 pM, glycogen phosphorylase flux was found to be 0.25 µmol/g liver/min (122), no glycogen cyling was found. The net glycogen phosphorylase flux of 0.25 µmol/g liver/min, fits with net glycogen phophorylase found 0.24 µmol/g liver/min after an overnight fast (81), mentioned above. However here glycogen cycling was 33 %, corresponding to a glycogen synthesis of 0.12 µmol/g liver/min and total glycogen phosphorylase of 0.36 µmol/g liver/min. At a plasma glucose concentration clamped at 10 mM and with insulin kept at 40 pM, the glycogen phosphorylase rate was measured to be 0.05 µmol/g liver/min (122), again after an overnight fast. Glycogen phosphorylase is stimulated by glycagon (7;16). This accounts

for the higher rate of glycogen phosphorylase at a glucose concentration of 10 mM determined by the relation showed in figure 13 (right) compared to the data from Petersen et al. (122). This data is also plotted in figure 13. This study also showed a 25% increase in glycogen phosphorylase rate at basal glucose (5 mM) and insulin (40 pM) concentrations with "high" 50 ng/l glycogen concentration compeared to at "low" 30 ng/l glycogen concentration. Regulation of glycogen phosphorylase by glucagon is not included in the model.

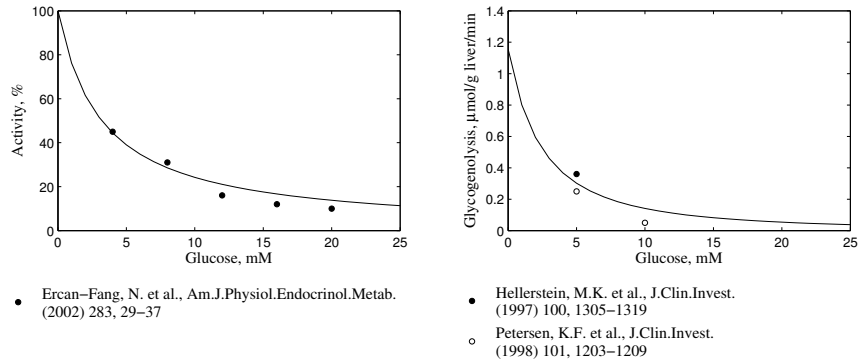

Figure 13: To the left – Effect of glucose on the relativ activity of human liver glycogen phosphorylase. The relationship can be described by a Mmichaelis-Mmenten type function; half maximal activity is at a glucose concentration of 3.2 mM. To the right – Rate of glycogen phosphorylase as a function of glucose. Hepatic orthophosphate concentration is 1.4 mM, hepatic glycogen concentration 250 mM.

$$GgP = \frac{V_{GgP}}{1 + \frac{K_4}{[Gg]} + \frac{K_{Pi}}{[Pi]} \cdot \left(1 + \frac{[G]}{K_{Pi,G}}\right) + \frac{K_1}{[Gg]} \cdot \frac{K_{Pi}}{[Pi]} \cdot \left(1 + \frac{[G]}{K_{i,G}}\right)} \cdot \frac{[Gg]}{K_{Gg}} \cdot \frac{K_{GgP,G}}{K_{GgP,G} + [G]}$$

eq. 39

The function describing the rate of glycogen breakdown is shown above. As mentioned, the rate of glycogen breakdown is stimulated by is products orthophosphate and glycogen.

This relation is described by a Michaelis-Menten like function (103). Glucose lowers the affinity of glycogen phophorylase to orthophosphate and, at the same time, it increases the maximal velocity. The glucose stimulation of glycogen phosphorylase is also decribed by a Michaelis-Menten type function. Furthermore, glycogen also increases the rate of glycogen breakdown, this effect is described in a linear manner. Parameter values are shown in
table **4**.

3.1.4 Glycogen synthesis

Glycogen synthase catalyses the rate-determining reaction in glycogen synthesis (148). Glycogen synthase is stimulated indirectly by glucose, on several levels. As for glycogen phoshorylase, glycogen synthase is regulated though phosphorylation and de-phophorylation of the enzyme, glycogen synthase is active in its phosphorylated form (7).

Glucose increases hepatic glucose 6-phosphate, which stimulates glycogen synthase activity and increases the affinity for its substrate UDP-glucose. As mention in an earlier section, glucose inhibits glycogen phosphorylase activity which results in increased glycogen synthase activity, through decreased inhibition of glycogen synthase by glycogen phosphorylase (16). Here glucose concentration is used as a stimulator of glycogen synthesis, due to the very complex indirect effect of glucose.

Glycogen synthesis rate at glucose concentrations of 5 mM is found to vanish (122). However, another study reports glycogen synthesis rates of 12 μmol/g liver/min in the overnight fasted state and a glycogen cycling of 33% (81), after an overnight fast. At glucose concentrations of 10 mM, the glycogen synthesis rate was found to be 0.05 umol/g liver/min (122), with a glycogen cycling of 100% (45;122). Glycogen synthesis rate is described by a Michaelis-Menten function. The model is simplified so that the glycogen synthesis flux depends on the hepatic glucose 6-phosphate concentration and

that the maximal velocity in enhanced in a linear way by glucose. The function is given by:

$$GgS = \frac{[G]}{K_{GgS,G}} \cdot \frac{V_{GgS} \cdot [G6P]}{K_{GgS} + [G6P]}$$

eq. 40

Model parameter values are shown in
table **4**.

3.1.5 Gluconeogenesis

It is widely believed that glucogenolysis and gluconeogenesis each contribute approximately 50% of glucose turnover in healthy subjects after an overnight fast (161), this gives a gluconeogenesis rate of about 0.23 µmol/g liver/min (~ 5 µmol/kg/min), corresponding to a total glucose output of 0.47 µmol/g liver/min (161).

3.1.6 Hepatic Glucose Metabolism Model Equations

In this section all differential equations and model fluxes are collected. Below are first the two differential equations, representing hepatic glucose 6-phosphate and hepatic glycogen:

$$\frac{d[G6P]}{dt} = \frac{1}{V} \cdot (GK - GPase + NEO - GgS + GgP)$$

eq. 41

$$\frac{d[Gg]}{dt} = \frac{1}{V} \cdot (GgS - GgP)$$

eq. 42

Herafter follow the four earlier described functions for Hepatic Glucose Metabolism Model flux shown, followed again by the parameters of the Hepatic Glucose Metabolism Model:

$$GK = \frac{V_{GK} \cdot [G]^{\alpha}}{K_{KG}{}^{\alpha} + [G]^{\alpha}}$$

eq. 37

$$GPase = \frac{V_{GPase} \cdot [G6P]}{K_{GPase} + [G6P]}$$

eq. 38

$$GgP = \frac{V_{GgP}}{1 + \frac{K_4}{[Gg]} + \frac{K_{Pi}}{[Pi]} \cdot \left(1 + \frac{[G]}{K_{Pi,G}}\right) + \frac{K_1}{[Gg]} \cdot \frac{K_{Pi}}{[Pi]} \cdot \left(1 + \frac{[G]}{K_{i,G}}\right)} \cdot \frac{[Gg]}{K_{Gg}} \cdot \frac{K_{GgP,G}}{K_{GgP,G} + [G]}$$

eq. 39

$$GgS = \frac{[G]}{K_{GgS,G}} \cdot \frac{V_{GgS} \cdot [G6P]}{K_{GgS} + [G6P]}$$

eq. 40

Table 4: Hepatic Glucose Metabolism Model Parameters

V	1.5	L	(32;135)
V_{GK}	1.8	µmol/g liver/min	Estimated from (167).
K_{GK}	7.8	mM	(124)
α	1.7		(105;124)
V_{GPase}	13	µmol/g liver/min	
K_{GPase}	2	mM	(84)
V_{GgS}	0.122	µmol/g liver/min	Estimated from glycogen synthase rate (81;122).
K_{GgS}	0.2	mM	(92)
$K_{GgS,G}$	4.2	mM	Estimated from glycogen synthase rate (81;122).
V_{GgP}	5.5	µmol/g liver/min	Estimated from overnight fast glycogenolysis rate (81;122).
K_4	0.92	mM	(103)
K_1	13	mM	(103)
K_{Pi}	5	mM	(54)
$K_{Pi,G}$	8	mM	(54)
K_{Gg}	250	mM	Estimated overnight fast glycogen content (135)
$K_{GgP,G}$	3.2	mM	(54)

3.2 SIMULATION OF HEPATIC GLUCOSE PRODUCTION

Through simulations with the hepatic glucose model the mechanisms described in the above section are evaluated, and the mechanism by which glucose regulates its own production is investigated. In the model of hepatic glucose production, the activity of glycogen synthase is indirectly stimulated by glucose, and glycogen phosphorylase is inhibited directly both allosteric and through regulation of activity. The apparent regulation of net glycogen formation/breakdown by glycogen itself is also explored further. Data suggests that net glycogenolysis decreases with decreasing glycogen concentration, see figure 12 (106). And, in muscle it was found that glycogen concentration suppresses net glycogen synthesis (77). In the hepatic glucose metabolism model, the regulation of glycogen formation/breakdown is through glycogen stimulation of glycogen phosphorylase. However, it has also been suggested that the mechanism for this regulation is through glycogen inhibition of glycogen synthasis (77). This will be investigated further in this section.

3.2.1 Glucose regulation of hepatic glucose metabolism

The model is used to explore four different situations regarding the mechanism by which glucose regulates its own production. First the effect of mass action, where there are no indirect stimulation of glycogen synthase by glucose neither any inhibition of glycogen phosphorylase activity by glucose. In a second situation the glucose stimulation of glycogen synthase is present. The third situation only has the glucose inhibition of glycogen phosphorylase by not the stimulation of glycogen synthase. And the last situation has both glucose stimulation of glycogen synthase and glucose inhibition of glycogen phosphorylase.

For all situations the relevant model version is used to determine quasi steady state for glucose concentrations between 4 and 17 mM. It is quasi steady state since the glycogen

concentration is not constant. The rate of gluconeogenesis is constant for all simulation at 0.265 µmol/g liver/min. The hepatic glucose output found through the simulations is compared to measured hepatic glucose output (45), during a 3-step hyperglycaemic glucose clamp, see figure 14. The data used are from young as well as older healthy subjects, normal BMI, mean age was 25 years and 59 years, respectively. During the clamp study, insulin and glucagon concentrations were kept at overnight fasting levels. Insulin concentration was 84 pM and glucagon 102 ng/l for young subjects and 72 pM and 173 ng/l in older subjects.

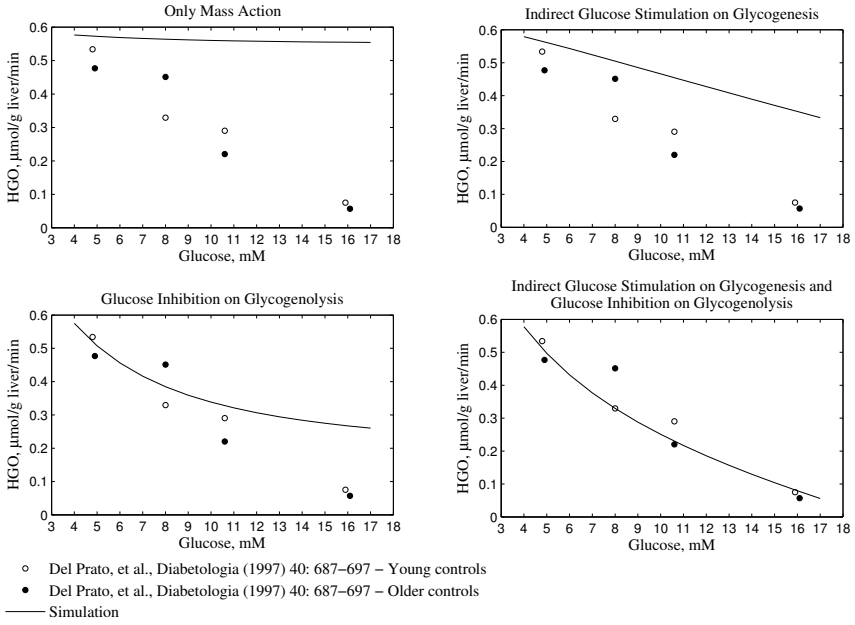

Figure 14: Hepatic glucose metabolism model simulation of hepatic glucose ouput, compared to hepatic glucose output measured during a 3 step glucose clamp where insulin and glycagon is kept at basal level. The figure shows simulations with four version of the hepatic glucose model.

From the simulation using the model version where only the mass action of glucose regulates hepatic glucose output (see figure 14 upper left corner), it is obvious the mass

action alone can not ensure the regulation of hepatic glucose production by glucose. The rates of glycogenesis and glycogenolysis are shown in figure 15.

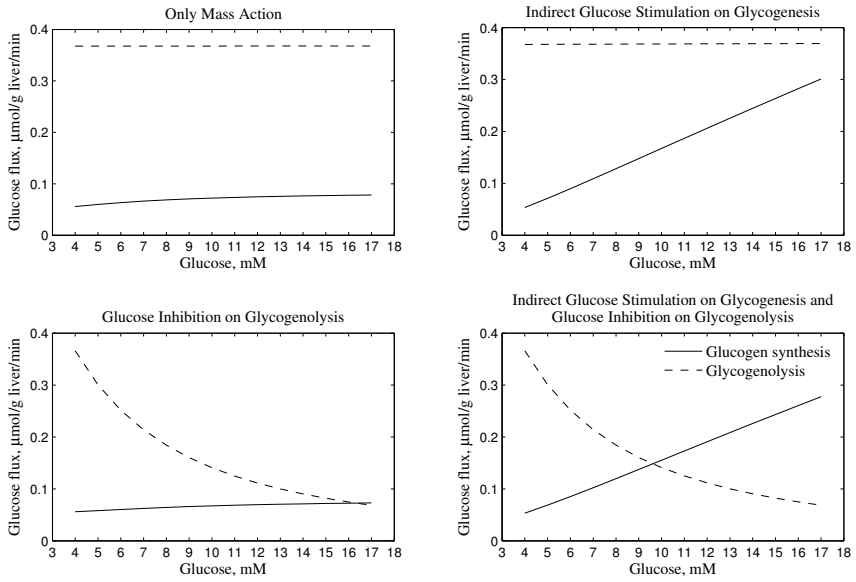

Figure 15: Four version of the hepatic glucose metabolism model simulating hepatic glucose output in quasi steady state as a function of glucose concentrations. The figures show glucogenesis and glycogenolysis rates.

In the second model version used (simulation is showed in the upper right corner of figure 14) glucose stimulates the activity of glycogen synthase. This mechanism alone gives some decrease of hepatic glucose output, altthough not enough to explain the relation between plasma glucose concentration and hepatic glucose output observed in the data. However, if the effect of glucose in glycogen synthase is increased two fold, relatively to the parameter values given in

table **4**, the observed hepatic glucose output in relation to glucose concentration can be explained only by mass action and glucose stimulation of glycogen synthesis (simulation not shown). However, since glucose stimulation of glycogen synthasis is indirect and in

part regulated through the inhibitory effect of glucose on glycogen phosphorylase, it does not seem reasonable that without the down regulation in phoshorylase the indirect glycogen synthase stimulation is two fold higher that with down regulation of phosphorylase.

Like with, the model version where the effect of glucose on hepatic glucose metabolism is through mass action and through glucose inhibition of the activity of glycogen phosphorylase and allosteric regulation the enzyme, is not able to explain the observed down regulation of hepatic glucose output with increasing glucose concentration. It is especially for high glucose concentrations (above 10 mM) that the glucose inhibition of glycogen phosphorylase fails to explain the observed relation between glucose concentration and hepatic glucose output. Increasing the inhibition effect of glucose will not be able to explain the rate of hepatic glucose output for the high glucose concentration, since glycogenolysis flux will have to be negative in order to reach the hepatic glucose output experimentally observed at a glucose concentration around 16 mM (see figure 15 - bottom left).

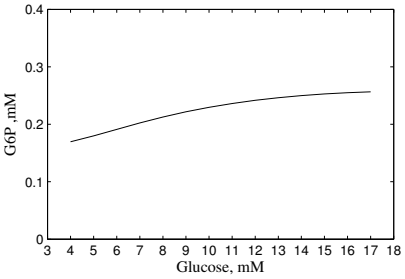

Figure 16: Simulated glucose 6-phosphate concentration from quasi steady state of hepatic glucose output simulation using the model defined in section "Hepatic Glucose Metabolism Model Equations". Including both glucose effects on glycogen synthase and glycogen phosphorylase.

When both the glucose stimulation of glycogen synthase and the glucose inhibition of glycogenolysis is taken in to account (this corresponds to the model defined in section "Hepatic Glucose Metabolism Model Equations") the model is able to reproduce the relation between hepatic glucose output and plasma glucose concentration observed in the 3 step hyperglycaemic clamp study (45), see figure 14 - bottom left. The rates of glycogen synthesis and glycogenolysis are shown in the lower right corner of figure 15, and the variation of the glucose 6-phosphate concentration with glucose concentration in figure 16. The simulated glucose 6-phosphate concentration is within the physiological range in the human liver, which is between 0.05 and 1 mM (54;54;84;158).

3.2.2 Glycogen regulation of hepatic glucose metabolim

To investigate glycogen regulation of hepatic glucose metabolism, two possible mechanisms are described; A mechanism where glycogen stimulates its own breakdown and a mechanism where glycogen inhibits its own synthesis. The model is used to see if either of the two mechanism can explain the experimentally observed decreases in glycogen synthesis with increasing glycogen content (76) and the decrease in glycogen breakdown with decreasing glycogen levels (106).

In figure 17 and figure 18 the hepatic glucose metabolism as described in "Hepatic Glucose Metabolism Model Equations" is used to simulate hepatic glucose output for 24 hours with a constant glucose concentration of 5 mM and initial glycogen concentration of 250 mM (figure 17) and with a constant glucose concentration of 15 mM and initial glycogen concentration of 250 mM (figure 18). Both in the situation of net glycogenolysis (plasma glucose 5 mM) and in the situation of net glycogenesis (plasma glucose 15 mM) the hepatic glucose metabolism model where glycogen regulates its own breakdown shows a linear correlation between glycogen content and net glycogenolysis and net glycogenesis, respectively. This corresponds to the experimentally observed linear relation between glycogen breakdown/synthesis and glycogen (77;106).

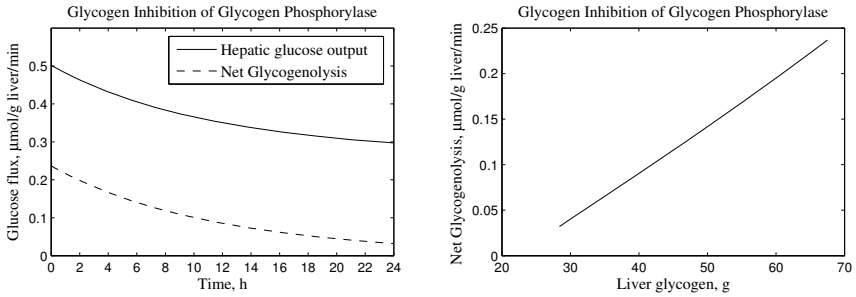

Figure 17: Simulation of hepatic glucose output, net glycogenolysis for 24 hours with initial glucogen concentration at 250 mM and constant plasma glucose concentration of 5 mM.

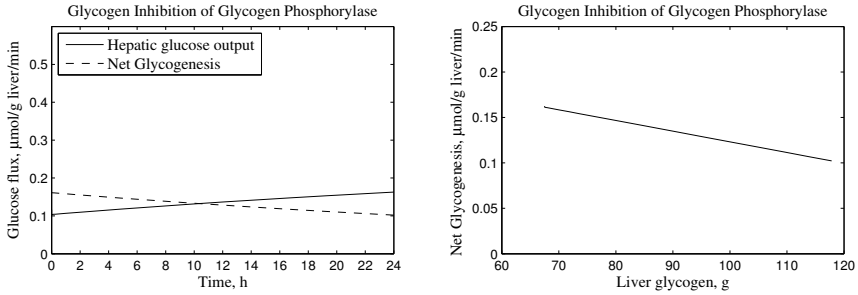

Figure 18: Simulation of hepatic glucose output, net glycogen synthesis for 24 hours with initial glucogen concentration at 250 mM and constant plasma glucose concentration of 15 mM.

In the literature it has been suggested that the glycogen inhibits its own synthesis through a mechanism related to the binding of both glycogen synthase and glycogen phosphatase to glycogen as part of a glycogen protein complex, which also includes glycogen phoshorylase (77). Glycogen phosphatase is the enzyme involved in the dephosphorylation of glycogen synthase to its active form (7). To see if a similar result could be obtained were glycogen, instead of stimulating its own breakdown, inhibits its own synthesis the model is modified so that, the function describing glycogen synthesis eq. 40 is modified to read:

$$GgS = \left(6.5 - \frac{[Gg]}{45}\right)\frac{[G]}{K_{GgS,G}} \cdot \frac{V_{GgS} \cdot [G6P]}{K_{GgS} + [G6P]}$$

eq. 43

and the function describing glycogen phosphorylase flux eq. 39 is modified to become:

$$GgP = \frac{V_{GgP}}{1 + \frac{K_4}{[Gg]} + \frac{K_{Pi}}{[Pi]} \cdot \left(1 + \frac{[G]}{K_{Pi,G}}\right) + \frac{K_1}{[Gg]} \cdot \frac{K_{Pi}}{[Pi]} \cdot \left(1 + \frac{[G]}{K_{i,G}}\right)} \cdot \frac{K_{GgP,G}}{K_{GgP,G} + [G]}$$

eq. 44

The parameters are the same as stated in table 4. The inhibition of glycogen synthase by glycogen is constructed so that at overnight fasted glycogen level (250 mM) the glycogen synthesis rate is not inhibited, and for zero glycogen the rate in 6.5 fold higher. This is done since the maximal rate of glycogen syntase (V_{GgS}) is estimated based on the overnight fasted glycogen synthesis rate.

The modified hepatic glucose metabolism model is used to simulate hepatic glucose output for 24 hours with a constant glucose concentration of 5 mM and initial glycogen concentration of 250 mM (figure 19) and with a constant glucose concentration of 15 mM and initial glycogen concentration of 250 mM (figure 20). According to the simulation with the modified hepatic glucose metabolism model also a mechanism where glycogen inhibits its own synthesis can also explain the linear relationship between net glycogenolysis and glycogen content, as well as between net glycogen synthesis and glycogen levels as observed experimentally (77;106).

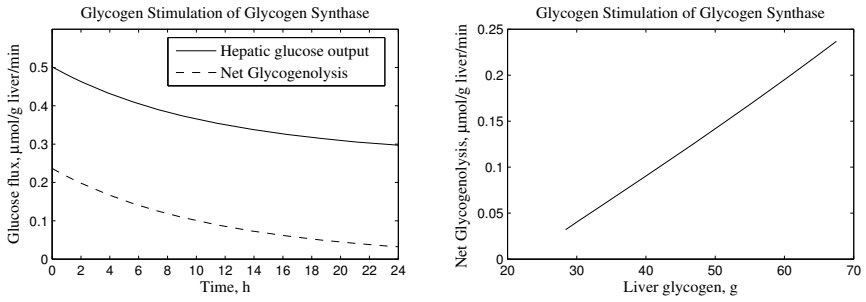

Figure 19: Simulation with modified hepatic glucose metabolism model of hepatic glucose output, net glycogenolysis for 24 hours with initial glucogen concentration at 250 mM and constant plasma glucose concentration of 5 mM.

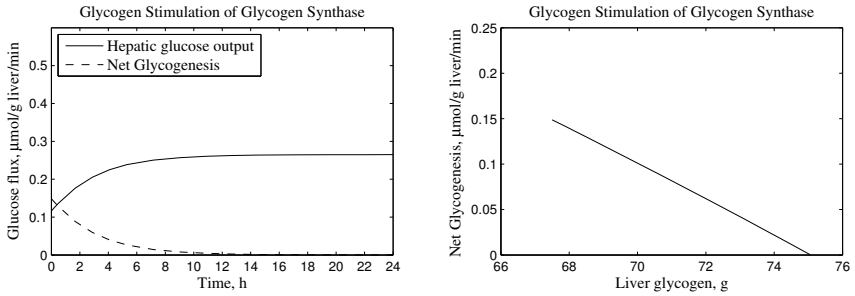

Figure 20: Simulation with modified hepatic glucose metabolism model of hepatic glucose output, net glycogenolysis for 24 hours with initial glucogen concentration at 250 mM and constant plasma glucose concentration of 15 mM.

In the situation where there is a net glycogenolysis (plasma glucose 5 mM) there no significant change in the relation of net glycogen breakdown and glycogen, between glycogen stimulation of glycogen breakdown and glycogen inhibition of glycogen synthesis.

3.3 DISCUSSION AND CRITIQUE OF THE HEPATIC GLUCOSE METABOLISM MODEL

The role of the liver in maintaining plasma glucose levels during fasting and its contribution to glucose homeostasis in the postprandial state is considerable. The hepatic glucose metabolism model presented here focus on the regulation of hepatic glucose metabolism by glycogen and glucose. The model is able to predict hepatic glucose output in relation to the plasma glucose concentration, which is compatible with the experimentally observed hepatic glucose output found during a three-step hyperglycaemic glucose clamp study where glucagon and insulin were kept at basal level (45). It was found that both stimulation of glycogen synthase by glucose and inhibition of glycogen phosphorylaser by glucose were necessary in order to explain the relation between hepatic glucose output and plasma glucose concentration experimentally observed (45).

The hepatic glucose metabolism model was also used to test if glycogen stimulation of glycogen breakdown or glycogen inhibition of glycogen synthesis could explain the linear relation between net glycogenolysis and glycogen content experimentally observed (77;106). It was found that both mechanisms could explain the linear relationship observed. And, of course, it could also be combination of both. The literature provides a suggestion as to how the mechanism of glycogen inhibition of it own synthesis could work, although it is only speculative (77). The idea is that glycogen binds to both glycogen synthase and glycogen phosphatise as part of a glycogen protein complex, which also include glycogen phoshorylase (77). How a mechanism for glycogen stimulation of its own breakdown works, is not known. However if glycogen in some way increases the activity of glycogen phosphorylase, then glycogen synthase activity will also be inhibited through the inhibitory effect of glycogen phosphorylase.

The stimulation of glycogen syntase by glucose in reality executed through allosteric regulation of glycogen synthase by glucose 6-phosphate and upregulation of active glycogen synthase through downregulation of active glycogen phosphorylase. However in

the hepatic glucose metabolism model described here, these mechanisms are grossly simplified, and the stimulation of glycogen synthase is directly regulated by the glucose concentration. Since this mechanism is important for the ability of the liver to regulate its glucose metabolism, further work should examine the indirect effect of glucose on glycogen synthesis more thoroughly.

The relation describing the mechanism for glycogen inhibition of its own synthesis is a linear function and so is the function describing the mechanism for glycogen stimulation of its own breakdown. It might be more realistic to describe the two mechanisms through a saturated function of michaelis-menten type. It could also be interesting investigate if a combination of glycogen stimulation of glycogen phosphorylase and inhibition of glycogen synthase can explain the experimentally observed relation between net glycogen synthesis/breakdown and glycogen.

In the hepatic glucose metabolism model the rate of gluconeogenesis is considered to be constant, and not to be influenced by glucose. However there is some evidence that glucose regulates the rate of glyconeogenesis (84).

3.3.1 Effect of Insulin on the Hepatic Glucose Metabolism

The hepatic glucose metabolism is also regulated by hormones. The dynamical response to plasma and portal insulin concentration is an obvious next step in further development of the hepatic glucose metabolism model. Within the time frame of the present study some preliminary investigations were made to quantify the effect of insulin on the hepatic glucose flux.

Glycogen phosphorylase is regulated by insulin and glucagon (16). Glucogenolysis flux was measured during hyperinsulima glucose clamp with a plasma glucose was 5 mM. At basal insulin concentrations (40 pM), glycogenolysis was measured to 0.2 μmol/g liver/min, and at insulin concentrations of 400 pM, glycogenolysis was 0.29 μmol/g

liver/min (122). However, in general insulin in thought to inhibit glycogenolysis, see figure 21. The data in figure 21 comes from dogs and might overestimate human glycogenolysis rates since the rate of hepatic glucose production is lower in dogs than in humans, at least in relation to hyperglycemia (28).

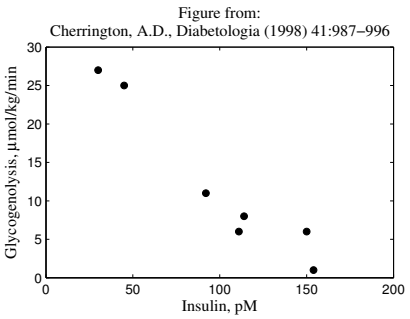

Figure 21: Rate of hepatic glycogen phosphorylase at increasing hepatic sinusoidal insulin concentrations, in conscious overnight fasting dogs (30).

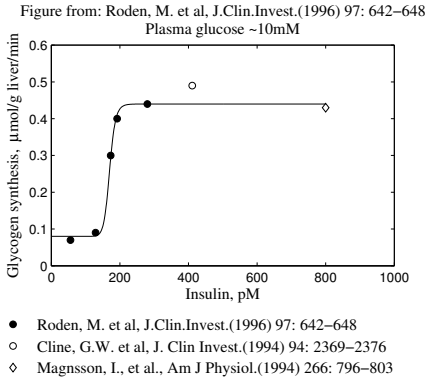

Figure 22: Rate of hepatic glycogen synthase (GgS) at different insulin levels, glucose levels are held constant at 10 mM - Data from (129).

Insulin stimulates glycogen synthesis by increasing the amount of glycogen synthase a (the active form) (16;129). The effect of insulin on glycogen synthesis is showed in figure 22. At a glucose concentration of 10 mM and basal insulin the rate of glycogen synthesis is 0.07 µmol/g liver/min (129). This is increased about 6 fold at an insulin concentration of 280 pM to about 0.44 µmol/g liver/min. The stimulation of glucose synthesis by insulin can be described by a Hill function with a Hill constant of 20 and a half maximal stimulation at 170 pM. The function is very steep, which means that insulin stimulation almost can be seen as a switch.

The effect of insulin on hepatic glucose metabolism can be subject to a time response (delay) of about 15 min (29).

Insulin also regulates gluconeogenesis (84). This regulation includes both direct and indirect effects (161). Indirectly, insulin inhibits gluconeogenesis through inhibition of the substrates; amino acids and glycerol (161).

4 POSTPRANDIAL LIPID METABOLISM

Due to the metabolic disease diabetes type 1 and type 2, and the dysfunction of glucose metabolism observed with these diseases there has been a strong focus on quantitative models of glucose metabolism, for instance the minimal models. However, as pointed out earlier, the regulation of fat and glucose metabolisms are connected. A decrease in the ability of insulin to inhibit release of fatty acids can, for instance, influence the utilisation of glucose; see Simulation of Hyperinsulinaemic Glucose Clamp. The literature also provides examples, which show that increased plasma non-estrified fatty acid is associated with impaired glucose uptake and decreased insulin sensitivity (12), whereas reduction in plasma non-esterified fatty acids is related to increased insulin sensitivity (139). The close relation between glucose and fat makes it interesting to focus more on the regulation of fat metabolism.

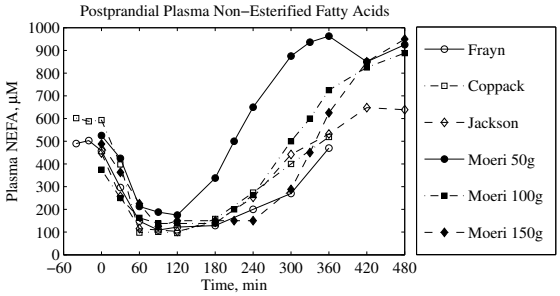

Figure 23: The figure shows the plasma non-esterified fatty acid profile for 6 studies where a mixed meal or OGGT is given after an overnight fast. Data is taken from (35;63;86;113).

When looking at models of postprandial (*overnight fast followed by a meal*) plasma non-esterified fatty acids, the time scale is often 300-360 minutes (121;136). Within this time interval the typical behaviour for plasma non-esterified fatty acid is to decrease from an overnight levels of 400-600 µM to around 100-200 µM about 60 min after a meal for there

after to increase again towards the initial level. For illustration here of see figure 23. This behaviour is captured well by the models describing plasma non-esterified fatty acid dynamics by Periwal *et al*, 2009 (121) and by Roy & Parker, 2006 (136).

In two of the studies shown in figure 23, Frayn *et al*, 1993 and Coppack *et al*, 1992 (35;63) the study is stopped after 360 min. Within this time frame the plasma non-esterified fatty acid concentration decreases from around 500-600 μM to around 100 μM about 60 min after the meal is given. Around 120-180 minutes after the meal plasma non-esterified fatty acid concentration increases again reaching initial level at the end of the study.

However, in the study by Jackson *et al*, 2005 (86) and the three OGGTs by Moeri *et al*, 1988 (113), the experiment was ended 480 min after the meal/OGGT was given. This discloses an extra dynamic effect in the plasma non-esterified fatty acid profile, where the plasma non-esterified fatty acid concentration keeps increasing after having reached initial level, and a plasma non-esterified fatty acid overshoot can be observed. The observed overshoot is not captured by the mentioned models of plasma non-esterified fatty acid dynamics, and might be due to a physiological mechanism not described by the model in Periwal *et al*, 2009 (121) and Roy & Parker, 2006 (136). The two models describe adipose tissue lipolysis, re-esterification of fatty acid into adipose tissue, and periphery uptake of fatty acids from plasma, as well as interaction among fatty acids, glucose and insulin.

During a normal day meals are usually eaten with an interval of 4-6 hours, or less. However this does not mean that the late postprandial plasma fatty acid overshoot which is observed 6-8 hours after a meal, is not interesting. The metabolic response to a second meal is not similar to the response observed after the first meal (after an overnight fast) (58). The reason for the difference between metabolic responses to the first and second

meal could be explained by this overshoot. Therefore, is it interesting to investigate the mechanism behind the late postprandial non-esterified fatty acid overshoot.

4.1 MODELLING PLASMA NON-ESTERIFIED FATTY ACID DYNAMICS

In the following a model of postprandial plasma non-esterified fatty acid dynamics will be setup, the model will be used to examine possible mechanisms resulting in the plasma non-esterified fatty acid overshoot observed in studies 5-8 hours after a meal following an overnight fast, see figure 23. The model is also used to examine if differences, for example between lean and obese subjects, seen in plasma insulin, triglyceride and non-esterified fatty acid profiles after a meal can be explained by changes in the lipid metabolism described by the plasma non-esterified fatty acid dynamics model.

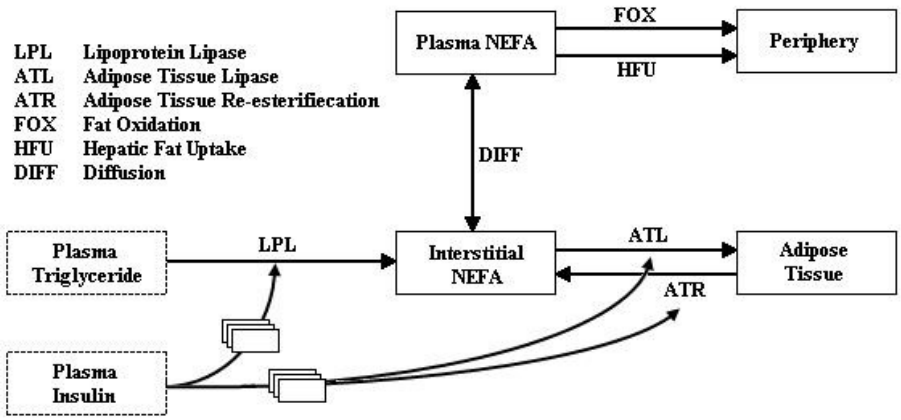

Figure 24: Schematic representation of Postprandial Plasma Non-Esterified Fatty Acid Model

The model consists of eight differential equations, with 20 parameters, in which two represents plasma non-esterified fatty acid concentrations and interstitial non-esterified fatty acid concentration, the remaining six differential equations represent two systems of 3. order delays. A schematic representation of the model is shown in figure 24, followed by all model equations. Non-esterified fatty acid enters plasma from the interstitial compartment, through diffusion, and is taken up by periphery tissue. The interstital space has an entry of non-esterified fatty acid both from adipose tissue lipolysis, and adipose

tissue lipoprotein lipase, and is removed through adipose tissue re-esterification. Non-esterified fatty acid can also enter or be removed from the interstitial space from/to plasma depending on the concentration gradient. The velocity relations are described by michaelis-menten type functions, except the exchange between plasma and interstital space. The parameters for the velocity function in the model are roughly estimated within the indication found in the published literature.

4.1.1 Adipose Tissue Lipolysis and Re-Esterification

The mobilization of stored fat takes place via hydrolysis, where adipose tissue triglycerides are hydrolysed into three fatty acids and one glycerol, all of which are released into the circulation for use by other organs. The initial and rate-limiting step lipolysis is the hydrolysis of triglyceride to yield one non-esterified fatty acid and diaglyceride (50). The key enzyme of this process in adipocytes is hormone-sensitive lipase, although new adipose tissue triglyceridelipases have been identified (50;168). In the postprandial state lipolysis is regulated primarily through the antilipolytic actions of insulin (40;50;66;150). Insulin sensitivity of lipolysis has a considerable variation in healthy humans (150), with reported half maximal suppression constant (*Ki*) between 10 pM to 140 pM (17;25;26;40;150). In the overnight fasted state (low insulin concentration ~ 50 pM) the rate of lipolysis is in the order of 30 - 40 μmol/kg fat mass/min for lean subjects (25;26;35;165) and 20-25 μmol/kg fat mass/min for obese subjects (26;35;165). The rate of lipolysis decreases as insulin increases. However even at very high insulin concentrations (above physiological concentrations), lipolysis can be observed. This indicates a basal lipolysis rate. A lipolysis rate of ~13 μmol/kg fat mass/min was found for both lean and obese persons at insulin concentrations above 13000 pM (25;26).

The function describing the adipose tissue lipase flux is shown below. The rate is inhibited by insulin and consists of a michaelis-menten type function dependent on insulin and a basal rate. The maximal velocity and the basal velocity depend on fat mass.

$$ATL = \frac{V_{ATL} \cdot K_{ATL}}{K_{ATL} + [I_{ATL}]} + B_{ATL}$$

eq. 45

Alteration in lipolysis are frequently associated with obesity, including an increase in basal rates of lipolysis that may contribute to the development of insulin resistance, as well as an impaired responsiveness to the antilipolysic effect on insulin (50).

In addition to the inhibitory effects on the enzymes in triglyceride hydrolysis, insulin also decreases net fatty acid release by increasing the rate of fatty acid re-estrification (39;50). In addition to the stimulatory effect of insulin on re-esterifiction, adipose tissue re-esterification also depends on substrate availability that is non-esterified fatty acid concentration (104). During basal conditions (overnight fast) adipose tissue re-esterification is around 20% of adipose tissue lipolysis rate, about 8 μmol/kg fat mass/min (25;164) in lean subjects. Half maximal rate of re-esterification is likely to occur at a non-esterified fatty acid concentration of 1500 μM, around albumin-binding saturation range (104). In basal non-esterified fatty acid concentration is considered to be around 500 μM (66) and re-esterifiction rate 8 μmol/kg fat mass/min, then the maximal re-esterification rate at basal level would be around 30 μmol/kg fat mass/min. As mentioned, insulin stimulates the rate of adipose re-esterification. Half maximal stimulation of re-esterification by insulin is found to be 120 pM (74). Maximal stimulation by insulin is set to 5, so that at basal level (overnight fast, insulin 50 pM) there are no effect of insulin on the re-esterification rate. The function describing the rate of adipose tissue re-esterification in presented below. The function consists of a non-esterified fatty acids dependent part and an insulin dependent part. As mentioned, insulin increases the maximal rate of adipose tissue re-esterification approximately by five fold at maximal stimulation.

$$ATR = \frac{V_{ATR} \cdot [NEFA_i]}{K_{ATR,FA} + [NEFA_i]} \cdot \frac{q \cdot [I_{AT}]}{K_{ATR,I} + [I_{AT}]}$$

eq. 46

Both for lipolysis and re-esterification the effect of insulin is associated with at small response time in the order of 10-30 min (35;55). This response time could represent the diffusion of insulin across the epithelial cells and the interstices, association of adipocyte insulin receptors, and in-/activation of intracellular processes.(15;89).

4.1.2 Lipoprotein Lipase

Triglyceride is, unlike glucose, not soluble in the plasma. Therefore, it is transported in the circulation in the form of lipoprotein particles (59;66). The two major lipoproteins are chylomicrons (from the diet) and VLDL particles (secreted by the liver). They are both hydrolysed by the Lipoprotein lipase (LPL) present in the capillary bed of the endothelial cells in a variety of tissues for instance in adipose tissue, skeletal muscle, and heart (44;59;66). Adipose tissue is the tissue with the highest activity of LPL, particularly in the postprandial state (35). In the basal state where plasma triglyceride concentration is around 1000 μM, the rate of LPL are approximately 100 μmol/min (35;56). In vitro studies indicate a C50 of around 3000 μM (22;33). The activity of adipose tissue LPL is stimulated by insulin over a relatively long time-course (4-6 hours) (35;66), while in muscle cells it is inhibited by insulin (66). The maximal activation of LPL by insulin in *in vitro* studies of human adipocytes are reported to 7 fold with maximal stimulation at 7000 pM insulin (3), 4.4 fold, with a EC50 of approximately 250 pM and with maximal stimulation at 1000 pM insulin (96). However, in *in vivo* studies half maximal stimulation of LPL by insulin was found to be at 200 pM (35;55;65). eq. 47 shows the functional relationship describing the rate of adipose tissue lipoprotein lipase. Again the rate consists of the product of two michaelis-menten functions, one depending on plasma triglyceride and the other on insulin concentration. As previously mentioned, the stimulatory effects of

insulin are delayed in relation to the actually insulin concentration, the effective insulin concentration on lipoprotein lipase is denoted I_{LPL}. In the present model this delay is represented by at 3.order delay, see the section "Postprandial Plasma Non-Esterified Fatty Acid Dynamics Model Equations" for the representation of a 3. order delay.

$$LPL = \frac{V_{LPL} \cdot [TG]}{K_{LPL,TG} + [TG]} \cdot \frac{p \cdot [I_{LPL}]}{K_{LPL,I} + [I_{LPL}]}$$

eq. 47

The presence of LPL on the capillary endothelium allows the lipoprotein particles passing through the capillary to be hydrolysed. The movement of fatty acid from the site of LPL action into the cells is not fully understood. It seems, however, to follow concentration gradients across the endothelium to the interstitial space and into the cells (59;65). In adipose tissue not all fatty acids released by LPL action are taken up by the adipocytes. Thus, there is a spillover of non-esterified fatty acids in to plasma (55;59).

4.1.3 Fatty Acid Uptake in Periphery Tissues

The fate of the non-esterified fatty acid taken up by periphery tissue is either to undergo oxidation or re-esterification to triglyceride. Both oxidation and re-esterification can in principle take place in most tissues. In muscle fatty acids are particularly taken up in the oxidative fibres. Under resting condition this uptake is closely related to plasma non-esterified fatty acid concentration, and with in the muscle cell fatty acids are oxidised in accordance with their rate of uptake (64). A relation between fatty acid oxidation and plasma non-esterified fatty acid concentration is shown in figure 25. There the relative rate of fatty acid oxidation (fatty acid oxidation relative to total oxidation) vs. plasma non-esterified fatty acid concentrations from four studies (2;11;113;159) are shown. The total oxidation in the four studies is on average 1.2 kcal/min, with a maximal variation of ± 25% in resting postprandial condition.

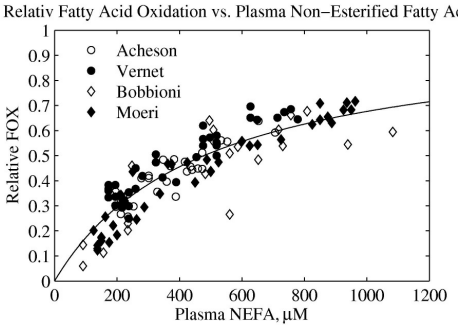

Figure 25: Relative fatty acid oxidation vs, plasma non-esterified fatty acid concentration under resting conditions. Experimental data (2;11;113;159) from different studies are marked, the full line represents a michaelis-menten type function (maximal velocity) Vm = 1 and (concentration for half maximal velocity)Km = 478 µM (R^2 = 0.82).

The function describing the relationship between plasma non-esterified fatty acids and fatty acid oxidation is shown in eq. 48.

$$FOX = \frac{V_{FOX} \cdot \lfloor NEFA_p \rfloor}{K_{FOX} + \lceil NEFA_p \rceil}$$

eq. 48

In the liver the two major fates of non-esterified fatty acid is re-esterification and oxidation (66). Complete oxidation is small, only 4-5% (110). In vitro hepatic non-esterified fatty acid uptake is substrate dependent and saturated at high non-esterified fatty acid levels. Its seems to be independent of any other nutrients or hormones (97;156). Maximal rate of hepatic non-esterified fatty acid uptake is around 600 µmol/min and half maximal rate at a concentration of 1500 µM, based on in vitro studies in rats (80). The function for hepatic fatty acid uptake is shown below.

$$HFU = \frac{V_{HFU} \cdot \lfloor NEFA_p \rfloor}{K_{HFU} + \lceil NEFA_p \rceil}$$

eq. 49

4.1.4 Transport of Non-Esterified Fatty Acid between Adipose Tissue Interstitium and Plasma

Transport of non-esterified fatty acid occurs via diffusion and/or via transport proteins. A number of transporters have been identified (4;79), but it is still debated whether or not the diffusion mechanism is the stronger. Whatever the mechanism, transport of non-esterified fatty acid into cells is regarded to be passive (i.e. not ATP-requiring) and concentration driven (6;67;75). The diffusion (or transport) of non-esterified fatty acid between plasma and interstitium depends on the concentration gradient between the two compartments, and on both permeability surface area (PS) and on perfusion (BF) in adipose tissue. If the transportation of non-esterified fatty acid between plasma and interstitium is described through a mass balance function, then the flux of non-esterified fatty acid from plasma to interstitium can be expressed as follows:

$$DIFF = PP \cdot \left(\left[NEFA_p \right] - \left[NEFA_i \right] \right)$$

eq. 50

For high permeability (PS >> BF) the value of PP will come close to the rate of perfusion. In adipose tissue the rate of perfusion is reported to be between 2 and 4 mL/100g fat mass/min (34) – around 0.3 L/min in a lean man (around 12 kg fat mass). Capillary permeability-surface area for palmitate was found to be 1.3 ml/g tissue/min at albumin concentrations of 0.44 mM in rabit hearts (6).

4.1.5 Other regulatory mechanisms

There are a number of additional regulators of non-esterified fatty acid metabolism besides those mentioned above. Catecholamines, cortisol and glucagon are hormones, other than insulin, that regulates non-esterified fatty acid metabolism (50). As an example catocholamines are known to stimulate lipolysis, and although catecholamines in plasma do increase acutely after a meal (141), the changes are small compared to what is needed for at significant change in lipolysis (128). And, as the focus here is on non-esterified fatty acid dynamics in the postprandial state, these effects are not considered in detail. Further

glycolysis is needed to produce glycerol-3-phosphate required for fatty acid re-esterification, thus it is possible that glucose can stimulate re-esterification of non-esterified fatty acids in adipose tissue. However, in experiments examining effects of glucose on adipose tissue metabolism, it was not possible to distinguish the effects of glucose from the effects of insulin (38;41;100). Again, looking at postprandial metabolism, it is assumed that glycolysis is sufficient to provide for the re-esterification in adipose tissue.

4.1.6 Postprandial Plasma Non-Esterified Fatty Acid Dynamics Model Equations and Parameters

All model differential equations and the equations representing model fluxes and model parameters are collected in this section. First all model differential equations are shown, the first 3 differential equations represent the 3. order delay on insulin's effect on lipoprotein lipase. The three differential equations describing the 3. order delay are under one described as eq. 51. Similar for the three equations describing the 3.order delay for insulin's delayed effect on adipose tissue lipase a re-esterification, which under one is denoted eq. 52.

$$\frac{dI_1}{dt} = \frac{3}{\tau_{LPL}}([I]-[I_1])$$
$$\frac{dI_2}{dt} = \frac{3}{\tau_{LPL}}([I_1]-[I_2])$$
$$\frac{dI_{LPL}}{dt} = \frac{3}{\tau_{LPL}}([I_2]-[I_{LPL}])$$

eq. 51

$$\frac{dI_4}{dt} = \frac{3}{\tau_{AT}}([I] - [I_4])$$
$$\frac{dI_5}{dt} = \frac{3}{\tau_{AT}}([I_4] - [I_5])$$
$$\frac{dI_{ATL}}{dt} = \frac{3}{\tau_{AT}}([I_5] - [I_{AT}])$$

eq. 52

$$\frac{dNEFA_i}{dt} = \frac{1}{V_i}(LPL + ATL - ATR + DIFF)$$

eq. 53

$$\frac{dNEFA_p}{dt} = \frac{1}{V_p}(-DIFF - FOX - HFU)$$

eq. 54

In the following all postprandial plasma non-esterified fatty acid model fluxes are repeated:

$$ATL = \frac{V_{ATL} \cdot K_{ATL}}{K_{ATL} + [I_{ATL}]} + B_{ATL}$$

eq. 45

$$ATR = \frac{V_{ATR} \cdot [FA_i]}{K_{ATR,FA} + [FA_i]} \cdot \frac{q \cdot [I_{AT}]}{K_{ATR,I} + [I_{AT}]}$$

eq. 46

$$LPL = \frac{V_{LPL} \cdot [TG]}{K_{LPL,TG} + [TG]} \cdot \frac{p \cdot [I_{LPL}]}{K_{LPL,I} + [I_{LPL}]}$$

eq. 47

$$FOX = \frac{V_{FOX} \cdot [FA_p]}{K_{FOX} + [FA_p]}$$

eq. 48

$$HFU = \frac{V_{HFU} \cdot [FA_p]}{K_{HFU} + [FA_p]}$$

eq. 49

$$DIFF = PP \cdot ([FA_p] - [FA_i])$$

eq. 50

Table 5: Postprandial Plasma Non-Esterified Fatty Acid Model Standard Parameters

V_i	0.8	L	Estimated from (99)
V_p	3	L	Estimated from (13)
τ_{LPL}	240	min	(35;66)
τ_{AT}	30	min	(35;55)
V_{LPL}	350		*Estimated from (35;56)
$K_{LPL,TG}$	3000	µM	(22;33).
p	5		(3;96)
$K_{LPL,I}$	200	pM	(35;55;65)
V_{ATL}	50	µmol/kg fat/min	*Estimated from (25;26;35;165)
K_{ATL}	50	µM	(17;25;26;40;150)
B_{ATL}	10	µmol/kg fat/min	(25;26)
V_{ATR}	30	µmol/kg fat/min	*Estimated from (25;164)
$K_{ATR,FA}$	1500	µM	(104)
q	5		Estimated from (3;96)
$K_{ATR,I}$	200	pM	Estimated from (74)
PS	0.025	L/kg fat/min	Estimated from (6;34)
V_{FOX}	444	µmol /min**	*Estimated from (2;11;113;159)
K_{FOX}	478	µM	*Estimated from (2;11;113;159)
V_{HFU}	600	µmol /min	*Estimated from (80)
K_{HFU}	1500	µM	(80)

* Estimation is based on the assumption about the mathematical relationship made here when describing the flux

** For energy expenditure of 1.2 kcal/min

4.2 TESTING POSSIBLE MECHANISM RESPONSIBLE FOR PLASMA NON-ESTERIFIED FATTY ACID OVERSHOOT IN THE LATE POSTPRANDIAL PHASE

In the late postprandial phase plasma non-esterified fatty acid exceeds the basal non-esterified fatty acid concentration. The model presented in the section "Postprandial Plasma Non-Esterified Fatty Acid Dynamics Model Equations" will be used to explore possible mechanisms responsible for the late postprandial non-esterified fatty acid overshoot. One of the processes suggested to drive the plasma non-esterified fatty acid overshoot in the late postprandial period is the increase in plasma chylomicrons and LPL preference towards chylomicrons to other lipoproteins. Another process is the long time response on insulin stimulation of Lipoprotein lipase rate, this effect is already incorporated in the model.

After an overnight fast chylomicron concentration is close to zero, usually less than 50 μM (66), and after a meal it typically rises to around 400-600 μM peaking around 3-4 hours after the meal (66). Lipoprotein lipase prefers larger particles (66;166), and in comparison to VLDL chylomicrons are cleared quickly from plasma. This mechanism of competition between VLDL and chylomicrons for LPL action is incorporated into the model by modifying the function describing lipoprotein lipase (eq. 47) as following:

$$LPL = \frac{V_{LPL} \cdot \left([TG_{VLDL}] + \varepsilon \cdot [TG_{Chylo}] \right)}{K_{LPL,TG} + [TG_{VLDL}] + \varepsilon \cdot [TG_{Chylo}]} \cdot \frac{p \cdot [I_{LPL}]}{K_{LPL,I} + [I_{LPL}]}$$

eq. 55

The parameter ε determines the competitive advances of chylomicrons towards lipoprotein lipase, the higher the value of ε the higher the affinity of chylomicrons for lipoprotein lipase gets in relation to VLDLs affinity for lipoprotein lipase. The affinity of chylomicrons toward lipoprotein lipase is found to be 50 times higher than that of VLDL (166). Similarly, it has been shown that removal of TG from chylomicrons is 10 time

greater than that form VLDL after a mixed meal (36). To explore the effort of this mechanism, on plasma non-esterified fatty acid dynamics in the late postprandial phase, the model is used to simulate postprandial non-esterified fatty acid concentrations after a mixed meal. To do so, data from a study measuring, among other things, plasma insulin, triglyceride and non-esterified fatty acid concentration regularly for 480 min after a mixed meal (43) are used (for more details on the study see the section "Simulation of Mixed Meal". Insulin and triglyceride are used at input to the model, and plasma non-esterified fatty acid concentration is used to compare to simulated plasma concentration. Plasma insulin and triglyceride concentration is showed in figure 26 – the points represent the experimental insulin and triglyceride concentrations, and the lines represent model input concentrations. Input concentrations are determined by linear interpolation between points.

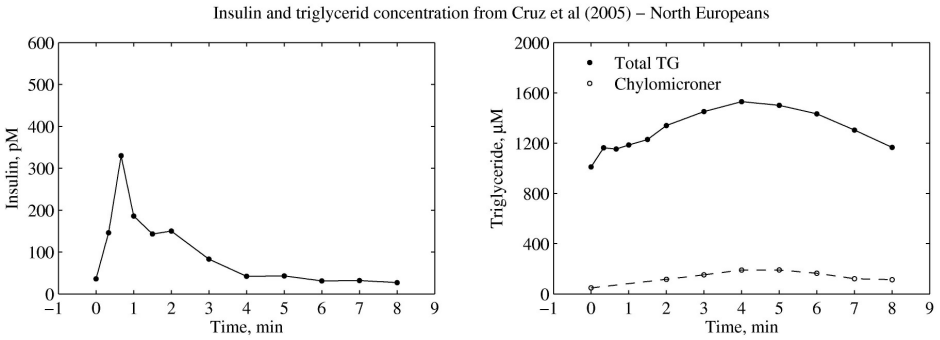

Figure 26: Plasma insulin (left) and triglyceride (right) during the postprandial phase for young healthy North European subjects (43). The points are the experimental measured plasma concentrations, and the lines represent model input concentrations. The plasma insulin and triglyceride concentration are used as input for the model simulation done in this section.

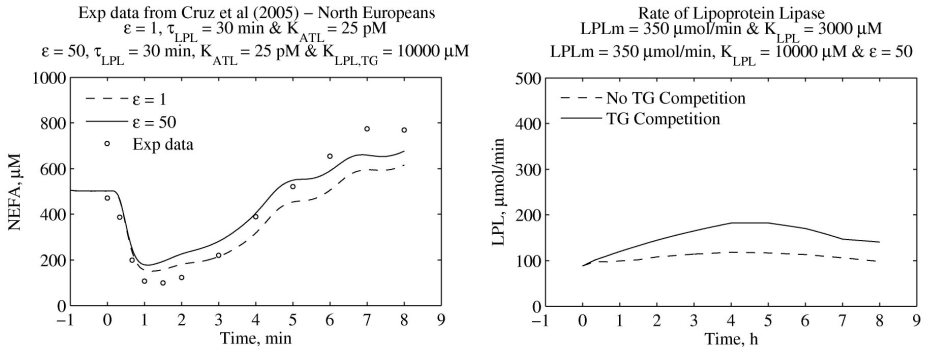

Figure 27: Left -Simulation of postprandial plasma non-esterified fatty acid metabolism, using the modified model, which includes competition between chylomicrons and VLDL-triglyceride towards lipoprotein lipase. Model input data is from Cruz et al (2005) – North European subjects (43), see figure 26. Right - Triglyceride dependent part of lipoprotein lipase rate. Full line is the lipoprotein lipase described by eq. 55 and the broken line is lipoprotein lipase described by eq. 47. Insulin stimulation is set to 1.

First we look at the effect of lipoprotein lipases preference towards chylomicrons, represented in eq. 55, without including the potential effect of lipoprotein lipases delayed response towards insulin. This is done by setting the response time (τ_{LPL}) to 30 min, the same as the time response for insulin's effect on adipose tissue lipase and adipose fatty acid re-esterification (τ_{AT}). The competitive advances of chylomicrons, ε, is set to 50, and half maximum triglyceride concentration for lipoprotein lipase rate, $K_{LPL,TG}$, is increased to reach a reasonable overnight fast lipoprotein lipase rate of around 100 µmol/min (35;56). The simulation is shown in figure 27 left. There is a small effect of including the competition between chylomicrons and VLDL triglyceride; however the effect is not high enough to capture the plasma non-esterified fatty acid overshoot seen in data. It also seems that the effect of the competition between VLDL and chylomicrons for hydrolysis, is not confined to increased lipoprotein lipase in the late postprandial phase, later than 360 min after the meal, but rather through most of the postprandial period, see also figure 27 right. The oscillation which can be observed in the simulation are a result of the methode input insulin is found. Input insulin is found by linear interpolation between the data

points of time series of experimental determined insulin, in this study insulin also excibits small oscillation in the late phase, see figure 26 left. In figure 27 (right) lipoprotein lipase rate during the simulation is shown, without the stimulation from insulin. Choosing ε equal to one corresponds to using eq. 47 to determine model lipoprotein lipase rate.

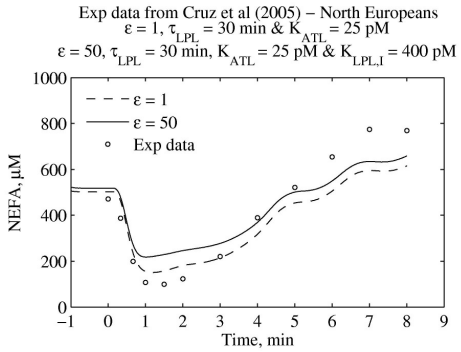

Figure 28: Simulation of postprandial plasma non-esterified fatty acid metabolism, using the modified model, which includes competition between chylomicrons and VLDL-triglyceride towards lipoprotein lipase. Model input data is from Cruz et al (2005) – North European subjects (43), see figure 26.

Instead of increasing $K_{LPL,TG}$, when considering the lipoprotein lipase rate with chylomicron/VLDL competition, insulin stimulation of lipoprotein lipase rate may be decreased by increasing the value of half maximal concentration for insulin stimulation, $K_{LPL,I}$. Such a simulation is shown in figure 28. Again there is a small effect of the chylomicron preferential lipoprotein lipase rate. However it seems to be biggest in the early phase of the postprandial period. The overall conclusion from this model is that it does not appear to be increased lipoprotein lipase rates due to increase in plasma chylomicrons after a meal that is responsible for the late postprandial plasma non-esterified fatty acid overhoot. This conclusion is also supported by experimental data. If the mechanism responsible for the plasma non-esterified fatty acid overshoot, alone is the increase in triglyceride (especially Chylomicrons) we could not observe the late

postprandial non-esterified fatty acid overshoot after an OGTT, where there is no release of Chylomicrones. However, after an OGTT an overshoot in plasma non-esterified fatty acid is observed – see figure 23 Moeri 50g, Moeri 100g and Moeri 150g. Hence, there must be another mechanism underlying the non-esterified fatty acid overshoot.

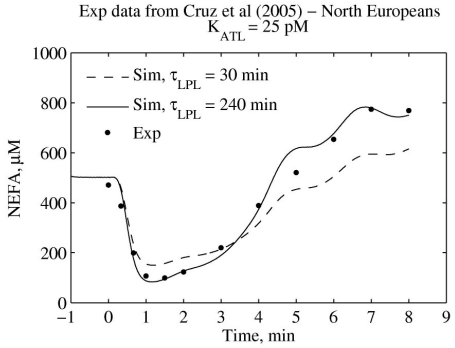

Figure 29: Simulation of postprandial non-esterified fatty acid dynamics with and without long time response on insulin effect on LPL. Again input data from Cruz et al (2005) – see figure 26

Even if chylomicrons increased affinity to lipoprotein lipase compared to VLDL is not the responsible mechanism driving the late postprandial non-esterified fatty acid overshoot, the mechanism could be very interesting when investigating the dynamics of plasma triglycerides, VLDL and chylomicrons. After a meal there is an increase in total plasma triglycerides, however this increase is not only due to the delivery of chylomicrons, but also to an increase in other lipoproteins such as VLDL. The competitive advances of chylomicrons towards lipoprotein lipase, could result in a simultaneous decrease in VLDL clearance by lipoprotein lipase and there by an increase in plasma VLDL concentration.

The other mechanism proposed to drive the late postprandial plasma non-esterified fatty acid overshoot is the long time response related to the effect of insulin on lipoprotein lipase. The model presented in the section “Postprandial Plasma Non-Esterified Fatty

Acid Dynamics Model Equations and Parameters" already includes insulin stimulation of lipoprotein lipase rate and the long time response on this stimulation. By removing the delay of insulin's effect on lipoprotein lipase, the model will be used to explore if insulin and its delayed effect on lipoprotein lipase is the mechanism driving the late postprandial non-esterified fatty acid overshoot. Figure 29 shows a simulation of postprandial plasma non-esterified fatty acid concentration with a time response to insulin stimulation (ε_{LPL}) of lipoprotein lipase of 30 min and of 240 min is shown. The effect of the long time response is clear. The late postprandial non-esterified fatty acid overshoot is increased, and with the time response of 240 min the simulation non-esterified fatty acid overshoot in close to what can be observed experientially. The long time response also decreases plasma non-esterified fatty acid nadir to a concentration similar to the experimental found plasma non-esterified fatty acid nadir around one hour after the meal. This also means that the delayed effect of insulin on lipoprotein lipase is important during the non-esterified fatty acid repression phase, where insulin is high. Lipoprotein lipase rate is stimulated by insulin, and without the response time on this stimulation the non-esterified fatty acid suppression will not be as big as indicated by several studies. The increased adipose re-esterifiction is not high enough to accommodate the increased release of fatty acids from lipoprotein lipase.

4.3 POSTPRANDIAL PLASMA NON-ESTERIFIED FATTY ACID DYNAMICS MODEL PARAMETER SENSITIVITY

The model uses plasma insulin concentration and plasma triglyceride concentration as input. In order to evaluate the model sensitivity to the input parameters, the steady state plasma non-esterified fatty acid concentration is determined for a variety of insulin and triglyceride concentrations see figure 30.

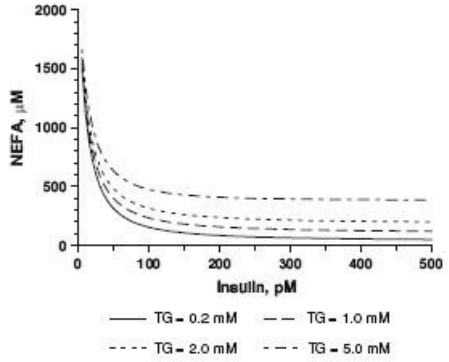

Figure 30: Model simulation - steady state plasma non-esterified fatty acid concentration vs. insulin concentration for four different TG concentrations. All functions and parameters are as described in the section "Postprandial Plasma Non-Esterified Fatty Acid Dynamics Model Equations and Parameters". Fat mass 12 kg.

For healthy subjects in the basal state (overnight fast), the insulin level is typically around 20-80 pM (60 pM (66)) and the triglyceride concentration is around 1000 µM (66). For an insulin concentration of 50 pM and a triglyceride concentration of 1000 µM the model finds the concentration of plasma non-esterified fatty acid to be 400 µM. This corresponds well with measured overnight fasted levels of plasma non-esterified fatty acid in humans (410 – 470 µM (57); 500 µM (66); 370 µM (37)). The model is especially sensitive to insulin concentrations between zero and 100 pM. This suggests that the steady state non-esterified fatty acid concentration is especially influenced by the antilipolytic effect of

insulin on adipose tissue lipolysis. As triglyceride concentration increases the interval where steady state non-esterified fatty acid level is sensitive to insulin decreases.

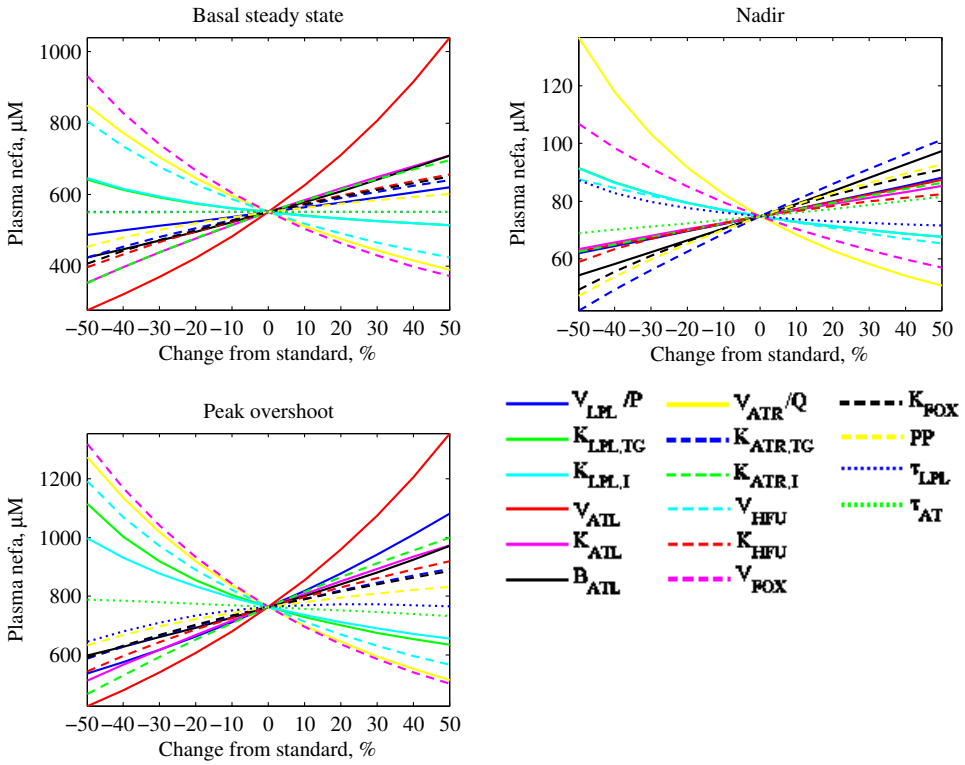

Figure 31: Parameter sensitivity analysis was done using input data from the Coppack study (35), mixed meal, lean subjects. All model parameters are varied ± 50%.

There is some uncertainty about the exact value of the model parameters, in fact it will not be reasonable to assume that any of the parameters has an exact value, and there is most certainly great variance between subject groups and even for the same person at different times. To evaluate the parameter sensitivity of the model simulations using data from a mixed meal lean subjects (Coppack study (35)) are used as input insulin and triglyceride concentrations (For more information about the study see section " Simulation of Mixed

Meal" measured insulin and triglyceride is shown in figure 34). In the study (35) plasma concentrations are measured regularly until 360 min after the test meal and therefore does not capture the late postprandial non-esterified fatty acid overshoot. To include the overshoot in the sensitivity analysis insulin and triglyceride concentrations are kept at 360 min level for simulation time later than that time point. The evaluate model parameter sensitivity simulations are made varying one parameter at a time, all model parameters are varied ± 50% from their standard value. For all simulations the same input data is used. Here the results of the model parameter sensitivity analysis (see figure 31) are presented by the value of plasma non-esterified fatty acid in three states; the overnight steady state plasma non-esterified fatty acid concentration (basal steady state); the minimum plasma non-esterified fatty acid concentration (nadir); and the maximal non-esterified fatty acid concentration (peak overshoot).

For several of the parameters the effect of varying the parameter value is very similar. The result of varying the parameter is often an increase or decrease of plasma non-esterified fatty acid concentration in all points. As an example; look at the parameter V_{FOX} (maximal

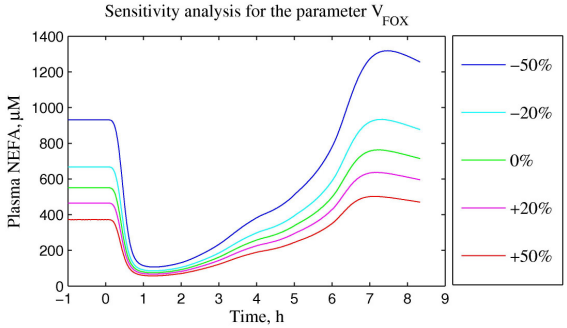

Figure 32: Sensitivity to changes in the parameter V_{FOX} for the dynamics of the postprandial non-esterified fatty acid model. The parameter FOXm was change ± 50% from the value set in table 5.

fatty acid oxidation) – the pink broken line in figure 31 also shown in figure 32. Varying V_{FOX} induces one of the highest changes in plasma non-esterified fatty acid concentration both in basal steady state, in nadir and in peak overshoot.

However, it does not change the general behaviour of the model, merely shifts the plasma non-esterified fatty acid curve upwards or downwards. The value of the parameter V_{FOX} depends on the value of whole body energy expenditure. Here it is considered constant at 1.2 kcal/min based on data for four studies (2;11;113;159), where whole body oxidation was measured regularly during the postprandial phase for both lean and obese subjects at rest. Mean total whole body oxidation form the four studies is 1.2 and maximal variation of - 25% and + 30%.

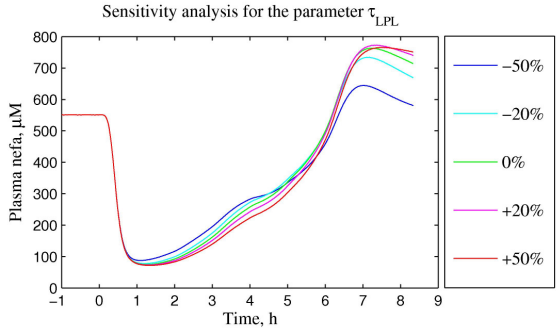

Figure 33: Sensitivity to changes in the parameter τ_{LPL} for the dynamics of the postprandial non-esterified fatty acid model. The parameter τLPL was change ± 50% from the value set in table 5.

The time response for the effect of insulin effect on lipoprotein lipase (τ_{LPL}) - dark blue dotted line figure 31 - is the parameter that has the highest impact on the overall behaviour of the model. In basal steady state the value of the parameter has no influence on the plasma non-esterified fatty acid level. But varying τ_{LPL} induces change in non-esterified fatty acid concentration both in nadir and peak overshoot. Even though, the change in plasma non-esterified fatty acid concentration in nadir and peak overshoot is one of the

smaller changes induced, it is the only parameter that increases plasma non-esterified fatty acid nadir concentration and reduces plasma non-esterified fatty acid peak overshoot concentration. This is also seen for τ_{LPL} decreased to 30 min (-87.5%) as shown in the section "Testing Possible Mechanism Responsible for Plasma Non-Esterified Fatty Acid Overshoot in the Late Postprandial Phase" figure 29. It is only when decreasing the value of τ_{LPL} this situation occurs, when increasing τ_{LPL} nadir non-esterified fatty acid concentration is decreased minimally; while peak overshoot concentration is fairly constant – at least with in the interval of τ_{LPL} investigated here.

The parameters V_{ATL}, Q, P, $K_{ATL,}$ $K_{ATR,I}$ and $K_{LPL,I}$ refer to functions connected to the effect of insulin on the system. Changing the V_{ATL}, Q or P will correspond to changing the amount of enzyme, while K_{ATL}, $K_{ATR,I}$ and $K_{LPL,I}$ refer to the affinity of the enzyme to insulin.

4.4 POSTPRANDIAL PLASMA NON-ESTERIFIED FATTY ACID DYNAMICS MODEL SIMULATIONS

The postprandial plasma non-esterified fatty acid dynamics model is used to simulate different studies investigating the plasma non-esterified fatty acid and insulin response after a meal or in connection to an oral glucose tolerance test (OGTT). Experimentally measured plasma insulin and triglyceride concentrations from different studies are used as inputs to the model. To obtain a full insulin and triglyceride profile, with an insulin and triglyceride concentration for every simulation time point, linear interpolation drawn between the measured data points is made to represent the concentrations in the time between measurements. With this input the model simulate a postprandial plasma non-esterified fatty acid profile, which is compared to experimentally measured concentrations. For the different studies, model parameters have been changed in order to get simulations that correspond to the experimentally observed plasma non-esterified fatty acid profile. The parameters changes may help us to detect changes in the regulation of the metabolic system. In general, it is parameters representing the affinity of insulin towards different stimulatory / inhibitory effects in the model that have to be changed in order to obtain a simulated plasma non-esterified fatty acid profiles that are similarly to the experimental observed profiles.

4.4.1 Simulation of Mixed Meal

In this section the postprandial plasma non-esterified fatty acid model is used to simulate the dynamical response of plasma non-esterified fatty acid to a mixed meal in healthy subjects. With a mixed meal we mean a meal consisting of fat and carbohydrate as well as protein.

The first simulation shown here is a simulation of the results obtained by Coppack *et al* (35). This simulation is meant as a control, in order to see if the model is able to replicate the experimental observed plasma non-esterified fatty acid response to a meal. The study consists of a control group of ten healthy subjects (five female), mean age 38 years, body mass 66 kg, height 1.70 m, BMI 23 kg/m^2 and fat mass 16 kg. The test meal contained a total of 3100 kJ (740 kcal), and was combined of 33.5 g fat, 93 g carbohydrate and 21.9 g protein. Plasma triglyceride, non-esterified fatty acid and insulin were measured in regularly intervals until 360 min after the test meal was given. The experimental data of plasma non-esterified fatty acid, insulin and triglyceride from the Coppack, *et al* (35) study of lean healthy controls is shown in figure 34, together with the model simulation of this study. In the plot to the left, the simulated plasma non-esterified fatty acid concentration can be compared with the experimental measured plasma non-esterified fatty acid concentration. In the this simulation all model parameters concur with the standard parameter set, see table 5. The model does a good job in capturing the dynamical behaviour of plasma non-esterified fatty acid in the postprandial state. Shortly after the meal is given (time zero) the plasma non-esterified fatty acid concentration decreases drastically reaching a nadir of about 75 μM at around 60 min after meal time. Hereafter, the plasma concentration increases, in a less drastic matter, reaching a concentration close to the initial plasma concentration at 360 min. The study is stopped after 360 min and no

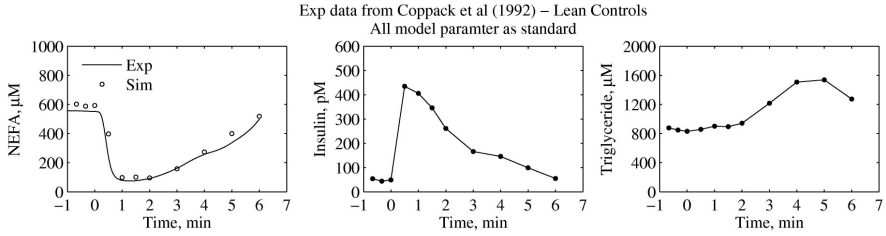

Figure 34: Model simulation of plasma non-esterified fatty acid concentration after a mixed meal given to healthy lean subjects, Coppack *et al* (1992). Plasma non-esterified fatty acid from study and the simulated plasma non-esterified fatty acid are shown in the plot to the left. The middle and right plots show plasma insulin and triglyceride from the experimental study; they are used as model input. All parameters are as in table 5.

overshoot can be observed. However, as noted, the plasma non-esterified fatty acid overshoot in the late postprandial phase is often observed after 360 min.

Next the model was used to simulate the postprandial plasma non-esterified fatty acid response after a mixed meal, given to 3 different ethnic groups, North European, South Asians and Latin Americans, study by Cruz, *et al.* (2001)(43). The study seek to investigate whether the higher susceptibility of coronary heart disease and diabetes in South Asian immigrants to the UK compared with the Caucasian population may reflect insulin resistance and altered postprandial lipid metabolism. The study consisted of 25

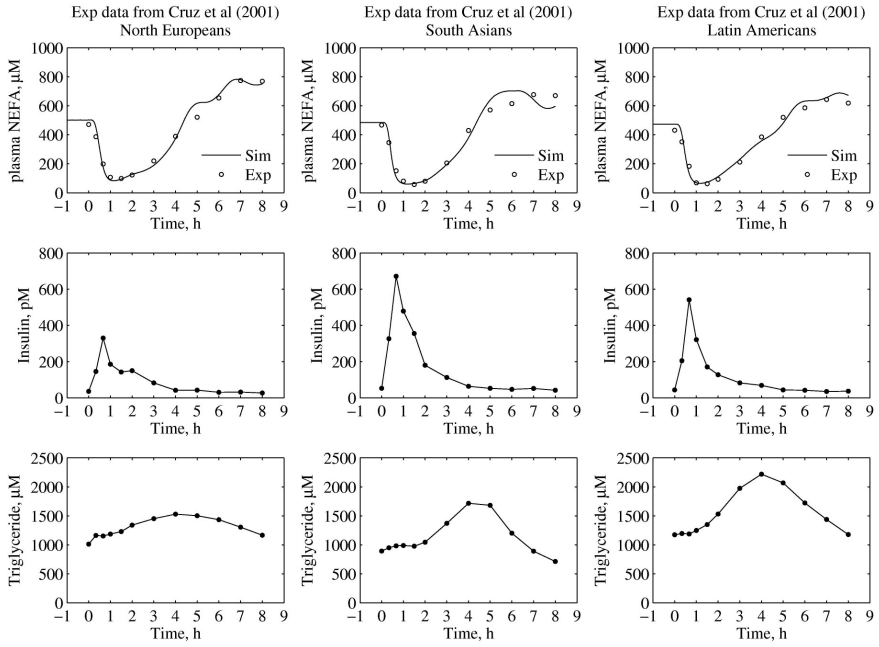

Figure 35: Simulation of studies in Cruz, et al (2001)(43), mixed meal given to 3 different ethnic groups. The plots in the top of the figure show model simulations and experientally measured plasma non-esterified fatty acid concentrations after a mixed meal. The middle and bottom plots show experientally measured insulin and plasma triglycerides after the mixed meal, respectively. The experiental insulin and triglyceride profiles are used as inputs to the model.

healthy men, age between 22-40 years and BMI 19-27 kg/m^2. The test meal provided 52% of the energy as fat, 40% as carbohydrate and 8% as protein, the total energy content was not reported. The meal was given after a 14 hour fast, and plasma triglyceride, glucose, insulin and non-esterified fatty acid was measured in regularly intervals for 480 min after the test meal were given. Model simulation of postprandial plasma non-esterified fatty acids, experimental input data and experimental data for plasma non-esterified fatty acids for all three groups are shown in figure 35.

Table 6: Changes in model parameter for simulation of the different ethnic groups (43).

	V_{ATL} μmol/kg fm/min	K_{ATL} pM	p	$K_{LPL,I}$ pM
Standard parameter	50	50	5	200
North Europeans	-	25	-	-
South Asians	-	45	3.5	-
Latin Americans	40	40	3.5	250

For the model simulation of the three studies to capture the experimental observed plasma non-esterified fatty acid profile, parameters had to be changed for all three groups. The changed parameters are shown in table 6 all other parameters are as in table 5. Fasting plasma insulin for the North Europeans is relative low (36 pM). This indicate high insulin sensitivity. Roughly fitting model plasma non-esterified fatty acid to the experimental measured can be done by decreasing K_{ATL} from 50 pM to 25 pM, implying increased affinity for insulin to inhibit adipose tissue lipase. Physiologically this also seems reasonably since K_{ATL}, which corresponds to EC50 for insulin inhibition on adipose tissue lipolysis has a considerable variation in healthy humans (150), with reported EC50 values between 10 pM to 140 pM (17;25;26;40;150). For the two other groups; the South Asians and the Latin Americans, fasting plasma insulin is 53 pM and 44 pM respectively, which does not indicate especially increased insulin sensitivity. However the peak insulin concentration, after the meal, is higher for both groups compared to the North Europeans, and so are plasma triglycerides (see figure 35). Despite the increased insulin and triglycerides responses there are no changes in the plasma non-esterified fatty acid response. This could indicate a reduced lipoprotein lipase rate. For the South Asian group;

the model could replicate the plasma non-esterified fatty acid dynamics profile by decreasing the stimulatory effect of insulin on the rate of lipoprotein lipase. For the Latin American group, the stimulatory effect of insulin was decreased further by also decreasing the affinity of insulin for lipoprotein lipase stimulation. If the model setup is accepted as a quantitative description of lipid metabolism, this simulation indicates the regulation of lipid metabolism is impaired in the South Asian and Latin American group.

4.4.2 Simulation of OGTT studies

During oral glucose tolerance tests plasma non-esterified fatty acid decreases almost immediately after glucose is given and minimal non-esterified fatty acid concentration can be observed about 30 min after peak insulin concentration. As for mixed meals, plasma non-esterified fatty acid concentration rebounds and overshoots its initial value, with out any increase in plasma triglyceride. The model is used to simulate oral glucose tolerance tests by Moeri *et al* (1988) (113). The study includes 8 healthy men age 22 years and BMI 21.7 kg/m^2. The amount of body fat is not reported, however a fat mass of 12 kg will be used. The study consisted of three OGTT; 50 g glucose, 100g and 150 g glucose. Plasma triglyceride concentration is not reported in the study, for the simulation the triglyceride concentration is considered constant at 1000 μM. Similar studies report little or no change in plasma triglyceride concentration during OGTT (23;91).

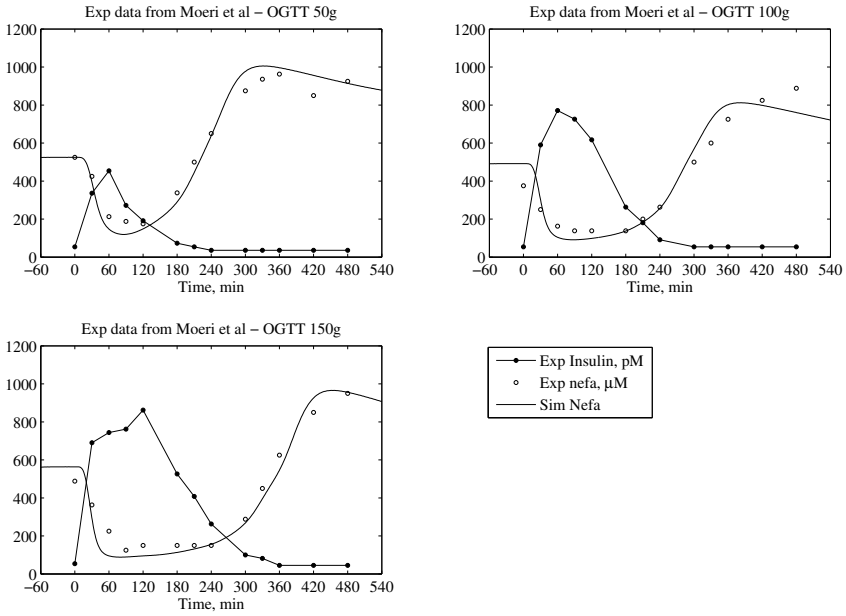

Figure 36: Experimental data from three OGTT's with 50 g, 100 g and 150 g glucose, in healthy subjects (113). Time series of plasma non-esterified fatty acid (○) and insulin (●) are shown for all three OGTT's, glucose is given at time zero, and the full line is the model simulation of plasma non-esterified fatty acid**.** Input plasma triglyceride is considered constant at 1000 µM through out the simulation, since no plasma triglyceride is reported in the studies.

For each of the glucose loads (50, 100, and 150 g), non-esterified fatty acids levels are simulated (figure 36) and compared with the experimental values. In order to get the best fit, some parameters were slightly adjusted from the standard parameters (the same parameters for all three experiments), see table 7, all other parameters are as stated in the standard parameters for the postprandial plasma non-estrified fatty acid model, see table 5. The parameter changes used for the simulation of OGTT are not unambiguous. However the selected combinations of parameters are those which are related to the effect of insulin, and are all within their physiological ranges.

Table 7: Changes in model parameter for simulation of OGTTs (113).

	K_{ATL} pM	q	p	$K_{LPL,I}$ pM
Standard parameter	50	5	5	200
OGTT	80	2.5	2.3	150

The time series of insulin and plasma non-esterified fatty acids measured during the three OGTTs (113) and the model simulation of the three OGTTs shows how the drop in the non-esterified fatty acids level depends on the amount of glucose ingested. Ingestion of a high amount of glucose results in the highest AUC of insulin. The postprandial non-esterified fatty acids dynamics can be described with four phases. In the first phase, the rise in insulin results in a suppression of adipose tissue lipase (ATL) and in non-esterified fatty acids. In the second phase, the non-esterified fatty acids levels are at its lowest while insulin remains high. In the third phase, the drop in insulin causes the non-esterified fatty acids levels to return to initial levels. In the last phase, insulin is at its initial level while non-esterified fatty acid concentration is increasing above its initial value. This gives an overshoot in plasma non-esterified fatty acids levels. This simulation of OGTT emphasises, the findings in the section "Testing Possible Mechanism Responsible for Plasma Non-Esterified Fatty Acid Overshoot in the Postprandial State" that the mechanism driving this overshoot is the delayed effect of insulin on lipoprotein lipase activity. However, the decrease in the parameters connected to insulin effect on lipoprotein lipase and adipose tissue re-esterification, could indicate influence of the plasma triglyceride concentration on the plasma non-esterified fatty acids also in the earlier phases of postprandial state should not be underestimated. During this simulation the plasma triglyceride concentration is kept constant at 1000 μM, since no plasma triglyceride concentration was reported in the studies.

Non-esterified fatty acids oxidation is substrate dependent and decreases in the early phase of the OGTT. In the same way, the simulation gives a drop in hepatic non-esterified fatty acids uptake, data not shown.

4.4.3 Simulation of mixed meal studies for obese and diabetic subjects

The last two simulations performed, with the postprandial plasma non-estrified model are simulations of a study of obese subjects and of obese diabetic subjects. The first study by Coppack et al (2002) (35), with 8 obese subjects (five female), age 45 years, BMI 42 kg/m^2, fat mass 48 kg. The test meal contained a total of 3100 kJ (740 kcal) and consisted of 33.5 g fat, 93 g carbohydrate and 21.9 g protein. Plasma triglyceride, non-esterified fatty acid and insulin were measured in regularly intervals 360 min after the test meal was

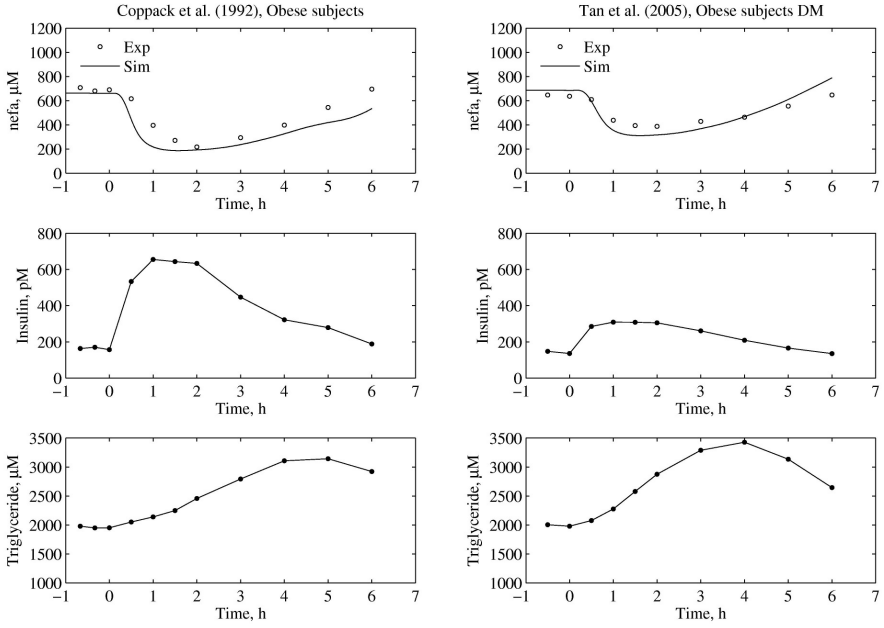

Figure 37: Simulation of postprandial non-esterified fatty acid dynamics of obese subjects from Coppack et al (1992)(35) and obese subjects with type 2 diabetes (DM) from Tan et al (2005)(151). Fat mass 48 kg for the obese and 40 kg the obese DM group (Fat mass not reported in Tan et al (2005), the used fat mass is estimated based on BMI). The only parameter changed from the standard is K_{ATL} = 110 pM.

given. The second study simulated is by Tan et al (2005) (151). It included 24 obese subjects with type 2 diabetes, fasting glucose between 7-12 mM, none were taking any

medication known to affect glucose metabolism. All subjects in the study were between 30-70 years and with a BMI 32.8 kg/m^2. Fat mass was not reported in the article, but in the simulation it is set to 40 kg, estimated on basis of BMI.

Table 8: Changes in model parameter for simulation of Coppack *et al* (1992) obese and Tan *et al* (2005) obese diabetics.

	K_{ATL} pM
Standard parameter	50
Coppack – obese	110
Tan – obese diabetic	110

For the model simulation of the obese and obese diabetic subjects to be compatible to measured plasma non-esterfied fatty acid concentrations, it required an increase in the insulin concentration for half maximal suppression of adipose tissue lipase, K_{ATL}. The high K_{ATL} concentration is in good agrement with the failure to suppress adipose tissue lipolysis in the normal manner, in response to postprandial hyperinsulinemia, which is often related to obesity (90). The increased insulin concentration for half maximal suppression of adipose tissue lipase, K_{ATL}, for obese is in accordance with the clinical observed (25;26). Unfortunately the duration of the studies simulated are not long enough

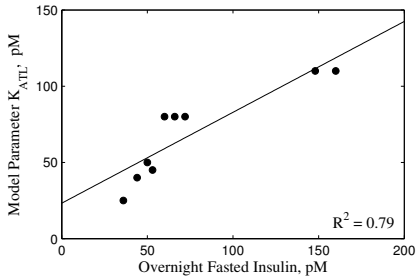

Figure 38: Relation between model parameter K_{ATL} and fasting insulin level.

to capture the plasma non-esterified fatty acid overshoot, as so we can not detect any changes in the regulation of lipoprotein lipase.

Common for all simulations shown above are that the parameter for half maximal inhibition of adipose tissue lipase (K_{ATL}) can be determined based on the level of basal insulin.

4.5 DISCUSSION AND CRITIQUE OF THE POSTPRANDIAL PLASMA NEFA DYNAMICS MODEL

The ability of the model to describe early postprandial plasma non-esterified fatty acid dynamics is fairly good. However several models are published which can describe this behaviour. Common for other models of non-esterified fatty acid metabolism (121), including the one described here, is the high inhibitory effect of insulin on adipose tissue lipase. When modelling different subjects/patient groups changing the parameter K_{ATL}, which describes insulin affinity for adipose tissue lipase, will make the model reaching compatible plasma non-esterified fatty acid levels. Moreover changing this parameter, in order to fit model simulation to data, seems reasonable since physiological realistic interval is very large. The model simulations shown above reveal a relation between the overnight fasted insulin concentration and the value of K_{ATL}. Low overnight fasted insulin concentration seems to require a high affinity of adipose tissue lipase towards insulin (low K_{ALT} value), see figure 35 – North Europeans. While high overnight fasting insulin concentration, as for obese subjects (see figure 37), seem to require a lower affinity of adipose tissue lipase towards insulin (high K_{ATL} values).

For the late postprandial period the current model is able to capture the plasma non-esterified fatty acid overshoot. According to this model the dynamics of this overshoot is controlled by the lipoprotein lipase, its sensitivity to insulin and, very importantly, the large response time in connection to the stimulatory effect of insulin on lipoprotein lipase. In relation to the lipoprotein lipase, the model is used to test if the effect of different lipoproteins on lipoprotein lipase is responsible for driving the late postprandial plasma non-esterified fatty acid overhoot. Chylomicrons are reported to have 50 fold higher affinity towards lipoprotein lipase than of VLDL. It was found that this mechanism could no explain the late postprandial plasma non-esterified fatty acid overshoot. However, in this connection it is important to note that the form of the function describing the competition between chylomicron-triglyceride and VLDL-triglyceride towards lipoprotein

lipase (eq. 55), is very simple. The advance of chylomicron-triglyceride is described by increasing the apparent chylomicro-triglyceride concentration, in relation the real chylomicron-triglyceride concentration. A more correct relation would be to use the michaelis-menten function for competitive inhibition. The function looks as follows:

$$v = \frac{V_{\max} \cdot [S]}{Km \cdot \left(1 + \frac{[I]}{Ki}\right) + [S]}$$

eq. 56

where v is the reaction rate, V_{max} the maximal velocity, and [S] the substrate concentration. Km is the half maximal velocity concentration of substrate, [I] the inhibitor concentration, and Ki is the inhibition constant. But the required information about the kinetics for the rate of chylomicron-triglyceride removal by lipoprotein lipase was not found.

The model was used to identify the mechanism responsible for the late postprandial plasma fatty acid overshoot observed experimentally. However it was not possible to use the model to investigate if this overshoot can account for the difference between the metabolic response to the first meal after an overnight fast and the second meal. This was not possible due to lack of data, the model needs plasma insulin and triglyceride as input, and it was not possible to find at study where these variables were measured and reported for both the first and the second meal.

5 ADIPOSE TISSUE DISTRIBUTION

Fat accumulation in the visceral area is believed to be particularly dangerous because it is highly correlated with cardiovascular and metabolic risk factors such as elevated blood pressure, dyslipidemia, insulin resistance, and type 2 diabetes (10;47;60;162). Thus, reduction of visceral adipose tissue (VAT) may be especially beneficial. Fortunately, negative energy balance appears to cause VAT to decrease faster than total fat mass (FM) (145) which may explain the early metabolic benefits of weight loss. But are some weight loss methods better than others at generating a targeted or selective reduction of VAT?

5.1 ALLOMETRIC RELATIONSHIP BETWEEN CHANGES OF VISCERAL FAT AND TOTAL FAT MASS

Several years ago, Smith et al. addressed the issue of selective reduction of VAT by reviewing published studies that measured VAT as well as total fat mass (FM) changes during weight loss and found that most weight loss interventions caused a preferential loss of VAT (145). These authors concluded that the absolute amount of VAT loss was related to both the amount of FM loss as well as the initial VAT (145), but a clear mathematical relationship between these variables was not determined.

This study updates and extends the observations of Smith et al. (145) and test the hypothesis that changes of VAT mass and FM are allometrically related according to the following differential equation:

$$\frac{dVAT}{dFM} = k \cdot \frac{VAT}{FM}$$

eq. 57

where k is a dimensionless constant and VAT and FM denote the initial values of visceral adipose tissue and total fat mass. This class of equation has a long and rich history and was first used by Huxley to describe the law of constant differential growth between various body parts of an organism (85). It is shown that this allometric relationship accurately describes the published data on changes of VAT and FM and that the same relationship holds regardless of gender or the type of weight loss intervention.

5.1.1 Method

Published studies were included in this analysis if FM and VAT were measured before and after a weight loss intervention in humans, regardless of the method of weight loss. Total fat mass was measured by dual energy X-ray absorptiometry (DEXA), underwater weighing, and air displacement plethysmography, via whole-body computed tomography (CT) or via magnetic resonance imaging (MRI). Studies measuring FM changes using bioelectric impedance or anthropomorphic methods, such as skin-folds, were excluded. MRI or CT imaging was used to assess VAT changes.

Since the hypothesized allometric equation is an expression involving VAT mass, converting cross-sectional VAT areas to volumes using the regression equations described by Shen (144) was done. (This procedure was unnecessary for studies that measured VAT volumes using multi-slice CT or MRI.) Since different regression equations are used to convert cross-sectional areas to volumes in men and women, it was required that the studies report the VAT areas for men and women separately. Furthermore, the regression equations required that the slice location had to be either at L4-L5 for either genders or 5 cm above L4-L5 for women and 10 cm above L4-L5 for men. L4-L5 referrer to the L4-L5 intervertebral space in the spinal cord. This is in the lower part of the spinal cord. We assumed an adipose tissue density of 0.93 kg/L.

A search for studies matching the above inclusion criteria in both PubMed and Web of Science databases using the search term “weight loss visceral adipose tissue” was done.

On July 4th 2007, the PubMed search returned 83 hits and the Web of Science search returned 335 hits, 65 of which were duplicates also found in the PubMed search. Examination of the abstracts reduced the number of studies possibly matching the search criteria to 131. Investigation of the methods sections of these remaining reports further narrowed the number of studies to a total of 34 that fulfilled the inclusion criteria. The citations from these 34 reports were then surveyed for studies not found by the initial search, and resulted in an additional 3 studies such that 37 total studies matched the inclusion criteria.

In appendix A, it is shown that the allometric hypothesis requires that the ratio of the change of VAT to the change of FM, $\Delta VAT/\Delta FM$, is proportional to the initial ratio of VAT to FM, VAT/FM .Therefore, these ratios were calculated and it was investigated whether or not a linear relationship existed. Typically, such an analysis would be completed using a weighted least-squares linear regression method that assumes that only the y coordinate is associated with uncertainty. However, in the present case this cannot be assumed since the data had uncertainties in both the x and y coordinates. Therefore a combination of the use of traditional weighted linear regression, which accounts for the uncertainties in the y direction, along with a Monte-Carlo strategy to take the uncertainties in the x direction into account, was used. For each Monte-Carlo iterate, a random set of x variables was chosen such that each x value was normally distributed about the data point with a standard deviation given by the uncertainty of each data point. For each Monte-Carlo iteration, a weighted least-squares regression procedure to fit to the line y = k*x were performed. The model parameter k was estimated as the average over 10000 Monte-Carlo simulations. All model statistics were then assessed based on this average linear model. Outlier assessment based on the Cook's distance and studentized residuals were calculated using the standard deviations of the data points.

The x variable (initial VAT/FM) and y variable (ΔVAT/ΔFM) in the analysis were transformations of the reported VAT and FM data. Since the initial VAT and FM

measurements were included in both x and y variable calculations, the data transformation introduced dependences between the variables that could possibly lead to spurious correlations (19). The analysis also included testing for spurious correlations by randomly shuffling the VAT and FM measurements 10000 times and calculated the coefficients of determination (i.e., the Pearson correlation coefficient squared, r^2) of the resulting x and y variables. If the data transformation procedure itself introduced significant correlations, then the r^2 calculated using the shuffled data should frequently exceed the r^2 determined from the un-shuffled data. The probability of a spurious correlation was estimated as the fraction of the 10000 r^2 values obtained using the shuffled data that exceeded the observed r^2 value of the original un-shuffled data.

5.1.2 Results

The systematic review produced a total of 37 weight loss intervention studies, representing 1407 subjects and 79 data points (see appendix B for table of data included in this study). The population comprised 24% men and 73% women, of which 27% were postmenopausal. The number of gender was not reported for 3% of the subjects. These studies investigated a wide range of weight loss interventions including caloric restriction (20;31;48;49;68;69;71;73;87;88;98;116;117;126;127;131-134;138;140;152;154;157;163), endurance exercise (12;46;53;69;98;102;115-117;119;126;131-134;137;138;143;153;154), resistance exercise (87;88;127;130;134), and bariatric surgery (24;70;101). One study reported data from women with type 2 diabetes (T2DM) (69) and another study investigated HIV positive women (53).

The loss of visceral fat mass relative to the total loss of fat mass ($\Delta VAT/\Delta FM$) was potted against the initial visceral fat mass divided by the total fat mass (VAT/FM). Figure 39 clearly shows a linear relationship between these two ratios which is consistent with our hypothesis that VAT and FM changes are allometrically related. The calculated dimensionless model parameter was $k = 1.3 \pm 0.1$ with an $R^2 = 0.73$ indicating that the model explained more than 70% of the variability in the reported data. We found no

evidence of spurious correlations since none of the 10000 shuffled VAT and FM data sets produced a coefficient of determination higher than that observed for the original data. The residuals of the model, plotted in figure 39 right, indicate no general trend. There were no outliers detected by examination of Cook's distance (maximum value was 0.04) or studentized residuals (maximum magnitude was 1.05). The chi-square was 4.6 and, based on an evaluation of the incomplete gamma function, the probability is less than 10^{-33} that the chi-square for a correct model should be less than the chi-square calculated for this model (123). In other words, the allometric model provides an excellent fit to the data.

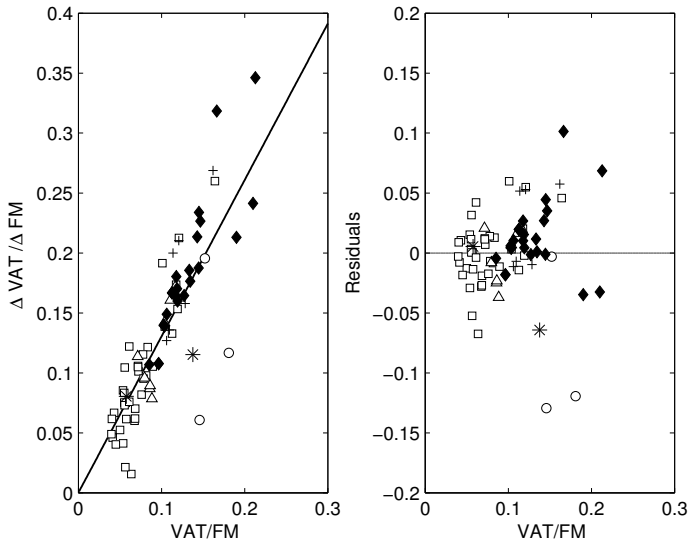

Figure 39: Left - Changes of visceral fat mass relative to the change of total fat mass (ΔVAT/ΔFM) versus the initial visceral fat mass divided by the total fat mass (VAT/FM) as compiled from 37 published studies of weight loss representing more than 1400 subjects. Male subjects (♦) had higher initial VAT to FM ratios compared to healthy pre-menopausal women (□), post-menopausal women (Δ), HIV positive women (◊), or women with type 2 diabetes (○). Crosses (+) indicate studies that reported a mixture of men and women. The line corresponds to the best fit allometric relationship to the weight loss data with $k = 1.3 \pm 0.1$ and $R^2 = 0.73$. Data from two weight gain interventions (*) are also plotted. Right - Residuals of the best fit allometric model versus the initial VAT to FM ratio.

Nevertheless, this measure of the model fit may be somewhat overestimated since the uncertainties for each data point were large due to the fact that access to data was limited to the reported group averages in each published study. (The average calculated uncertainty of the data points was $\hat{\sigma}_x = 0.05$ and $\hat{\sigma}_y = 0.3$ in the x and y directions, respectively.) For clarity, the error bars are omitted from the figures.

Both men and women were described by the same allometric relationship, where k = 1.3 ± 0.2 for both groups calculated separately which was the same as the overall best fit line with k = 1.3 ± 0.1. However, the male subjects on average had a higher initial VAT to FM ratio as indicated by the closed black diamonds (♦) in comparison to the open symbols

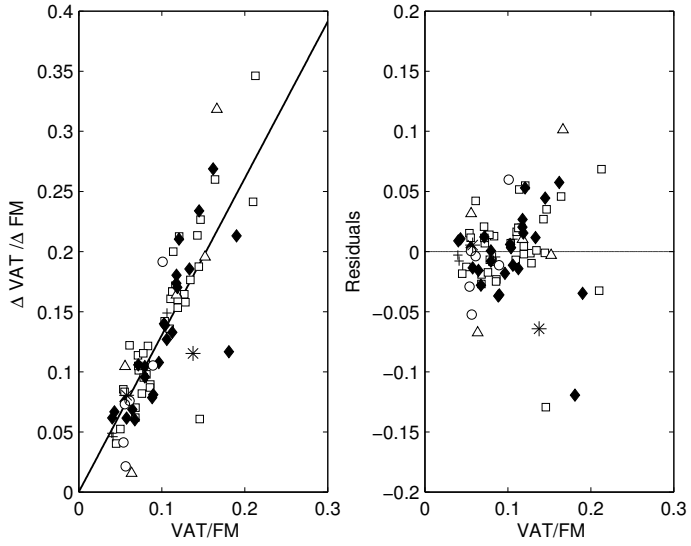

Figure 40: Left -The same data as in Figure 1 are represented according to the type of weight loss intervention as follows: caloric restriction alone (□), caloric restriction with aerobic exercise (♦), caloric restriction with resistance exercise (+), exercise alone (Δ), and bariatric surgery (○). Data from two weight gain interventions (*) are also plotted. Right - Residuals of the best fit allometric model versus the initial VAT to FM ratio.

(women) in figure 39 left. Crosses indicate studies that reported a mixture of men and women (+).

Figure 40 (left and right) depicts the same data coded by weight loss intervention. The allometric relationship applied equally well to all weight-loss interventions as can be seen from the fact that no particular intervention deviated systematically from the overall best fit line with k = 1.3 ± 0.1. The calculated allometric constants determined separately for each group were no different from the overall best fit value since k = 1.2 ± 0.2 for caloric restriction alone (□), k = 1.4 ± 0.2 for caloric restriction with aerobic exercise (♦), k = 1.3 ± 3 for caloric restriction with resistance exercise (+), k = 1.5 ± 0.7 for exercise alone (Δ), and k = 1.4 ± 1 for bariatric surgery (○).

5.1.3 Discussion of Allometric Relationship

VAT is often considered to be a labile fat depot based on the observed preferential loss of VAT with weight loss (145), along with the *in vitro* observations that visceral adipocytes are more lipolytically active (108;112), and are therefore believed to have a higher fat turnover rate when compared with subcutaneous adipocytes. Others have hypothesized that VAT is a secondary fat storage pool that accumulates during positive energy balance only after subcutaneous stores are full (146). Some have suggested that exercise specifically mobilizes VAT as a result of preferential stimulation of VAT lipolysis (114). Here, it is demonstrated that the VAT changes in parallel with FM changes and that the magnitude of VAT change is primarily determined by FM change according to an allometric relationship and does not depend on the method of weight loss.

Allometric equations have historically been used to describe relationships between the relative growth of various body parts of an organism (85). To see this, eq. 57 can be rearranged as follows:

$$\frac{1}{VAT}\frac{dVAT}{dt} = k \cdot \frac{1}{FM}\frac{dFM}{dt}$$

eq. 58

thereby indicating that the relative growth rates of VAT and FM are proportional to each other. The fact that the best fit value of the constant k was greater than 1 (i.e., k = 1.3 ± 0.1) corresponds to the observation of preferential VAT changes versus FM changes. The fact that this same value for k adequately describes both genders as well as a wide variety of weight loss interventions suggests that differences between men and women can be explained by the initial VAT to FM ratio and there is no preferential benefit of one weight loss intervention over another.

Also data matching our inclusion criteria from two weight gain interventions was found, one examining recovery of anorexic women (109) and the other was an overfeeding study of healthy young men (18). These weight gain data also appeared to follow the allometric relationship as depicted by asterisks (*) in figure 39 and figure 40, but they were not used in the model fitting procedure. Future work should investigate the applicability of the allometric relationship in weight gain studies.

In their 1999 review of VAT changes with weight loss, Smith et al. introduced a selectivity index to facilitate comparisons between weight loss interventions and quantify their ability to selectively target VAT (145). The selectivity index was defined as the percent change of VAT divided by the percent change of FM which is mathematically identical to the allometric constant k. The observation that the same value of k adequately represented various types of weight loss interventions conforms to Smith et al.'s conclusion that no clear pattern was detected for the selectivity index across the interventions (145). However, Smith et al. claimed that the selectivity index depended on the initial proportion of visceral fat in a subset of studies that reported single slice area ratios of initial VAT to subcutaneous adipose tissue (SAT). In this subset of data, also a

weak positive correlations between the selectivity index with both the initial VAT/FM and VAT/SAT (r^2 = 0.26 and 0.29, respectively) was found. However, there is a high probability that these correlations were spurious since shuffled data produced higher r^2 values than the un-shuffled data 15% of the time. Furthermore, the autors found no significant correlations of the selectivity index as a function of initial VAT/FM in the full dataset (r^2 = 0.03). Thus, the data are consistent with a constant selectivity index identical to the allometric constant k which is independent of the initial proportion of VAT.

The allometric equation (eq. 57) can be integrated to give a power law relationship:

$$VAT = b \cdot FM^{k}$$

eq. 59

where b is a parameter that sets the baseline amount of VAT for a given initial FM. Unlike many reported allometric relationships, the value of b is not a universal constant in this case. Rather, b depends on gender as well as other potential factors that contribute to determining the baseline VAT. Thus, the typical log-log plots often used to assess allometric relationships in this case produces a scatter of points since the values of the parameter b vary widely across race and gender groups (not shown).

The allometric model also predicts that VAT is lost preferentially compared with subcutaneous adipose tissue (SAT) with modest weigh loss, but the effect is attenuated with greater weight loss, which is documented in the literature (27). For a more comprehensive description of this conclusion see appendix A.

The most obvious limitation of the present analysis is that the calculated uncertainties of the data points are quite large due to the fact that we only had access to the reported average values from the published studies. Future studies should investigate these relationships using data on body composition change in individual subjects. Despite this

limitation, a clear relationship was apparent in the data and the allometric model described this relationship remarkably well. This analysis therefore suggests that changes of VAT mass are determined primarily by FM changes as well as the initial ratio of VAT to FM and is independent of gender or the method of weight loss intervention. In conclusion, it is suggested that future investigation should use the allometric model prediction as a null hypothesis to test for an additional independent effect of weight loss on visceral fat loss.

6 DISCUSSION AND CONCLUSION

The five models described here were used to investigate different aspects of glucose and fat metabolism and the regulation of the two metabolic pathways. The models were applied both to look for relations between hormones and metabolic fluxes, and to identify mechanism relevant for specific metabolic phenomena.

The glucose and fat metabolism steady state model illustrated the importance of considering the interplay between the two metabolic pathways when interpreting experimental results from, for example, glucose clamp studies. Fat metabolism in indirectly regulated by glucose metabolism through insulin, and glucose metabolism is regulated indirectly by fat metabolism through the rate of glucose oxidation. The glucose and fat steady state model combined with the simple model of hexokinase showed the different aspects in the regulation of glucose transport, and it was pointed out that glucose transport and its stimulation by insulin is not the only processes to consider when describing plasma glucose concentrations. It is equally important to consider glucose utilisation within the cells. This could be oxidation, lactate formation, lipogenesis or glycogen formation.

The next model described in this thesis, involves the formation and breakdown of glycogen in the liver. The hepatic glucose metabolism model was used to demonstrate the regulatory effect of glucose on both glycogen synthesis and glycogen breakdown is necessary to describe the relation between glucose concentration and hepatic glucose output, under conditions similar to the overnight fasted state (insulin and glucagon at basal level). This section also showed that the rate of glycogen synthesis and breakdown is regulated by glycogen it self. Although it was not possible to identify the mechanism behind this regulation, it could only be concluded that both glycogen inhibition of glycogen synthase and glycogen stimulation of glycogen phophorylase can explain the relation between net glycogen synthesis/breakdown observed experimentally.

The postprandial plasma non-estrified fatty acid model was used to identify the mechanism responsible for the experimentally observed late postprandial plasma fatty acid overshoot. The model showed that the overshoot can be explained by insulin delayed effect on lipoprotein lipase and not by the differential affinity of lipoprotein lipase towards chylomicron-triglyceride and VLDL-triglyceride as otherwise suggested in the literature (9). Although the mechanism responsible for the late postprandial fatty acid overshoot was identified in was not possible to investigate if this overshoot can explain the experimentally observed difference between the metabolic response to the first meal and the second meal after an overnight fast (58).

The postprandial plasma non-esterified fatty acid model was able to replicate different studies of postprandial plasma fatty acid dynamics. However, only with a change in some of the model parameter values. It was found the a linear relation between overnight fasted insulin concentration and the parameter K_{ATL}, which is related to the affinity of insulin towards adipose tissue lipase, could explain some of the changes in fat metabolism for the different subject groups.

The last model included in this thesis describes the allometric relationship between visceral fat and total fat mass. This is the first model to reveal an allometric relationship between changes of visceral and total fat mass that holds for both genders as well as for a wide variety of weight loss interventions including bariatric surgery, caloric restriction with or without exercise, and exercise alone. From this relationship it can be concluded that changes of visceral fat are primarily determined by total fat mass changes and bythe initial visceral to total fat mass ratio. For future investigations of visceral fat loss the allometric model predictions could be used as a null hypothesis to test for an additional independent effect of weight loss.

7 LIST OF REFERENCES

1 Acheson KJ, Schutz Y, Bessard T, Anantharaman K, Flatt JP, Jequier E. Glycogen storage capacity and de novo lipogenesis during massive carbohydrate overfeeding in man. American Journal of Clinical Nutrition 1988;**48/2**:240-247.

2 Acheson KJ, Schutz Y, Bessard T, Ravussin E, Jequier E, Flatt JP. Nutritional influences on lipogenesis and thermogenesis after a carbohydrate meal. Am J Physiol 1984;**246/1 Pt 1**:E62-E70.

3 Appel B, Fried SK. Effects of insulin and dexamethasone on lipoprotein lipase in human adipose tissue. Am J Physiol 1992;**262/5 Pt 1**:E695-E699.

4 Armstrong DT, Steele R, Altszuler N, Dunn A, Bishop JS, de Bodo RC. Regulation of plasma free fatty acid turnover. Am J Physiol 1961;**201/1**:9-15.

5 Baba H, Zhang XJ, Wolfe RR. Glycerol Gluconeogenesis in Fasting Humans. Nutrition 1995;**11**:149-153.

6 Bassingthwaighte JB, Noodleman L, van der Vusse G, Glatz JFC. Modeling of palmitate transport in the heart. Molecular and Cellular Biochemistry 1989;**88**:51-58.

7 Berg JM, Tymoczko JL, Stryer L. *Biochemistry*. 5 edn. W. H. Freeman and Company: New York, 2002.

8 Bergman R, Refai M. Dynamic control of hepatic glucose metabolism: Studies by experiment and computer simulation. Annals of Biomedical Engineering 1975;**3/4**:411-432.

9 Bickerton AST, Roberts R, Fielding BA, Hodson L, Blaak EE, Wagenmakers AJM, Gilbert M, Krape F, Frayn KN. Preferential uptake of Dietary Fatty Acids in Adipose Tissue and Muscle in the Postprandial Period. Diabetes 2007;**/56**:168-176.

10 Bjorntorp P. "Portal" adipose tissue as a generator of risk factors for cardiovascular disease and diabetes. Arterioscler Thromb Vasc Biol 1990;**10/4**:493-496.

11 Bobbioni-Harsch E, Habicht F, Lehmann T, James RW, Rohner-Jeanrenaud F, Golay A. Energy expenditure and substrates oxidative patterns, after glucose, fat or mixed load in normal weight subjects. Eur J Clin Nutr 1997;**51/6**:370-374.

12 Boden G, Chen XH, Ruiz J, White JV, Rossetti L. Mechanisms of fatty acid-induced inhibition of glucose-uptake. J Clin Inv 1994;**93/6**:2438-2446.

13 Boer P. Estimated lean body mass as an index for normalization of body fluid volumes in humans. Am J Physiol 1984;**247/4 Pt 2**:F632-F636.

14 Boesiger P, Buchli D, Meier D, Steinmann B, Gitzelmann R. Changes of Liver Metabolite Concentrations in Adults with disorders of Fructose Metabolism after Interveous Fructose be 31P Magnetic Resonanse Spectroscopy. Pediatric Researce 1994;**36**:436-440.

15 Bolinder J, Kager L, Ostman J, Arner P. Differences at the receptor and postreceptor levels between human omental and subcutaneous adipose tissue in the action of insulin on lipolysis. Diabetes 1983;**32/2**:117-123.

16 Bollen M, Keppens S, Stalmans W. Specific features of glycogen metabolism in the liver. Biochem J 1998;**336**:19-31.

17 Bonadonna RC, Groop LC, Zych K, Shank M, DeFronzo RA. Dose-dependent effect of insulin on plasma free fatty acid turnover and oxidation in humans. Am J Physiol 1990;**259/5 22-5**:E736-E750.

18 Bouchard C, Tremblay A, Després J, Nadeau A, Lupien P, Thériault G, Dussault J, Moorjani S, Pinault S, Fournier G. The response to long-term overfeeding in identical twins. N Engl J Med 1990;**322/21**:1477-1482.

19 Brett M. When is a correlation between non-independent variables "spurious". OIKOS 2004;**105/3**:647-656.

20 Brochu M, Tchernof A, Turner AN, Ades PA, Poehlman ET. Is there a threshold of visceral fat loss that improves the metabolic profile in obese postmenopausal women? Metabolism 2003;**52/5**:599-604.

21 Brooks GA. Lactate shuttles in nature. Biochem Soc Trans 2002;**30/2**:258-264.

22 Brunzell JD, Hazzard WR, Porte D, Bierman EL. Evidence for a common, saturable, triglyceride removal mechanism for chylomicrons and very low density lipoproteins in man. J Clin Inv 1973;**52/7**:1578-1585.

23 Bulow J, Simonsen L, Wiggins D, Humphreys SM, Frayn KN, Powell D, Gibbons GF. Co-ordination of hepatic and adipose tissue lipid metabolism after oral glucose. J Lipid Res 1999;**40/11**:2034-2043.

24 Busetto L, Tregnaghi A, De Marchi F, Segato G, Foletto M, Sergi G, Favretti F, Lise M, Enzi G. Liver Volume and Visceral Obesity in Women with Hepatic Steatosis Undergoing Gastric Banding. Obesity 2002;**10/5**:408-411.

25 Campbell PJ, Carlson MG, Hill JO, Nurjhan N. Regulation of free fatty acid metabolism by insulin in humans: Role of lipolysis and reesterification. Am J Physiol 1992;**263/6 PART 1**:E1063-E1069.

26 Campbell PJ, Carlson MG, Nurjhan N. Fat metabolism in human obesity. Am J Physiol Endocrinol Metab 1994;**266/4**:E600-E605.

27 Chaston TB, Dixon JB. Factors associated with percent change in visceral versus subcutaneous abdominal fat during weight loss: findings from a systematic review. Int J Obes 2008;**32/4**:619-628.

28 Cherrington AD. Control of glucose production in vivo by insulin and glucagon. In: Jefferson LS, Cherrington AD (eds). *Handbook of Physiology, Section 7: The Endocrine system, Volume 2: The Endocrine Pancreas and Regulation Metabolism.* Oxfort University Press: 2001.

29 Cherrington AD. Control of Glucose Uptake and Release by the Liver In Vivo. Diabetes 1999;**48**:1198-1214.

30 Cherrington AD, Edgerton D, Sindelar DK. The direct and indirect effects of insulin on hepatic glucose production in vivo. Diabetologia 1998;**41/9**:987-996.

31 Chowdhury B, Kvist H, Andersson B, Björntorp P, Sjöström L. CT-determined changes in adipose tissue distribution during a small weight reduction in obese males. Int J Obes Relat Metab Disord 1993;**17/2**:685-691.

32 Cline GW, Rothman DL, Magnusson I, Katz LD, Shulman GI. 13C-nuclear magnetic resonance spectroscopy studies of hepatic glucose metabolism in normal subjects and subjects with insulin-dependent diabetes mellitus. J Clin Invest 1994;**94/6**:2369-2376.

33 Connelly PW, Maguire GF, Vezina C, Hegele RA, Kuksis A. Kinetics of lipolysis of very low density lipoproteins by lipoprotein lipase. Importance of particle number and noncompetitive inhibition by particles with low triglyceride content. J Biol Chem 1994;**269/32**:20554-20560.

34 Coppack SW, Chinkes DL, Miles JM, Patterson BW, Klein S. A multicompartmental model of in vivo adipose tissue glycerol kinetics and capillary permeability in lean and obese humans. Diabetes 2005;**54/7**:1934-1941.

35 Coppack SW, Evans RD, Fisher RM, Frayn KN, Gibbons GF, Humphreys SM, Kirk ML, Potts JL, Hockaday TD. Adipose tissue metabolism in obesity: lipase action in vivo before and after a mixed meal. Metabolism 1992;**41/3**:264-272.

36 Coppack SW, Fisher RM, Gibbons GF, Humphreys SM, McDonough MJ, Potts JL, Frayn KN. Postprandial substrate deposition in human forearm and adipose tissues in vivo. Clin Sci (Lond) 1990;**79/4**:339-348.

37 Coppack SW, Frayn KN. Adipose tissue balance technique: application in human disease. In: Walker M, Butler P, Rizza RA (eds). *The Diabetes Annual 13.* 2000.

38 Coppack SW, Frayn KN, Humphreys SM. Plasma triacylglycerol extraction in human adipose tissue in vivo: effects of glucose ingestion and insulin infusion. Eur J Clin Nutr 1989;**43/7**:493-496.

39 Coppack SW, Frayn KN, Humphreys SM, Dhar H, Hockaday TD. Effects of insulin on human adipose tissue metabolism in vivo. Clin Sci (Colch) 1989;**77/6**:663-670.

40 Coppack SW, Jensen MD, Miles JM. In vivo regulation of lipolysis in humans. J Lipid Res 1994;**35/2**:177-193.

41 Coppack SW, Persson M, Judd RL, Miles JM. Glycerol and nonesterified fatty acid metabolism in human muscle and adipose tissue in vivo. Am J Physiol 1999;**276/2 Pt 1**:E233-E240.

42 Cornish-Bowden A, Ca¦rdenas ML. Hexokinase and [`]glucokinase' in liver metabolism. Trends in Biochemical Sciences 1991;**16**:281-282.

43 Cruz ML, Evans K, Frayn K. Postprandial lipid metabolsim and insulin sensitivity in young Northern Europeans, South Asians and Latin Americans in the UK. Atherosclerosis 2001;**159**:441-449.

44 Cryer A. Tissue lipoprotein lipase activity and its action in lipoprotein metabolism. Int J Biochem 1981;**13/5**:525-541.

45 Del Prato S, Matsuda M, Simonson DC, Groop LC, Sheehan P, Leonetti F, Bonadonna RC, DeFronzo RA. Studies on the mass action effect of glucose in NIDDM and IDDM: evidence for glucose resistance. Diabetologia 1997;**40/6**:387-397.

46 Despres JP, Pouliot MC, Moorjani S, Nadeau A, Tremblay A, Lupien PJ, Theriault G, Bouchard C. Loss of abdominal fat and metabolic response to exercise training in obese women. Am J Physiol Endocrinol Metab 1991;**261/2**:E159-E167.

47 Despres JP, Lemieux I. Abdominal obesity and metabolic syndrome. Nature 2006;**444/7121**:881-887.

48 Doucet E, St-Pierre S, Alméras N, Imbeault P, Mauriège P, Pascot A, Després J-P, Tremblay JA. Reduction of visceral adipose tissue during weight loss. Eur J Clin Nutr 2002;**56/4**:297-304.

49 Doucet E, St-Pierre S, Almeras N, Mauriege P, Despres JP, Richard D, Bouchard C, Tremblay A. Fasting Insulin Levels Influence Plasma Leptin Levels Independently from the Contribution of Adiposity: Evidence from Both a Cross-Sectional and an Intervention Study. J Clin Endocrinol Metab 2000;**85/11**:4231-4237.

50 Duncan RE, Ahmadian M, Jeworski K, Sarkadi-Nagy E, Sul HS. Regulation of Lipolysis in Adipocytes. Annu Rev Nutr 2007.

51 Edelman SV, Laakso M, Wallence P, Brechtel G, Brechtel G, Olefsky JM, Baron AD. Kinetics of insulin-mediated and non-insulin-mediated glcuose uptake in humans. Diabetes 1990;**39**:955-964.

52 El-Refai M, Bergman RN. Simulation study of control of hepatic glycogen synthesis by glucose and insulin. AJP - Legacy 1976;**231/5**:1608-1619.

53 Engelson ES, Agin D, Kenya S, Werber-Zion G, Luty B, Albu JB, Kotler DP. Body composition and metabolic effects of a diet and exercise weight loss regimen on obese, HIV-infected women. Metabolism 2006;**55/10**:1327-1336.

54 Ercan-Fang N, Gannon MC, Rath VL, Treadway JL, Taylor MR, Nuttall FQ. Integrated effects of multiple modulators on human liver glycogen phosphorylase a. Am J Physiol Endocrinol Metab 2002;**283/1**:E29-E37.

55 Evans K, Burdge GC, Wootton SA, Clark ML, Frayn KN. Regulation of dietary fatty acid entrapment in subcutaneous adipose tissue and skeletal muscle. Diabetes 2002;**51/9**:2684-2690.

56 Evans K, Clark ML, Frayn KN. Effects of an oral and intravenous fat load on adipose tissue and forearm lipid metabolism. Am J Physiol Endocrinol Metab 1999;**276/2**:E241-E248.

57 Fery F, Plat L, Balasse EO. Effect of fasting on the intracellular metabolic partition of intravenously infused glucose in humans. Am J Physiol Endocrinol Metab 1999;**277/5**:E815-E823.

58 Fielding BA, Callow J, Owen RM, Samra JS, Matthews DR, Frayn KN. Postprandial lipemia: the origin of an early peak studied by specific dietary fatty acid intake during sequential meals. American Journal of Clinical Nutrition 1996;**63/1**:36-41.

59 Fielding BA, Frayn KN. Lipoprotein lipase and the disposition of dietary fatty acids. Br J Nutr 1998;**80/6**:495-502.

60 Fox CS, Massaro JM, Hoffmann U, Pou KM, Maurovich-Horvat P, Liu CY, Vasan RS, Murabito JM, Meigs JB, Cupples LA, D'Agostino RB, Sr., O'Donnell CJ. Abdominal Visceral and Subcutaneous Adipose Tissue Compartments: Association With Metabolic Risk Factors in the Framingham Heart Study. Circulation 2007;**116/1**:39-48.

61 Frayn KN. *Metabolic Regulation. A Human Perspective.* Portland Press: 1999.

62 Frayn KN. Calculation of substrate oxidation rates in vivo from gaseous exchange. J Appl Physiol 1983;**55/2**:628-634.

63 Frayn KN, Coppack SW, Humphreys SM, Clark ML, Evans RD. Periprandial regulation of lipid metabolism in insulin-treated diabetes mellitus. Metabolism 1993;**42/4**:504-510.

64 Frayn KN, Karpe F, Fielding BA, Macdonald IA, Coppack SW. Integrative physiology of human adipose tissue. Int J Obes Relat Metab Disord 2003;**27/8**:875-888.

65 Frayn KN, Shadid S, Hamlani R, Humphreys SM, Clark ML, Fielding BA, Boland O, Coppack SW. Regulation of fatty acid movement in human adipose tissue in the postabsorptive-to-postprandial transition. Am J Physiol 1994;**266/3 Pt 1**:E308-E317.

66 Frayn KN. *Metabolic Regulation: A Human Perspective*. 2 edn. Blackwell Science Ltd: 2003.

67 Frohnert BI, Bernlohr DA. Regulation of fatty acid transporters in mammalian cells. Progress in Lipid Research 2000;**39/1**:83-107.

68 Fujioka S, Matsuzawa Y, Tokunaga K, Kawamoto T, Kobatake T, Keno Y, Kotani K, Yoshida S, Tarui S. Improvement of glucose and lipid metabolism associated with selective reduction of intra-abdominal visceral fat in premenopausal women with visceral fat obesity. Int J Obes 1991;**15/12**:853-859.

69 Giannopoulou I, Ploutz-Snyder LL, Carhart R, Weinstock RS, Fernhall B, Goulopoulou S, Kanaley JA. Exercise Is Required for Visceral Fat Loss in Postmenopausal Women with Type 2 Diabetes. J Clin Endocrinol Metab 2005;**90/3**:1511-1518.

70 Gletsu N, Lin E, Khaitan L, Lynch SA, Ramshaw B, Raziano R, Torres WE, Ziegler TR, Papanicolaou DA, Smith CD. Changes in C-Reactive Protein Predict Insulin Sensitivity in Severely Obese Individuals After Weight Loss Surgery. Journal of Gastrointestinal Surgery 2005;**9/8**:1119-1128.

71 Goodpaster BH, Kelley DE, Wing RR, Meier A, Thaete FL. Effects of weight loss on regional fat distribution and insulin sensitivity in obesity. Diabetes 1999;**48/4**:839-847.

72 Gottesman I, Mandarino L, Geric J. Estimation and kinetic analysis of insulin-independent glucose uptake in humans subjects. Am J Physiol 1983;**244**:632.

73 Gower BA, Weinsier RL, Jordan JM, Hunter GR, Desmond R. Effects of weight loss on changes in insulin sensitivity and lipid concentrations in premenopausal African American and white women. American Journal of Clinical Nutrition 2002;**76/5**:923-927.

74 Groop LC, Saloranta C, Shank M, Bonadonna RC, Ferrannini E, DeFronzo RA. The role of free fatty acid metabolism in the pathogenesis of insulin resistance in obesity and noninsulin-dependent diabetes mellitus. J Clin Endocrin Metab 1991;**72/1**:96-107.

75 Hamilton JA, Kamp F. How are free fatty acids transported in membranes? Is it by proteins or by free diffusion through the lipids? Diabetes 1999;**48/12**:2255-2269.

76 Hansen BF, Asp S, Kim B, Richter EA. Glycogen concentration in human skeletal muscle: effect of prolonged insulin and glucose infusion. Scand J Med Sci Sports 1999;**9**:209-213.

77 Hansen, B. F. Limits to Glycogen Storage. 1998. Laboratory of Human Physiology, August Krogh Institute, University of Copenhagen.
Ref Type: Thesis/Dissertation

78 Hansen, R. N. Glucose Homeostasis: A biosimuoation approach. 2004. Cobenhagen, Department of Physics, Technical University of Denmark.
Ref Type: Thesis/Dissertation

79 Havel RJ, Naimark A, Borchgrevink CF. Turnover rate and oxidation of free fatty acids of blood plasma in man durin gexercise: Studies during continuous infusion of palmitate-1-C14. J Clin Inv 1963;**42/7**:1054-1063.

80 Heimberg, M., Wilcox, H. G., Dunn, G. D., Woodside, W. F., Brent, K. J., and Soler-Argilaga, C. Studies on the Regualtion of Secretion of the Very Low Density Lipoprotein, and on Ketogenesis by the Liver. Lundquist, F. and Tygstrup, N. 6, 119-141. 1973. Copenhagen, Scandinavian University Books. Alfred Benzon Symposium. 1973.
Ref Type: Conference Proceeding

81 Hellerstein MK, Neese RA, Linfoot P, Christiansen M, Turner S, Letscher A. Hepatic gluconeogenic fluxes and glycogen turnover during fasting in humans. A stable isotope study. J Clin Invest 1997;**100/5**:1305-1319.

82 Hother-Nielsen O, Henriksen JE, Holst JJ, Beck-Nielsen. Effects of ´Insulin on Glucose Turnover Rates in Vivo: Isotopedilution versus Constant Specific Activity Technique. Metabolism 2009;**45**:82-91.

83 Hue L. The role of futile cycles in the regulation of carbohydrate metabolism in the liver. Advances in Enzymology and Related Areas of Molecular Biology 1981;**52**.

84 Hue L. Regulation of gluconeogenesis in liver. In: Jefferson LS, Cherrington AC (eds). *Handbook of Physiology, Section 7: The Endocrine system, Volume 2: The Endocrine Pancreas and Regulation Metabolism.* Oxford University Press: 2001, pp. 649-657.

85 Huxley J. *Problems of Relative Growth*. Methuen & Co. Ltd: London, 1932.

86 Jackson KG, Wolstencroft EJ, Bateman PA, Yaqoob P, Williams CM. Acute effects of meal fatty acids on postprandial NEFA, glucose and apo E response: implications for insulin sensitivity and lipoprotein regulation? British Journal of Nutrition 2005;**93/05**:693-700.

87 Janssen I, Ross R. Effects of sex on the change in visceral, subcutaneous adipose tissue and skeletal muscle in response to weight loss. Int J Obes Relat Metab Disord 1999;**23/10**:1035-1046.

88 Janssen I, Fortier A, Hudson R, Ross R. Effects of an Energy-Restrictive Diet With or Without Exercise on Abdominal Fat, Intermuscular Fat, and Metabolic Risk Factors in Obese Women. Diabetes Care 2002;**25/3**:431-438.

89 Jansson PA, Fowelin JP, von Schenck HP, Smith UP, Lonnroth PN. Measurement by microdialysis of the insulin concentration in subcutaneous interstitial fluid. Importance of the endothelial barrier for insulin. Diabetes 1993;**42/10**:1469-1473.

90 Jensen MD. Role of Body Fat Distribution and the Metabolic Complications of Obesity. J Clin Endocrinol Metab 2008;**93/11_Supplement_1**:s57-s63.

91 Karpe F, Fielding BA, Ardilouze JL, Ilic V, Macdonald IA, Frayn KN. Effects of insulin on adipose tissue blood flow in man. J Physiol 2002;**540/Pt 3**:1087-1093.

92 Kim J, Saidel G, Cabrera M. Multi-Scale Computational Model of Fuel Homeostasis During Exercise: Effect of Hormonal Control. Annals of Biomedical Engineering 2007;**35/1**:69-90.

93 Klip A, Marette A. Regulation of glucose transporters by insulin and exercise: cellular effects and implication for diabetes. In: Jefferson LS, Cherrington AD (eds). *Handbook of Physiology, Section 7: The Endocrine system, Volume 2: The Endocrine Pancreas and Regulation Metabolism.* Oxfort University Press: 2001.

94 Knox WE. *Enzyme Patterns in Fetal, Adult, and Neoplastic Rat Tissue*. 2 edn. Karger AG: Basel (Switzerland), 1976.

95 Knudsen GM, Hasselbalch SG, Hertx MM, Raulson OB. High Dose Insulin does not increase Glucose Transfer across the Blood-Brain Barrier in Humans: a re-evaluation. Eur J Clin Invest 1999;**29**:687-691.

96 Knutson VP. The Release of Lipoprotein Lipase from 3T3-L1 Adipocytes Is Regulated by Microvessel Endothelial Cells in an Insulin-Dependent Manner. Endocrinology 2000;**141/2**:693-701.

97 Kohout M, Kohoutova B, Heimberg M. The regulation of hepatic triglyceride metabolism by free fatty acids. J Biol Chem 1971;**246/16**:5067-5074.

98 Larson-Meyer DE, Heilbronn LK, Redman LM, Newcomer BR, Frisard MI, Anton S, Smith SR, Alfonso A, Ravussin E, the Pennington CALERIE Team. Effect of Calorie Restriction With or Without Exercise on Insulin Sensitivity, {beta}-Cell Function, Fat Cell Size, and Ectopic Lipid in Overweight Subjects. Diabetes Care 2006;**29/6**:1337-1344.

99 Levitt DG. The pharmacokinetics of the interstitial space in humans. BMC Clinical Pharmacology 2003;**3**.

100 Lewis GF, Carpentier A, Adeli K, Giacca A. Disordered fat storage and mobilization in the pathogenesis of insulin resistance and type 2 diabetes. Endocr Rev 2002;**23/2**:201-229.

101 Lin E, Phillips LS, Ziegler TR, Schmotzer B, Wu K, Gu LH, Khaitan L, Lynch SA, Torres WE, Smith CD, Gletsu-Miller N. Increases in Adiponectin Predict Improved Liver, but Not Peripheral, Insulin Sensitivity in Severely Obese Women During Weight Loss. Diabetes 2007;**56/3**:735-742.

102 Lynch NA, Nicklas BJ, Berman DM, Dennis KE, Goldberg AP. Reductions in visceral fat during weight loss and walking are associated with improvements in {V}O2 max. J Appl Physiol 2001;**90/1**:99-104.

103 Maddaiah VT, Madsen NB. Kinetics of Purified Liver Phosphorylase. J Biol Chem 1966;**241**:3873-3881.

104 Madsen J, Bulow J, Nielsen NE. Inhibition of fatty acid mobilization by arterial free fatty acid concentration. Acta Physiol Scand 1986;**127/2**:161-166.

105 Magnuson M, Matschinsky F. Glucokinase as a Glucose Sensor: Past, Present and Future. In: *Glucokinase and Glycemic Disease: From Basics to Novel Therapeutics.* Front Diabetes.: Basel, 2004, pp. 1-17.

106 Magnusson I, Rothman DL, Jucker B, Cline GW, Shulman RG, Shulman GI. Liver glycogen turnover in fed and fasted humans. Am J Physiol 1994;**266/5 Pt 1**:E796-E803.

107 Magnusson I, Rothman DL, Katz LD, Shulman RG, Shulman GI. Increased rate of gluconeogenesis in type II diabetes mellitus. A 13C nuclear magnetic resonance study. J Clin Invest 1992;**90/4**:1323-1327.

108 Mauriege P, Marette A, Atgie C, Bouchard C, Theriault G, Bukowiecki LK, Marceau P, Biron S, Nadeau A, Despres JP. Regional variation in adipose tissue metabolism of severely obese premenopausal women. J Lipid Res 1995;**36/4**:672-684.

109 Mayer L, Walsh BT, Pierson RN, Jr., Heymsfield SB, Gallagher D, Wang J, Parides MK, Leibel RL, Warren MP, Killory E, Glasofer D. Body fat redistribution after weight gain in women with anorexia nervosa. American Journal of Clinical Nutrition 2005;**81/6**:1286-1291.

110 McGarry JD, Foster DW. The regulation of ketogenesis from oleic acid and the influence of antiketogenic agents. J Biol Chem 1971;**246/20**:6247-6253.

111 McGarry JD, Foster DW. Regulation of Hepatic Fatty Acid Oxidation and Ketone Body Production. Annual Review of Biochemistry 2003;**49/1**:395-420.

112 Mittelman SD, Van Citters GW, Kirkman EL, Bergman RN. Extreme Insulin Resistance of the Central Adipose Depot In Vivo. Diabetes 2002;**51/3**:755-761.

113 Moeri R, Golay A, Schutz Y, Temler E, Jequier E, Felber JP. Oxidative and nonoxidative glucose metabolism following graded doses of oral glucose in man. Diabete Metab 1988;**14/1**:1-7.

114 Mourier A, Gautier J, De Kerviler E, Bigard A, Villette J, Garnier J, Duvallet A, Guezennec C, Cathelineau G. Mobilization of visceral adipose tissue related to the improvement in insulin sensitivity in response to physical training in NIDDM. Effects of branched-chain amino acid supplements. Diabetes Care 1997;**20/3**:385-891.

115 Nicklas BJ, Dennis KE, Berman DM, Sorkin J, Ryan AS, Goldberg AP. Lifestyle Intervention of Hypocaloric Dieting and Walking Reduces Abdominal Obesity and Improves Coronary Heart Disease Risk Factors in Obese, Postmenopausal, African-American and Caucasian Women. J Gerontol A Biol Sci Med Sci 2003;**58/2**:M181-M189.

116 Okura T, Nakata Y, Tanaka K. Effects of Exercise Intensity on Physical Fitness and Risk Factors for Coronary Heart Disease. Obesity 2003;**11/9**:1131-1139.

117 Okura T, Tanaka K, Nakanishi T, Lee DJ, Nakata Y, Wee SW, Shimokata H. Effects of Obesity Phenotype on Coronary Heart Disease Risk Factors in Response to Weight Loss. Obesity 2002;**10/8**:757-766.

118 Owen OE, Reichard GAJr, Markus H, Boden G, Mozzoli AM, Shulman CR. Rapid Intravenous Sodium Acetoacetate Infusion in Man. Metabolic and kinetic responses. J Clin Invest 1973;**52**:144-150.

119 Pare A, Dumont M, Lemieux I, Brochu M, Almeras N, Lemieux S, 'homme D, Despres JP. Is the Relationship between Adipose Tissue and Waist Girth Altered by Weight Loss in Obese Men? Obesity 2001;**9/9**:526-534.

120 Patel MS, Jomain-Baum M, Ballard FJ, Hanson RW. Pathway of carbon flow during fatty acid synthesis from lactate and pyruvate in rat adipose tissue. J Lipid Res 1971;**12**:179-191.

121 Periwal V, Chow CC, Bergman RN, Ricks M, Vega GL, Sumner AE. Evaluation of quantitative models of the effect of insulin on lipolysis and glucose disposal. Am J Physiol Regul Integr Comp Physiol 2008;**295/4**:R1089-R1096.

122 Petersen KF, Laurent D, Rothman DL, Cline GW, Shulman GI. Mechanism by which glucose and insulin inhibit net hepatic glycogenolysis in humans. J Clin Invest 1998;**101/6**:1203-1209.

123 Press W. *Numerical recipes: the art of scientific computing*. Cambridge University Press: New York, 1986.

124 Ralph EC, Thomson J, Almaden J, Sun S. Glucose modulation of glucokinase activation by small molecules. Biochemistry 2008;**47/17**:5028-5036.

125 Rasmussen BB, Wolfe RR. Regulation of fatty acid oxidation in skeletal muscle. Annu Rev Nutr 1999;**19**:463-484.

126 Redman LM, Heilbronn LK, Martin CK, Alfonso A, Smith SR, Ravussin E, for the Pennington CALERIE Team. Effect of Calorie Restriction with or without Exercise on Body Composition and Fat Distribution. J Clin Endocrinol Metab 2007;**92/3**:865-872.

127 Rice B, Janssen I, Hudson R, Ross R. Effects of aerobic or resistance exercise and/or diet on glucose tolerance and plasma insulin levels in obese men. Diabetes Care 1999;**22/5**:684-691.

128 Richelsen B, Pedersen SB, Moller-Pedersen T, Bak JF. Regional differences in triglyceride breakdown in human adipose tissue: effects of catecholamines, insulin, and prostaglandin E2. Metabolism 1991;**40/9**:990-996.

129 Roden M, Perseghin G, Petersen KF, Hwang JH, Cline GW, Gerow K, Rothman DL, Shulman GI. The Roles of Insulin and Glucagon in the Regulation of Hepatic Glycogen Synthesis and Turnover i Humans. J Clin Invest 1996;**7/3**:642-648.

130 Ross R, Rissanen J. Mobilization of visceral and subcutaneous adipose tissue in response to energy restriction and exercise. American Journal of Clinical Nutrition 1994;**60/5**:695-703.

131 Ross R, Rissanen J, Hudson R. Sensitivity associated with the identification of visceral adipose tissue levels using waist circumference in men adn women: effects of weight loss. Int J Obes Relat Metab Disord 1996;**20/6**:533-538.

132 Ross R, Dagnone D, Jones PJH, Smith H, Paddags A, Hudson R, Janssen I. Reduction in Obesity and Related Comorbid Conditions after Diet-Induced Weight Loss or Exercise-Induced Weight Loss in Men: A Randomized, Controlled Trial. Ann Intern Med 2000;**133/2**:92-103.

133 Ross R, Janssen I, Dawson J, Kungl AM, Kuk JL, Wong SL, Nguyen-Duy TB, Lee S, Kilpatrick K, Hudson R. Exercise-Induced Reduction in Obesity and Insulin Resistance in Women: a Randomized Controlled Trial[ast][ast]. Obesity 2004;**12/5**:789-798.

134 Ross R, Rissanen J, Pedwell H, Clifford J, Shragge P. Influence of diet and exercise on skeletal muscle and visceral adipose tissue in men. J Appl Physiol 1996;**81/6**:2445-2455.

135 Rothman DL, Magnusson I, Katz LD, Shulman RG, Shulman GI. Quantitation of hepatic glycogenolysis and gluconeogenesis in fasting humans with 13C NMR. Science 1991;**254/5031**:573-576.

136 Roy A, Parker RS. Dynamic Modeling of Free Fatty Acid, Glucose, and Insulin: An Extended "Minimal Model". Diabetes Technology & Therapeutics 2006;**8/6**:617-626.

137 Ryan AS, Nicklas BJ. Reductions in Plasma Cytokine Levels With Weight Loss Improve Insulin Sensitivity in Overweight and Obese Postmenopausal Women. Diabetes Care 2004;**27/7**:1699-1705.

138 Ryan AS, Nicklas BJ, Berman DM. Aerobic Exercise Is Necessary to Improve Glucose Utilization with Moderate Weight Loss in Women[ast]. Obesity 2006;**14/6**:1064-1072.

139 Santomauro AT, Boden G, Silva ME, Rocha DM, Santos RF, Ursich MJ, Strassmann PG, Wajchenberg BL. Overnight lowering of free fatty acids with Acipimox improves insulin resistance and glucose tolerance in obese diabetic and nondiabetic subjects. Diabetes 1999;**48/9**:1836-1841.

140 Santosa S, Demonty I, Lichtenstein AH, Jones PJH. Cholesterol metabolism and body composition in women: the effects of moderate weight loss. Int J Obes 2007;**31/6**:933-941.

141 Schwartz RS, Ravussin E, Massari M, O'Connell M, Robbins DC. The thermic effect of carbohydrate versus fat feeding in man. Metabolism 1985;**34/3**:285-293.

142 Segal HL, Washko ME. Studies of Liver Glucose 6-phosphatase. The Journal fo Biological Chemistry 1959;**234**:1937-1941.

143 Shadid S, Jensen MD. Effects of Pioglitazone Versus Diet and Exercise on Metabolic Health and Fat Distribution in Upper Body Obesity. Diabetes Care 2003;**26/11**:3148-3152.

144 Shen W, Punyanitya M, Wang Z, Gallagher D, St-Onge MP, Albu J, Heymsfield SB, Heshka S. Visceral adipose tissue: relations between singel-slice areas and totla volume. Am J Clin Nutr 2004;**23/4**:329-335.

145 Smith SR, Zachwieja JJ. Visceral adipose tissue: a critical review of intervention strategies. Int J Obes Relat Metab Disord 1999;**23/4**:329-335.

146 Sniderman AD, Bhopal R, Prabhakaran D, Sarrafzadegan N, Tchernof A. Why might South Asians be so susceptible to central obesity and its atherogenic consequences? The adipose tissue overflow hypothesis. Int J Epidemiol 2007;**36/1**:220-225.

147 Soop M, Nygren J, Brismar K, Thorell A, Ljungqvist O. The hyperinsulinaemic-euglycaemic glucose clamp: reproducibility and metabolic effects of prolonged insulin infusion in healthy subjects. Clin Sci 2000;**98/4**:367-374.

148 Stalmans W, Bollen M, Mvumbi L. Control of Glycogen Synthesis in Health and Disease. Diabetes/Metabolism Reviews 1987;**3**:127-161.

149 Stingl H, Chandramouli V, Schumann W, Brehm A, Nowotny P, Waldh+ñusl W, Landau B, Roden M. Changes in hepatic glycogen cycling during a glucose load in healthy humans. Diabetologia 2006;**49/2**:360-368.

150 Stumvoll M, Wahl HG, Machicao F, Haring H. Insulin sensitivity of glucose disposal and lipolysis: No influence of common genetic varainats in IRS-1 and CAPN10. Diabetolog 2002;**45/5**:651-656.

151 Tan GD, Fielding BA, Currie JM, Humphreys SM, Désage M, Frayn KN, Vidal H, Karpe F. The effects of rosiglitazone on fatty acid and triglyceride metabolism in type 2 diabetes. Diabetologia 2005;**48**:83-95.

152 Tchernof A, Starling RD, Turner A, Shuldiner AR, Walston JD, Silver K, Poehlman ET. Impaired capacity to lose visceral adipose tissue during weight reduction in obese postmenopausal women with the Trp64Arg beta3-adrenoceptor gene variant. Diabetes 2000;**49/10**:1709-1713.

153 Thamer C, Machann J, Stefan N, Haap M, Schafer S, Brenner S, Kantartzis K, Claussen C, Schick F, Haring H, Fritsche A. High Visceral Fat Mass and High Liver Fat Are Associated with Resistance to Lifestyle Intervention[ast]. Obesity 2007;**15/2**:531-538.

154 Thong FSL, Hudson R, Ross R, Janssen I, Graham TE. Plasma leptin in moderately obese men: independent effects of weight loss and aerobic exercise. Am J Physiol Endocrinol Metab 2000;**279/2**:E307-E313.

155 Toews CJ. Kinetic studies with Skeletal-Muscle Hexokinase. Biochem J 1966;**100**:739-744.

156 Van Harken DR, Dixon CW, Heimberg M. Hepatic lipid metabolism in experimental diabetes. V. The effect of concentration of oleate on metabolism of triglycerides and on ketogenesis. J Biol Chem 1969;**244/9**:2278-2285.

157 van Rossum EFC, Nicklas BJ, Dennis KE, Berman DM, Goldberg AP. Leptin Responses to Weight Loss in Postmenopausal Women: Relationship to Sex-Hormone Binding Globulin and Visceral Obesity. Obesity 2000;**8/1**:29-35.

158 Van Schaftingen E, Gerin I. The glucose-6-phosphatase system. Biochem J 2002;**362/Pt 3**:513-532.

159 Vernet O, Christin L, Schutz Y, Danforth E, Jequier E. Enteral versus parenteral nutrition: comparison of energy metabolism in lean and moderately obese women. Am J Clin Nutr 1986;**43/2**:194-209.

160 Vogel WK, Keenan RP, Gelev CW, Neet KE. The regulatory kinetic properties of porcine hepatic glucokinase. Molecular and Cellular Biochemistry 1989;**86/2**:171-179.

161 Wahren J, Ekberg K. Splanchnic Regulation of Glucose Production. Annu Rev Nutr 2007.

162 Wajchenberg BL. Subcutaneous and Visceral Adipose Tissue: Their Relation to the Metabolic Syndrome. Endocrine Reviews 2000;**21/6**:697-738.

163 Weinsier RL, Hunter GR, Gower BA, Schutz Y, Darnell BE, Zuckerman PA. Body fat distribution in white and black women: different patterns of intraabdominal and subcutaneous abdominal adipose tissue utilization with weight loss. American Journal of Clinical Nutrition 2001;**74/5**:631-636.

164 Wolfe RR, Klein S, Carraro F, Weber JM. Role of triglyceride-fatty acid cycle in controlling fat metabolism in humans during and after exercise. Am J Physiol 1990;**258/2 Pt 1**:E382-E389.

165 Wolfe RR, Peters EJ, Klein S, Holland OB, Rosenblatt J, Gary H, Jr. Effect of short-term fasting on lipolytic responsiveness in normal and obese human subjects. Am J Physiol Endocrinol Metab 1987;**252/2**:E189-E196.

166 Xiang SQ, Cianflone K, Kalant D, Sniderman AD. Differential binding of triglyceride-rich lipoproteins to lipoprotein lipase. J Lipid Res 1999;**40/9**:1655-1663.

167 Youn JH, Ader M, Bergman RN. Glucose phosphorylation is not rate limiting for accumulation of glycogen from glucose in perfused livers from fasted rats. J Biol Chem 1989;**264/1**:168-172.

168 Zimmermann R, Strauss JG, Haemmerle G, Schoiswohl G, Birner-Gruenberger R, Riederer M, Lass A, Neuberger G, Eisenhaber F, Hermetter A, Zechner R. Fat mobilization in adipose tissue is promoted by adipose triglyceride lipase. Science 2004;**306/5700**:1383-1386.